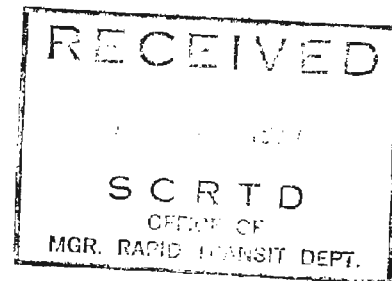


Report No. DOT-TST 76T-16

ANALYSIS OF INTERACTION BETWEEN TWO PARALLEL TUNNELS



AUGUST 1976

FINAL REPORT

Prepared for

U.S. Department of Transportation
OFFICE OF THE SECRETARY
AND
FEDERAL RAILROAD ADMINISTRATION
Washington, D.C. 20590

TF
230
.R36
c.1

NOTICE

This document is disseminated under the sponsorship of the Department of Transportation in the interest of information exchange. The United States Government assumes no liability for its contents or use thereof.

1. Report No. DOT-TST 76T-16		2. Government Accession No.		3. Recipient's Catalog No.	
4. Title and Subtitle ANALYSIS OF INTERACTION BETWEEN TWO PARALLEL TUNNELS				5. Report Date August, 1976	
				6. Performing Organization Code	
7. Author(s) R. E. Ranken and J. Ghaboussi				8. Performing Organization Report No. UILU-ENG-76-2020	
				10. Work Unit No. (TRAIS)	
9. Performing Organization Name and Address Department of Civil Engineering University of Illinois at Urbana-Champaign Urbana, IL 61801				11. Contract or Grant No. DOT FR 30022	
				13. Type of Report and Period Covered FINAL REPORT August 1975-August 1976	
12. Sponsoring Agency Name and Address U.S. Department of Transportation Office of the Secretary and Federal Railroad Administration Washington, D.C. 20590				14. Sponsoring Agency Code	
				15. Supplementary Notes	
16. Abstract <p>The finite element method of analysis was used to study the behavior and interaction of two circular and parallel tunnels. Depth of burial, tunnel spacing and construction sequence were the system variables considered in greatest detail.</p> <p>Throughout the investigation, which was restricted to two-dimensional analyses, the ground mass was assumed to be a continuous, isotropic and homogeneous medium with a free-field stress system corresponding to the self-weight of the medium and $K_0 = 0.5$. Except for three elasto-plastic analyses, all of the analyses assumed linear-elastic stress-strain behavior for the medium. The simulated support conditions approximated the installation of the liner either right at the tunnel face or far behind the face. Depths of cover equal to one tunnel diameter and five tunnel diameters were considered.</p> <p>In one series of analyses it was assumed that both tunnels advanced together at the same rate. In addition, the position of liner installation was considered to be the same in both tunnels. Three pillar width to tunnel diameter ratios ($W/D = 1.0, 0.5$ and 0.25) were simulated in this series of analyses.</p> <p>In a second set of analyses the construction sequence was altered such that the face of one tunnel was far ahead of the face of the second tunnel. Here only one pillar width ($W/D = 0.5$) was examined. Tunnel I was simulated as having been lined right at the face, lined behind the face but ahead of Tunnel II, or not lined until after passage of Tunnel II. Tunnel II was assumed to have been lined either right at the face or far behind the face.</p>					
17. Key Words Tunnels; Two Tunnel Interaction; Tunnel Liners; Soil-Liner Interaction; Finite Element Analysis.			18. Distribution Statement Document is available to the public through the National Technical Infor- mation Service, Springfield, VA 22151		
19. Security Classif. (of this report) Unclassified		20. Security Classif. (of this page) Unclassified		21. No. of Pages 125	22. Price

00948

100
100
100
100

PREFACE

Research described in this report was performed by the Department of Civil Engineering at the University of Illinois at Urbana-Champaign, Urbana, Illinois from August 1975 to August 1976.

The project was sponsored by the U.S. Department of Transportation, through Contract No. DOT FR 30022. The sponsor's technical representative was Mr. Russell K. McFarland of the Office of the Secretary.

The report was reviewed by Dr. R. B. Peck, Consultant to the project, and Professor E. J. Cording. Their helpful advice is gratefully acknowledged.

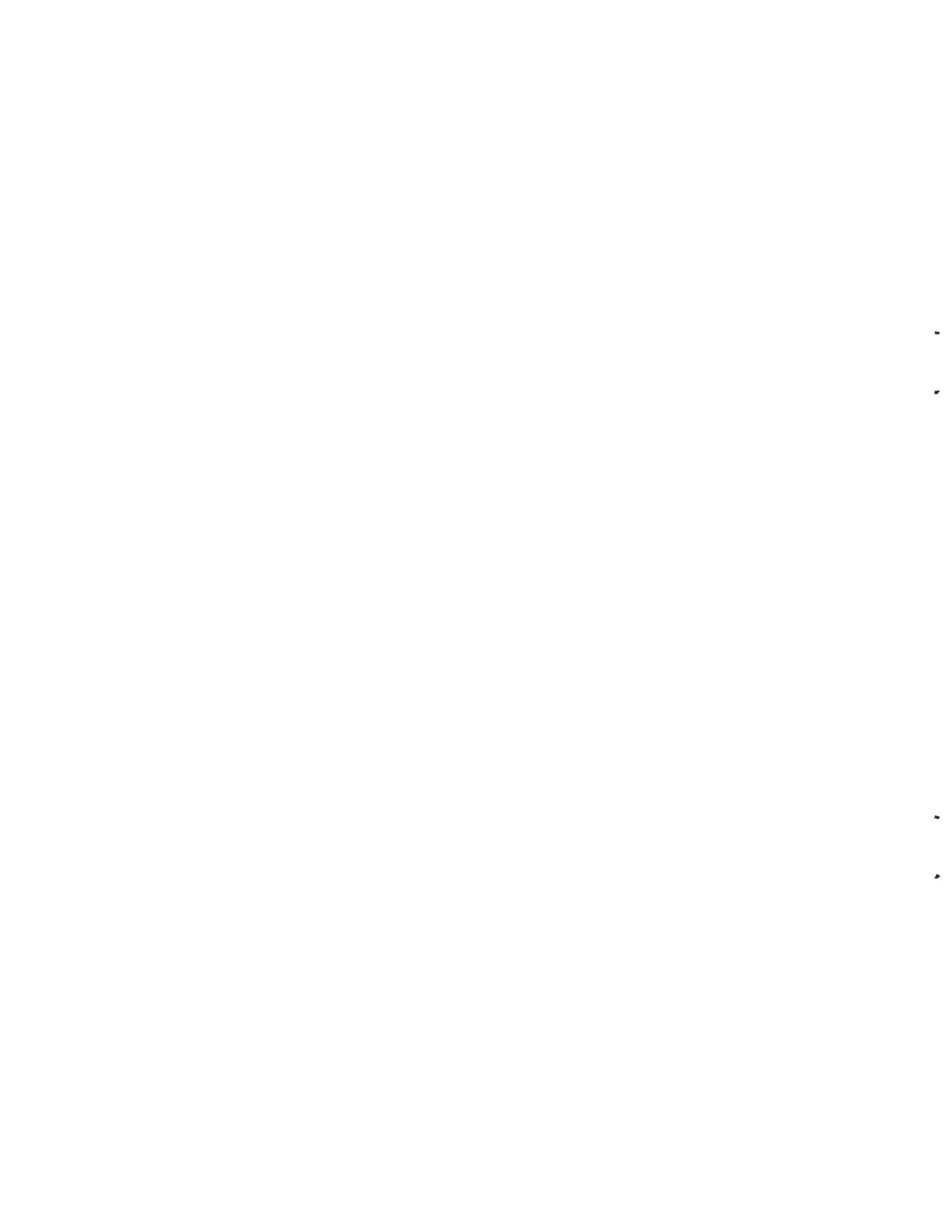


TABLE OF CONTENTS

Chapter		Page
1	INTRODUCTION	1-1
	1.1 OBJECTIVES	1-1
	1.2 GENERAL	1-1
	1.3 PREVIOUS STUDIES	1-7
2	METHOD OF ANALYSIS	2-1
	2.1 GENERAL	2-1
	2.2 FINITE ELEMENT MESH	2-1
	2.3 CONSTRUCTION SEQUENCE	2-3
3	RESULTS OF ANALYSIS	3-1
	3.1 GENERAL	3-1
	3.2 TWO TUNNELS CONSTRUCTED SIMULTANEOUSLY- THE SYMMETRICAL CASE.	3-2
	3.2.1 MEDIUM STRESSES.	3-2
	3.2.2 TUNNEL AND SURFACE DISPLACEMENTS	3-13
	3.2.3 LINER FORCES AND MOMENTS.	3-22
	3.3 SECOND TUNNEL CONSTRUCTED ADJACENT TO AN EXISTING TUNNEL -- THE UNSYMMETRICAL CASE	3-32
	3.3.1 MEDIUM STRESSES.	3-32
	3.3.2 TUNNEL AND SURFACE DISPLACEMENTS	3-37
	3.3.3 LINER FORCES AND MOMENTS.	3-53
	3.4 ELASTO-PLASTIC ANALYSES.	3-59
4	DISCUSSION OF RESULTS	4-1
	4.1 GENERAL	4-1
	4.2 SURFACE SETTLEMENTS	4-4
	4.3 LINER FORCES, MOMENTS AND STRESSES	4-20
5	SUMMARY AND CONCLUSIONS.	5-1
	REFERENCES	R-1



LIST OF FIGURES

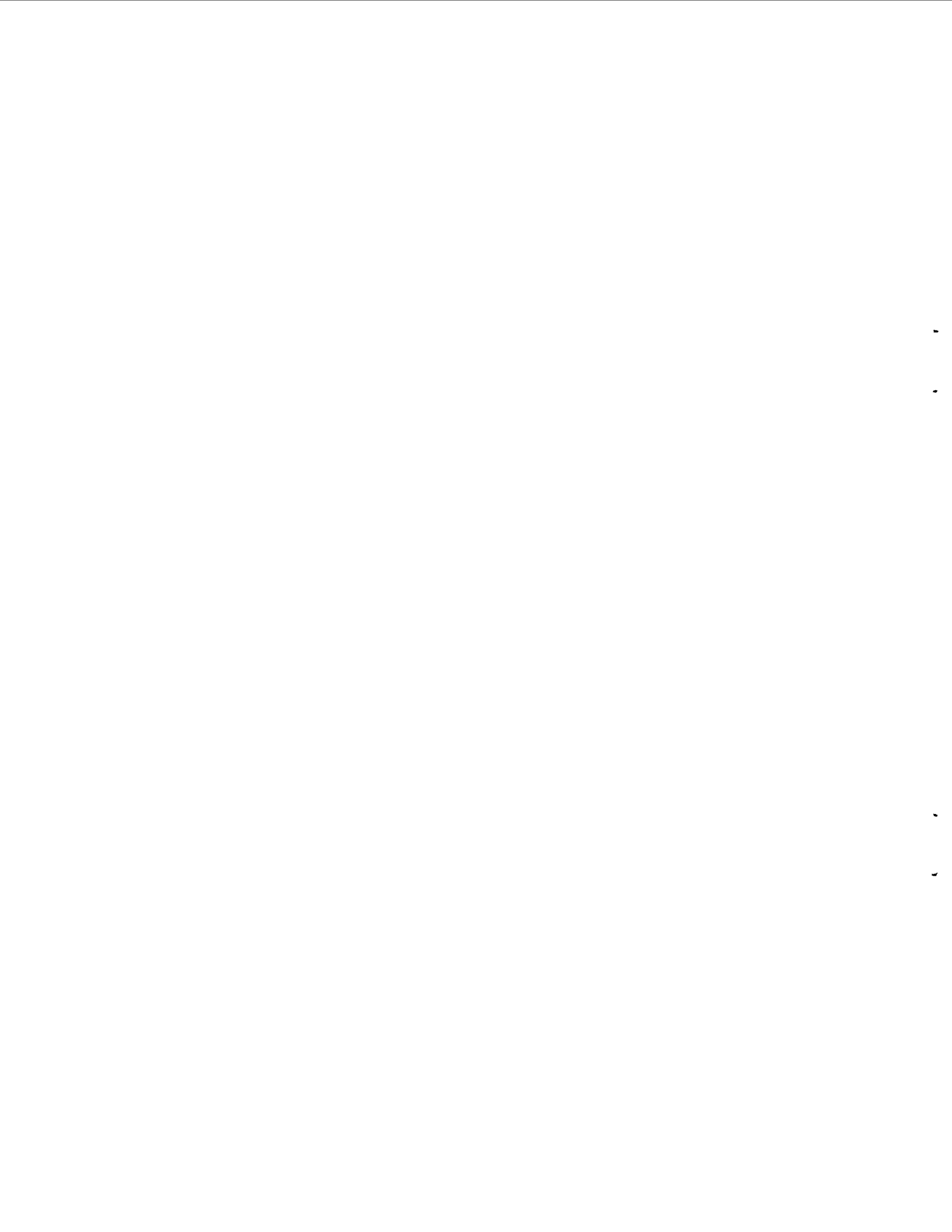
Figures		Page
1.1	RELATIVE POSITION OF TWO TUNNEL FACES	1-6
2.1	GEOMETRICAL CONFIGURATION OF THE PROBLEM AND DIMENSIONAL SYMBOLS	2-2
2.2	TYPICAL FINITE ELEMENT MESH FOR A SYMMETRICAL CASE	2-4
2.3	TYPICAL FINITE ELEMENT MESH FOR AN UNSYMMETRICAL CASE	2-5
3.1	STRESS DISTRIBUTIONS AROUND SINGLE UNLINED TUNNEL (ST4, H/D = 5.5)	3-6
3.2	STRESS DISTRIBUTIONS AROUND TWO PARALLEL UNLINED TUNNELS (TB4, H/D = 5.5, W/D = 1.0)	3-8
3.3	STRESS DISTRIBUTIONS AROUND TWO PARALLEL UNLINED TUNNELS (TB8, H/D = 5.5, W/D = 0.5)	3-9
3.4	STRESS DISTRIBUTIONS AROUND TWO PARALLEL UNLINED TUNNELS (TB12, H/D = 5.5, W/D = 0.25)	3-10
3.5	STRESS DISTRIBUTIONS AROUND TWO PARALLEL LINED TUNNELS (TB11, H/D = 5.5, W/D = 0.25)	3-12
3.6	UNLINED TUNNEL DISPLACEMENTS FOR THE SYMMETRICAL CASE (H/D = 1.5).	3-14
3.7	UNLINED TUNNEL DISPLACEMENTS FOR THE SYMMETRICAL CASE (H/D = 5.5).	3-15
3.8	LINED TUNNEL DISPLACEMENTS FOR THE SYMMETRICAL CASE (H/D = 1.5)	3-16
3.9	LINED TUNNEL DISPLACEMENTS FOR THE SYMMETRICAL CASE (H/D = 5.5).	3-17

	Page
3.10 SURFACE DISPLACEMENT FOR UNLINED TUNNELS (H/D = 1.5)	3-20
3.11 SURFACE DISPLACEMENTS FOR UNLINED TUNNELS (H/D = 5.5)	3-21
3.12 SURFACE DISPLACEMENTS FOR LINED TUNNELS (H/D = 1.5)	3-23
3.13 SURFACE DISPLACEMENTS FOR LINED TUNNELS (H/D = 5.5)	3-24
3.14 DISTRIBUTIONS OF LINER THRUST FOR THE SHALLOW TUNNELS	3-25
3.15 DISTRIBUTIONS OF LINER MOMENTS FOR THE SHALLOW TUNNELS	3-26
3.16 DISTRIBUTIONS OF LINER SHEAR FOR THE SHALLOW TUNNELS	3-27
3.17 DISTRIBUTIONS OF LINER THRUST FOR THE DEEP TUNNELS	3-28
3.18 DISTRIBUTIONS OF LINER MOMENTS FOR THE DEEP TUNNELS	3-29
3.19 DISTRIBUTIONS OF LINER SHEAR FOR THE DEEP TUNNELS	3-30
3.20 STRESS DISTRIBUTIONS FROM UNSYM- METRICAL ANALYSIS TB32 (H/D = 5.5, W/D = 0.5)	3-34
3.21 STRESS DISTRIBUTIONS FROM UNSYM- METRICAL ANALYSIS TB33 (H/D = 5.5, W/D = 0.5)	3-35
3.22 STRESS DISTRIBUTIONS FROM UNSYM- METRICAL ANALYSIS TB15 (H/D = 1.5, W/D = 0.5)	3-36
3.23 TUNNEL DISPLACEMENTS FOR TB13 (H/D = 1.5).	3-39
3.24 TUNNEL DISPLACEMENTS FOR TB14 (H/D = 1.5).	3-40

	Page
3.25 TUNNEL DISPLACEMENTS FOR TB15 (H/D = 1.5).	3-42
3.26 TUNNEL DISPLACEMENTS FOR TB16 (H/D = 1.5).	3-43
3.27 TUNNEL DISPLACEMENTS FOR TB17 (H/D = 1.5).	3-45
3.28 TUNNEL DISPLACEMENTS FOR TB30 (H/D = 5.5).	3-46
3.29 TUNNEL DISPLACEMENTS FOR TB31 (H/D = 5.5).	3-47
3.30 TUNNEL DISPLACEMENTS FOR TB32 (H/D = 5.5).	3-48
3.31 TUNNEL DISPLACEMENTS FOR TB33 (H/D = 5.5).	3-49
3.32 TUNNEL DISPLACEMENTS FOR TB34 (H/D = 5.5).	3-50
3.33 SURFACE DISPLACEMENTS FOR THE SHALLOW TUNNELS (H/D = 1.5) - UNSYMMETRICAL CASE	3-52
3.34 SURFACE DISPLACEMENTS FOR THE DEEP TUNNELS (H/D = 5.5) - UNSYMMETRICAL CASE	3-54
3.35 PLASTIC ZONES	3-62
3.36 LINEAR-ELASTIC AND ELASTO-PLASTIC TUNNEL DISPLACEMENTS FOR SINGLE TUNNEL (ST4, ST4EP) AND SYMMET- RICAL CASE (TB8, TB8EP).	3-63
3.37 LINEAR-ELASTIC AND ELASTO-PLASTIC TUNNEL DISPLACEMENTS FOR THE UNSYMMETRICAL CASE	3-64
3.38 VARIATION OF VERTICAL GROUND DIS- PLACEMENTS WITH DEPTH - SINGLE TUNNEL AND SYMMETRICAL CASE LINEAR-ELASTIC AND ELASTO-PLASTIC ANALYSES.	3-66

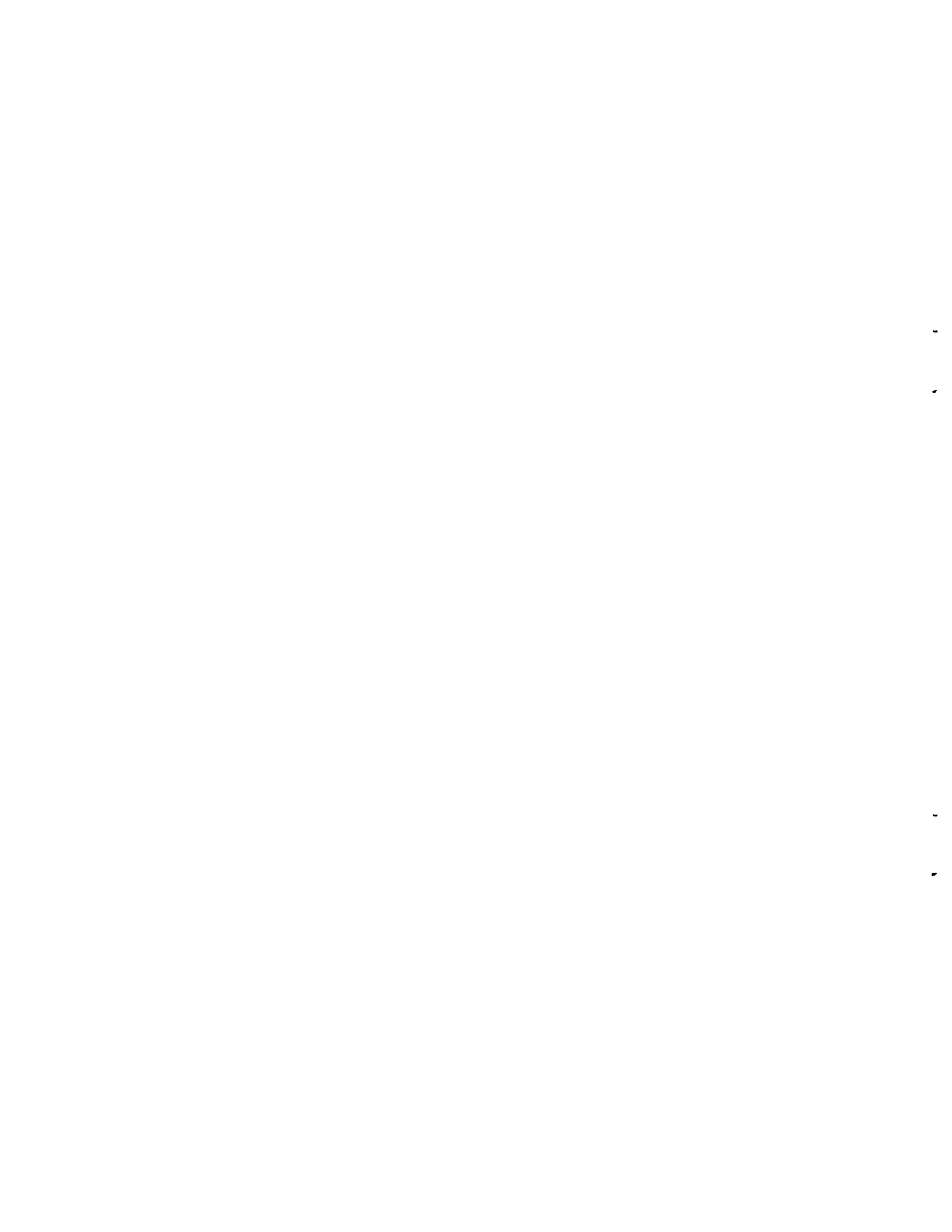
	Page
3.39 VARIATION OF VERTICAL GROUND DIS- PLACEMENTS WITH DEPTH - UNSYMMET- RICAL CASE LINEAR-ELASTIC AND ELASTO-PLASTIC ANALYSES.	3-67
3.40 DISTRIBUTION OF LINER THRUST CHANGES (TUNNEL I) DUE TO PASSAGE OF TUNNEL II (TB32, TB32EP)	3-69
3.41 DISTRIBUTION OF CHANGES IN BENDING MOMENTS IN LINER OF TUNNEL I DUE TO PASSAGE OF TUNNEL II (TB32, TB32EP).	3-70
4.1 SHAPE OF SETTLEMENT TROUGH AS CALCULATED FROM GAUSSIAN ERROR FUNCTION.	4-5
4.2 RELATIONSHIP BETWEEN β AND WIDTH OF SETTLEMENT TROUGH (MODIFIED AFTER CORDING AND HANSMIRE [10]).	4-6
4.3 COMPARISON OF SURFACE SETTLEMENTS FROM SINGLE TUNNEL FINITE ELEMENT ANALYSES AND NORMAL PROBABILITY CURVE	4-8
4.4 SCHEMATIC REPRESENTATION OF ADDITIONAL SURFACE SETTLEMENT ARISING FROM TWO- TUNNEL INTERACTION (SYMMETRICAL CASE)	4-10
4.5 SETTLEMENT TROUGHS FROM SYMMETRICAL TWO TUNNEL ANALYSES AND FROM SUPER- IMPOSING TWO SINGLE TUNNEL TROUGHS - H/D = 1.5	4-11
4.6 SETTLEMENT TROUGHS FROM SYMMETRICAL TWO TUNNEL ANALYSES AND FROM SUPER- IMPOSING TWO SINGLE TUNNEL TROUGHS - H/D = 5.5	4-13
4.7 SETTLEMENT TROUGHS FROM UNSYMMETRICAL TWO TUNNEL ANALYSES AND FROM SUPER- IMPOSING TWO SINGLE TUNNEL TROUGHS	4-14

	Page
4.8 DISTRIBUTION OF INTERACTION SETTLEMENTS OBTAINED FROM FINITE ELEMENT ANALYSES OF TWO UNLINED TUNNELS (UNSYMMETRICAL CASE).	4-16
4.9 INTERACTION SETTLEMENT VOLUME AT GROUND SURFACE VERSUS PILLAR WIDTH	4-18



LIST OF TABLES

Table		Page
3.1	SUMMARY OF SINGLE TUNNEL ANALYSES	3-3
3.2	SUMMARY OF SYMMETRICAL ANALYSES	3-4
3.3	SUMMARY OF UNSYMMETRICAL ANALYSES	3-5
3.4	MAXIMUM LINER FORCE AND MOMENT COEFFICIENTS FOR THE SYMMETRICAL CASE	3-31
3.5	THRUST COEFFICIENTS ($T/\gamma H a$) FROM THE LINED TUNNEL ANALYSES - UNSYMMET- RICAL CASE	3-55
3.6	MOMENT COEFFICIENTS ($M/\gamma H a^2$) FROM THE LINED TUNNEL ANALYSES - UNSYMMETRICAL CASE	3-56
3.7	SHEAR COEFFICIENTS ($V/\gamma H a$) FROM THE LINED TUNNEL ANALYSES - UNSYM- METRICAL CASE	3-57
4.1	MAXIMUM AND MINIMUM STRESSES AT SELECTED LOCATIONS AROUND LINER FOR ANALYSES TB32 AND TB32EP	4-23



CHAPTER 1

INTRODUCTION

1.1 OBJECTIVES

Presented in this report are the results of a finite element study on behavior and interaction of two circular and parallel tunnels. The objectives of this research are:

1. The study of the interaction of two parallel tunnels and the effect of such interaction on stresses and displacements around the tunnels and on support loads.
2. The parametric study of two tunnel systems to determine the effect of various parameters such as distance between the centers of the tunnels, depth, and construction sequence.

The results of this study are expected to enhance the understanding of the behavior of two tunnel systems and provide information to aid design and construction of two parallel tunnels.

1.2 GENERAL

The construction of a tunnel modifies the state of displacements and stresses in a zone around the tunnel. The size of this zone depends on: ground conditions--type of soil or rock, in situ stresses and properties of the medium; geometric parameters--depth and radius of the tunnel; and characteristics of the support system. If two tunnels are constructed far apart such that the zones of influence do not overlap, then the individual tunnels

can be considered separately and analyzed as such. However, if the zones of influence of the two tunnels overlap, the behavior of each of the tunnels will be different from that of a single tunnel as some degree of interaction between the two tunnels will take place. Interaction of tunnels will affect the state of displacement and stresses around the tunnels, ground surface displacements, and support loads. It can generally be expected that the surface settlements resulting from the construction of two tunnels will be greater than the sum of the settlements resulting from each tunnel alone. The stress distribution around two tunnels and support loads are too complex to lend themselves to a general statement and they require a comprehensive study.

There are two distinct problems related to the design and construction of two tunnels in soft ground: 1) Additional loads and distortions are imposed on the lining of the first tunnel due to passage of the second tunnel, and 2) the ground settlements due to excavation of the second tunnel may be appreciably greater than those that occurred during excavation of the first tunnel, and may result in damage to structures and utilities at the ground surface.

In the design and construction of two tunnels, designers must determine whether or not the distortions and load increases on the lining of the first tunnel due to passage of the second tunnel will be great enough to cause unacceptable damage to the lining. In many cases, the installation of the permanent lining for the first tunnel is delayed until after the second tunnel has passed. The finite element analyses in this report provide a means of evaluating the influence of the excavation of the second tunnel on the loads and distortions of the first.

Ground settlements due to excavation of a second tunnel are usually greater than the settlements due to excavation of the first tunnel for two reasons: 1) the first tunnel may disturb the soil around and above the second tunnel so that the soil will be weaker and have a greater tendency to displace into the second tunnel as it is mined, or the soil will have increased in volume during passage of the first tunnel and will undergo volume decreases during passage of the second tunnel, and 2) the pillar between the two tunnels will be more highly stressed and less confined than the abutments adjacent to single tunnels. It therefore will undergo greater settlement than the abutments of single tunnels.

Linear-elastic finite element analyses do not model the disturbance of the soil and volume changes in the soil as they occur around tunnels in real soils. However, the results from this type of analysis can be used to investigate the compression of the pillar and abutments around two tunnels and its influence on ground movement. Linear analyses will therefore be of use in evaluating field measurements and determining if the additional ground movements due to two tunnel excavation are related to pillar compression or to other causes.

An important factor which will affect the distribution of stresses and displacements around the two tunnels is the sequence of excavation and liner installation in each tunnel. Regarding the sequence of construction, the following situations are considered:

1. Two tunnels constructed simultaneously - In this case, the conditions encountered by each tunnel will be similar barring some possible cross variation of the ground or surface conditions. Ideally this case will be symmetric about a vertical

plane passing through the mid-distance between the two tunnels. The tunnels will be advancing through stressed media with the stress and displacement conditions ahead of the tunnels altered by the approach of both the tunnels.

2. A second tunnel is constructed adjacent to an existing tunnel - In this case, the second tunnel is constructed within a medium which has higher stresses than encountered at the same location if the first tunnel was not present. Also the material properties of the medium have been modified by the first tunnel. The construction of the second tunnel will change the support load on the first tunnel. The construction of an adjacent tunnel requires special design consideration for both tunnels regarding support requirements.

In the case of two tunnels being driven simultaneously, the faces of the two tunnels need not necessarily be at the same longitudinal position; the face of one tunnel can be ahead of the face of the second tunnel by a certain distance. This may well be the rule rather than the exception, as two tunnels cannot be expected to advance at the same rate.

The results of a previous study [1] have indicated that a transition zone of three-dimensional stress exists immediately ahead and behind the face of an advancing tunnel. The size of this zone depends on the type of medium and the support condition. The zone of significant stress and displacement changes can be considered to be approximately two tunnel diameters ahead of,

and also behind, the face when the ground remains elastic. Based on this information, the following cases can be considered regarding the distance between the faces of two tunnels. If the distance along the tunnel line between the faces of two tunnels is less than four tunnel diameters, the zones of influence around the tunnel faces overlap and interaction is taking place at the tunnel face, Fig. 1.1a. The state of stress near the tunnel face is clearly three-dimensional and any two-dimensional analysis of this case will suffer from drastic approximations. When the distance between the faces of two tunnels is about one tunnel diameter or less, the stress condition around the tunnels can be reasonably considered to be symmetric, as in case (1) discussed above, and a two-dimensional analysis may be a good approximation.

For the case of the distance between the tunnel faces being greater than four tunnel diameters, the zones of influence around tunnel faces are separated, Fig. 1.1b. This case is similar to case (2) discussed above. The first tunnel encounters stress conditions, and produces distributions of stresses and displacements in its zone of influence, similar to that of a single tunnel. The second tunnel encounters a stress field which has been modified by passing of the first tunnel and it is subjected to support loads which are basically different than those of the first tunnel. The passing of the second tunnel itself also alters the stress condition and modifies the support load in the first tunnel. The tendency is for increase in the support loads due to passing of an adjacent tunnel.

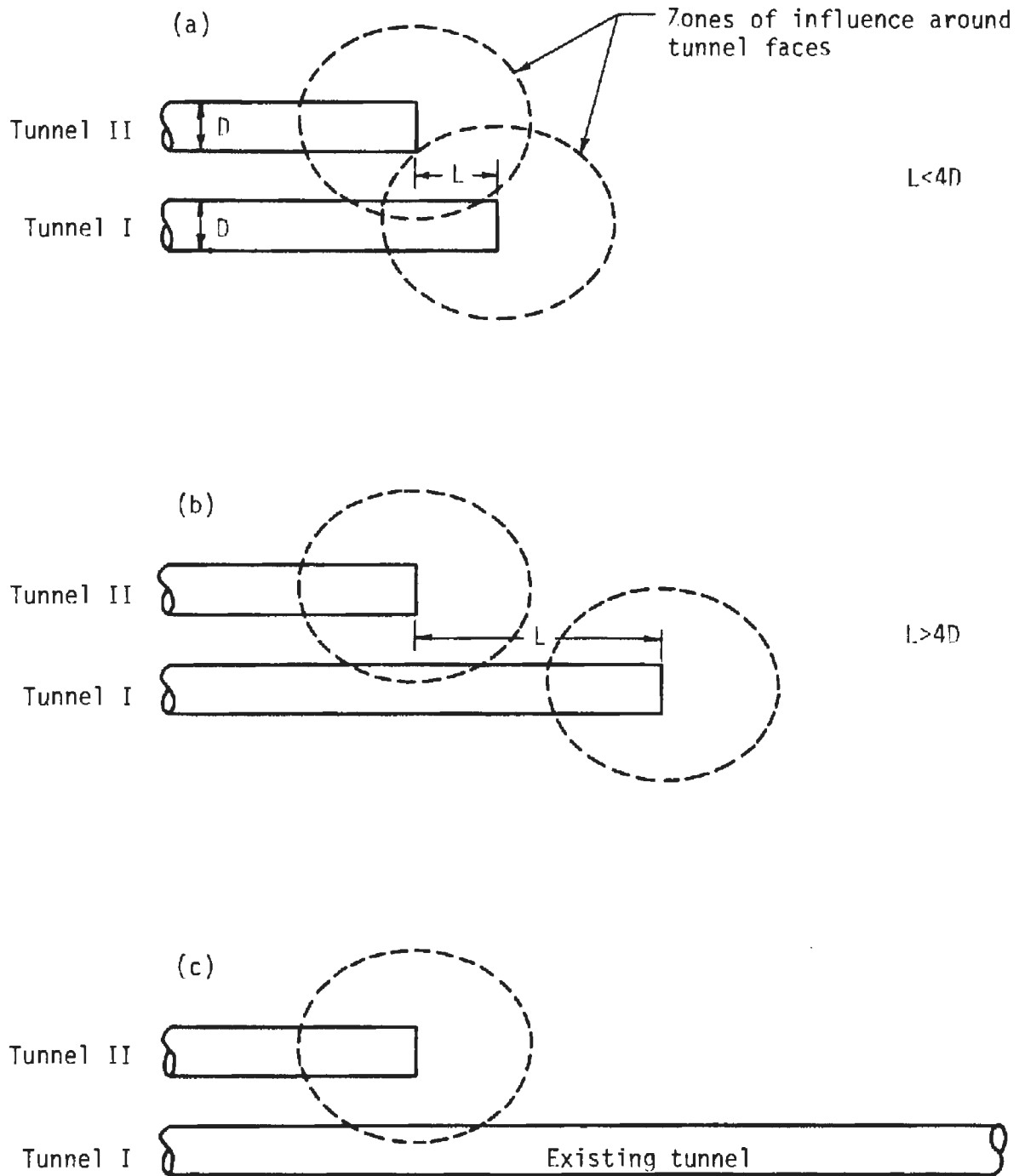


FIGURE 1.1 RELATIVE POSITION OF TWO TUNNEL FACES

1.3 PREVIOUS STUDIES

Fotieva and Sheinin [2] have studied the case of a tunnel driven adjacent to an existing and lined tunnel. They have developed a closed form linear elastic solution for this problem. Using their method they have analyzed an example problem of a lined tunnel of 19.7 ft (6 m) diameter at a depth of 118 ft (36 m). The medium has a modulus of $E \approx 700,000$ psi (4825 MPa) and Poisson's ratio of $\nu = 0.4$. The liner of 7.9 in. (20 cm) thick has a modulus of $E = 4,300,000$ psi (30×10^3 MPa) and Poisson's ratio of $\nu = 0.2$. A second tunnel of the same diameter is driven adjacent to this existing tunnel at a central distance of 26 ft (8 m) which gives a pillar width to tunnel diameter ratio of $W/D = 0.33$. The driving of the second tunnel causes additional stresses in the liner of the existing tunnel with a maximum thrust coefficient of $T/\gamma H a = 0.24$ and a maximum moment coefficient of $M/\gamma H a^2 = 0.0053$. These are significant additional liner forces which need to be taken into account.

Barla and Ottoviani [3] have used finite element method to study the case of two parallel unlined tunnels excavated simultaneously. They have used linear elastic and nonlinear variable moduli material properties in their analyses. They have reported results of a parametric study which cover a range of geometric parameters of: depth to diameter ratios of 0.75 to 3; pillar width to diameter ratios of 0.25 to 1.0; and two tunnel diameter values of 19.7 and 39.4 ft (6 and 12 m). Their results seem to indicate that the interaction between two tunnels becomes negligible for values of pillar width ratio of $W/D = 1.0$ or greater. They report large stresses in the zone between

the two tunnels for small values of pillar width ratios, $W/D \leq 0.5$. Zones of tensile stresses develop around the tunnels at shallow depths, $H/D \leq 1.0$.

Peck, et al., [4] have discussed the problem of two parallel or intersecting tunnels of different diameters at adjacent or stacked relative positions. They have given some general guidelines for liner design of the two tunnel systems.

Several researchers have reported the results of measurements made during and following construction of two or more parallel tunnels. Deere, et al., [5] gave an excellent summary of the available data prior to 1969. Most cases correspond to those illustrated by parts b or c of Fig. 1.1. In other words, measurements were made as a second tunnel was driven past a test section set up in an existing tunnel or one whose heading was a considerable distance ahead of the test section.

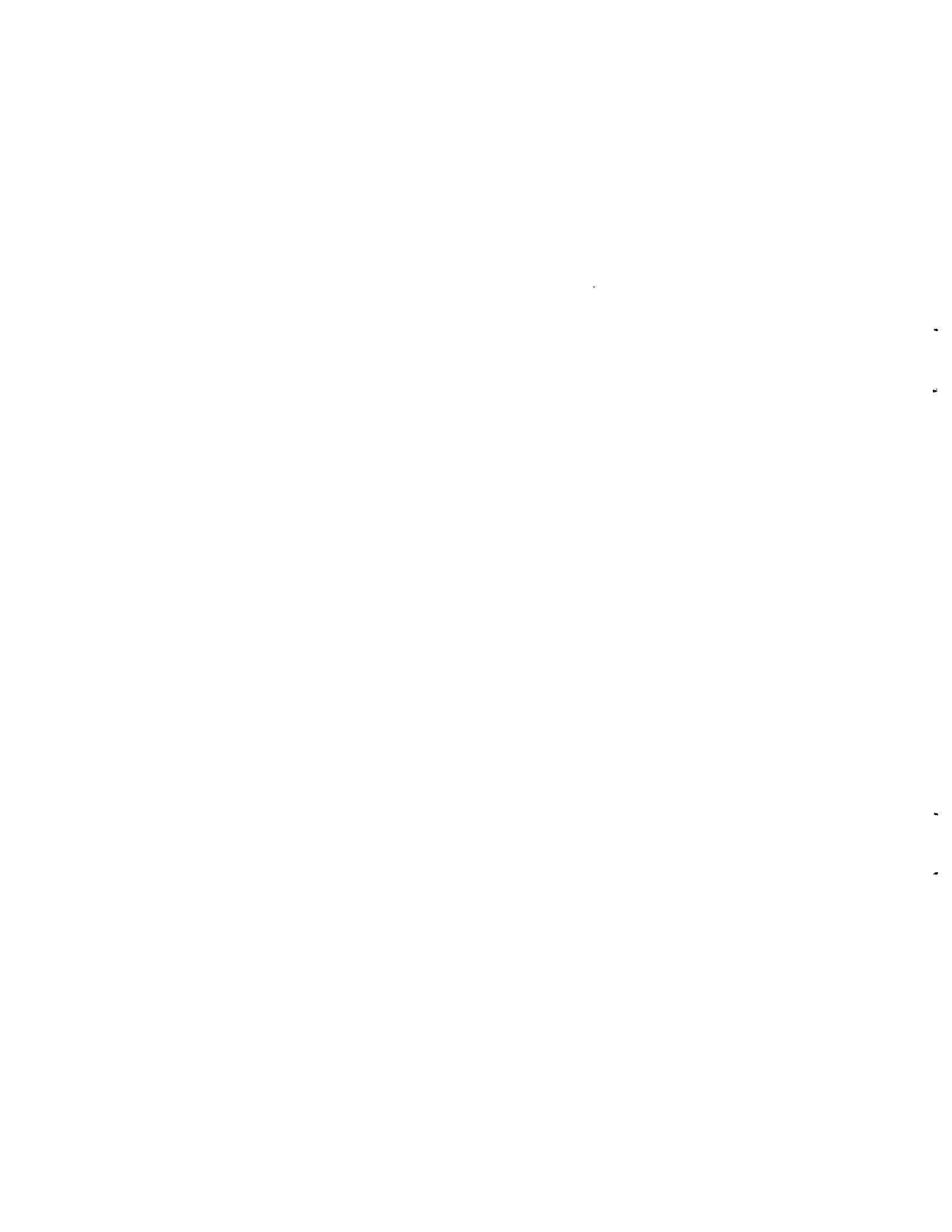
Ward and Thomas [6] reported on two parallel tunnels constructed in London clay. These particular tunnels were lined with precast concrete segments which had a thickness of 9 in. (23 cm). The tunnels were approximately 13 ft (4 m) in diameter and were separated by a pillar of 8 ft (2.4 m) minimum thickness ($W/D \approx 0.6$). Passage of the second tunnel caused an additional maximum distortion of the first tunnel of $\Delta a/a = 0.12$ percent. In addition, the average radial pressure acting on the first tunnel was increased by 8.33 psi (57 kPa). After 40 months the total maximum distortion of the first tunnel was 0.32 percent and the total average radial pressure was estimated to be approximately 48 psi (331 kPa).

Terzaghi [7] reported measurements taken on tunnels constructed in Chicago clay. These tunnels had a horseshoe shaped cross section and were lined

with steel ribs and liner plates. The tunnels were 20 ft (6.1 m) in diameter and were constructed at a distance of 28.5 ft (8.7 m) center-to-center, giving a pillar width of 8.5 ft (2.6 m) ($W/D = 0.425$). As the second tunnel was mined past, the springline nearest the second tunnel displaced outward 0.2 in. (5 mm) while the opposite springline moved outward only 0.04 in. (1 mm). This yielded a distortion of the first tunnel of $\Delta a/a = 0.10$ percent.

Contact pressures between the soil and the concrete invert of tunnel 1 were measured using Carlson cell slabs. As tunnel 2 passed on the north side, the contact pressure under the north rib increased and thereafter remained greater than those under the south rib which was farthest from tunnel 2.

Settlements of the street surface were also recorded as the two tunnels were advanced. Different settlement profiles were obtained for different spacings between the two tunnels. When the tunnels were constructed so that there was no pillar between them ($W/D = 0$), settlements due to the first tunnel were consistently greater than those due to the second tunnel. Ground displacements around tunnel 2 were restricted by the presence of the tunnel 1 liner. When the tunnels were mined leaving a pillar between them ($W/D = 0.425$) support provided by the tunnel 1 liner was not available. Instead the clay above tunnel 2 had to be supported by the relatively weak clay pillar. As a result, settlements due to the second tunnel were everywhere greater than those due to the first tunnel.



CHAPTER 2

METHOD OF ANALYSIS

2.1 GENERAL

A previous study of advancing tunnels, [1], has shown that the long term distribution of stresses and displacements around the tunnel as well as the liner forces at points far behind the face are strongly influenced by events and construction details at the advancing face of the tunnel. Clearly, the stress condition around the face of a tunnel is three-dimensional, and only a three-dimensional analysis can give an accurate picture of tunnel behavior. However, three-dimensional analyses are very costly and difficult to perform, especially in the nonlinear range of material behavior. Useful information can be obtained from two-dimensional analyses and the knowledge of the effects at the tunnel face may be used to develop approximate scaling factors. Therefore, this investigation is restricted to two-dimensional analyses. A schematic representation of the problem along with the symbols for various dimensions used in this study are given in Fig. 2.1.

2.2 FINITE ELEMENT MESH

A finite element mesh was developed for a region of the soil containing the two tunnels. Two-dimensional plane-strain quadrilateral finite elements with four corner nodes were used in the analyses. The liners were modeled by beam elements. Typical plots of automatically generated finite element meshes for half of the region (symmetric case of simultaneous

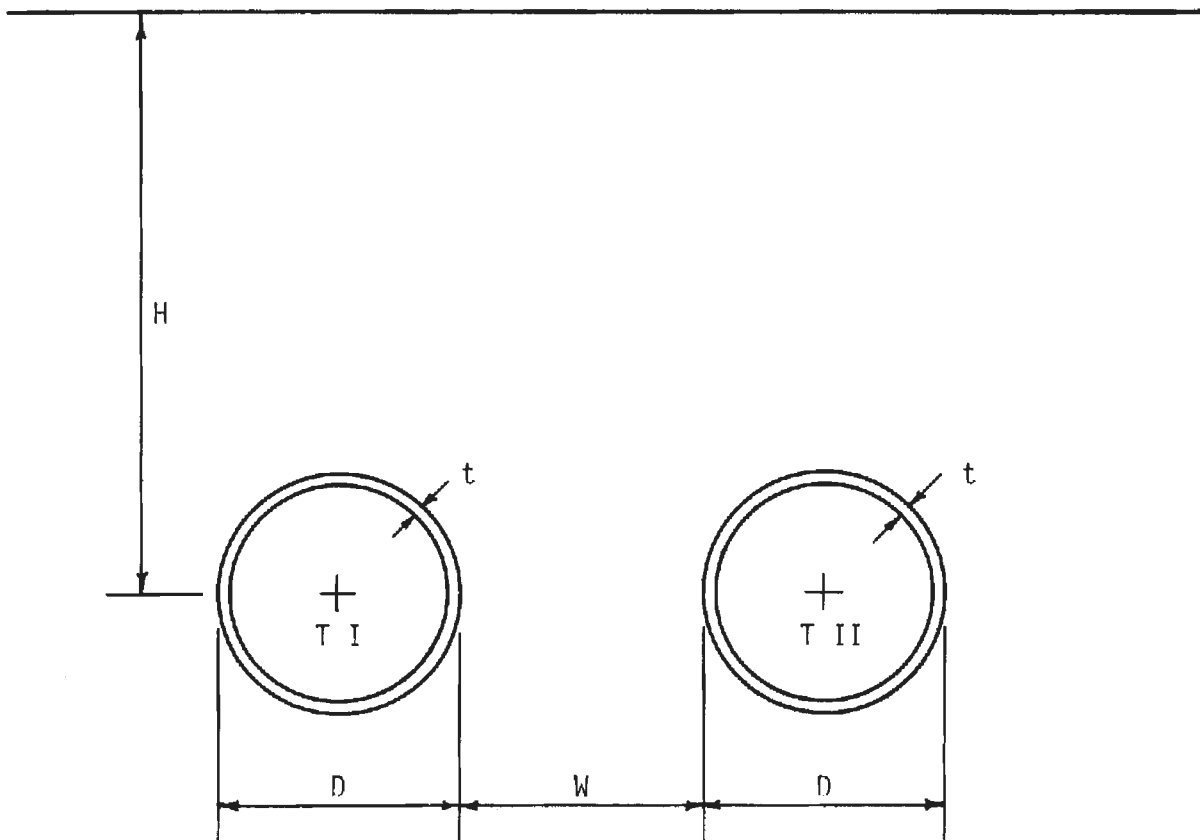


FIGURE 2.1 GEOMETRICAL CONFIGURATION OF THE PROBLEM AND DIMENSIONAL SYMBOLS

excavation of two tunnels) and the whole region (unsymmetric case) are shown in Figs. 2.2 and 2.3, respectively.

Initially the finite element model is subjected to the self weight of the medium to simulate the in situ stress condition. At this stage the base of the finite element model has a displacement boundary condition allowing horizontal movement but restricting vertical displacement, and the sides have a force boundary condition, consisting of a triangular force distribution corresponding to the lateral stresses resulting from the weight of the medium. By varying the rate of increase of this boundary lateral force with depth different K_0 conditions can be simulated.

The excavation of the tunnel is achieved at the subsequent step of the analysis by not incorporating in this step the soil elements located within the perimeter of the tunnel. At the excavation step the base and sides of the finite element mesh are fixed and no further movements are allowed, except along the plane of symmetry which is allowed vertical movements when half the region is analyzed. If a lined tunnel is being analyzed, the liner elements are activated at this or the following step.

2.3 CONSTRUCTION SEQUENCE

Basically two types of sequence of excavation and liner placement are considered. For the case of simultaneous excavation of two tunnels only half the mesh is used in the analysis and only two cases are analyzed: both tunnels are unlined; or both tunnels are lined and the liners are placed instantaneously upon excavation. In the case of two tunnels being excavated at different stages, the whole region containing the two tunnels is used in

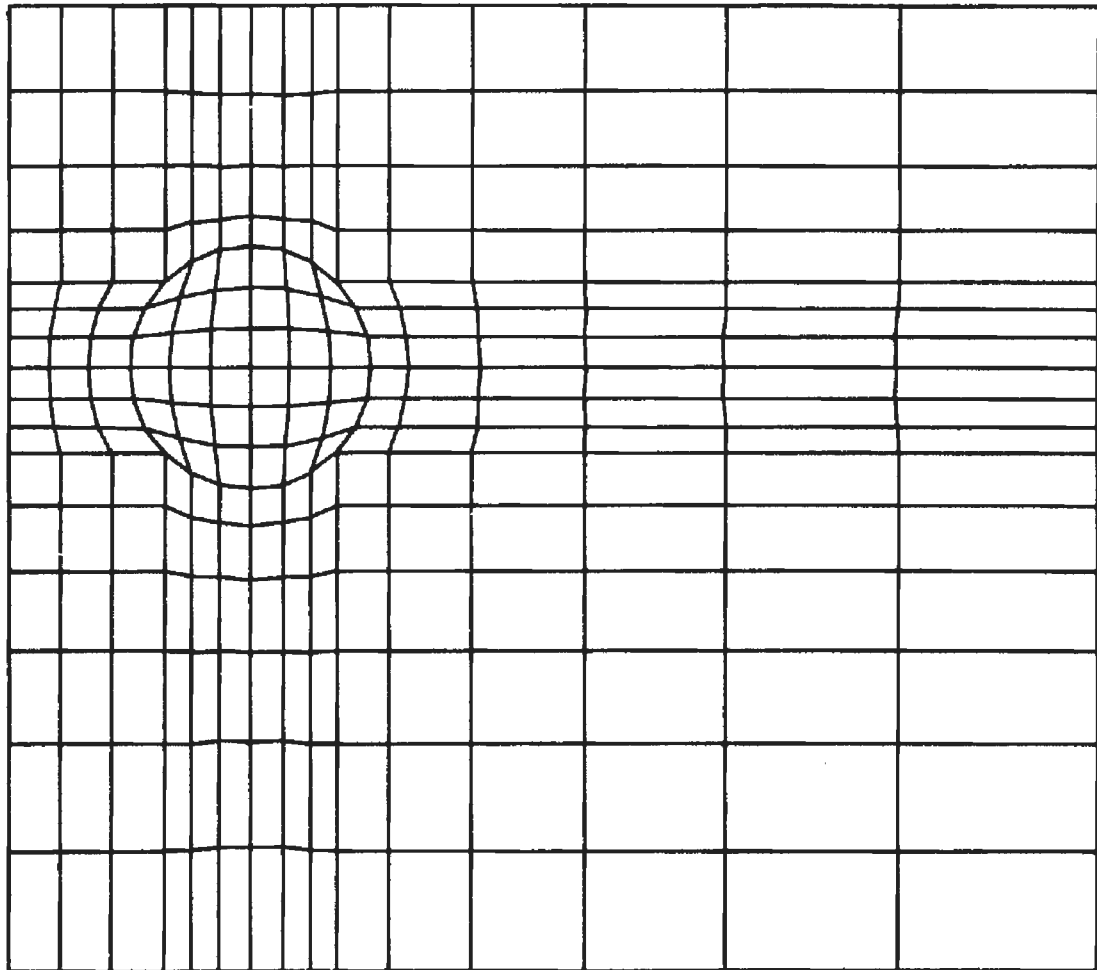


FIGURE 2.2 TYPICAL FINITE ELEMENT MESH
FOR A SYMMETRICAL CASE

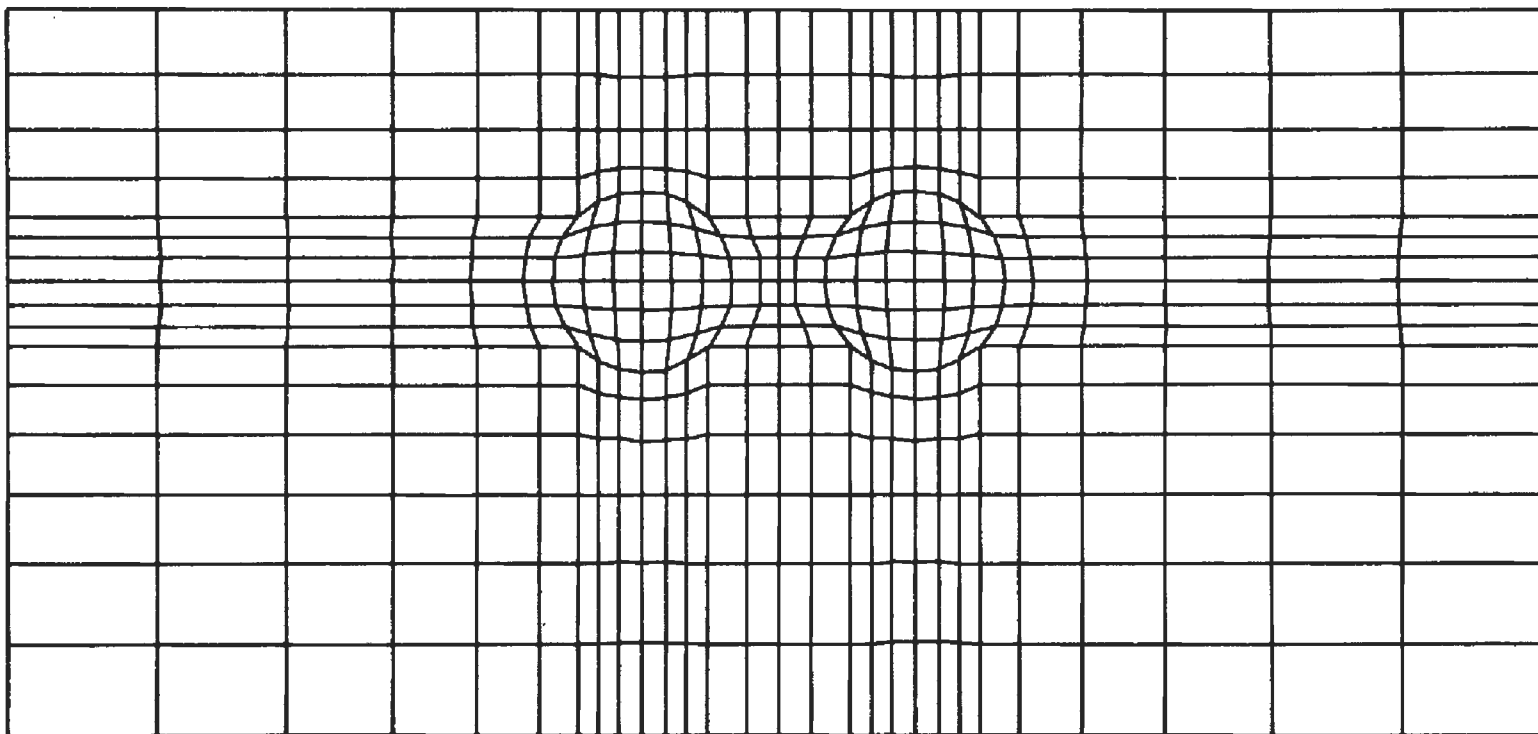


FIGURE 2.3 TYPICAL FINITE ELEMENT MESH FOR AN UNSYMMETRICAL CASE

the analysis and the number of possible combinations, considering the excavation and liner placement of the two tunnels, is greater. The following sequences of excavation and liner placement have been considered in this study.

- a. Step 1. excavate tunnel I
Step 2. excavate tunnel II
- b. Step 1. excavate and line tunnel I
Step 2. excavate and line tunnel II
- c. Step 1. excavate and line tunnel I
Step 2. excavate tunnel II
- d. Step 1. excavate tunnel I
Step 2. line tunnel I and excavate and line tunnel II
- e. Step 1. excavate tunnel I
Step 2. line tunnel I and excavate tunnel II

The liners modeled in these studies are so proportioned that they, in effect, simulate a form of final, permanent support. Installation of such a liner right at the tunnel heading is simulated by installing the liner on the same step in which excavation occurs.

There are two possible interpretations of the support conditions simulated by those analyses in which a tunnel is left unlined. For all except tunnel I in the unsymmetrical analyses of types d and e, the tunnel(s) can be considered to be either left entirely unlined or lined far behind the face. This second interpretation applies because instantaneous (elastic) medium displacements occur entirely within a zone extending one to two tunnel diameters ahead of and behind the face of an unlined tunnel. Thus, a liner installed at

a distance greater than this behind the face of a tunnel through an elastic medium would remain undisturbed (stress free) because there would be no interaction between the medium and the liner. A time-independent analysis of an "unlined" tunnel does not necessarily imply that the tunnel is to be left entirely unlined (which, in many types of ground, would lead to the eventual collapse of the tunnel). It implies only that, with respect to the instantaneous response of the medium to excavation of the opening, the tunnel is effectively unlined.

For unsymmetrical analyses of types d and e it is assumed that tunnel I is lined at a point that is more than one or two diameters behind the face of tunnel I but ahead of the face of tunnel II. Thus, the section of liner at this point remains undisturbed until tunnel II approaches and passes. The resulting deformation of and forces in the tunnel I liner are due solely to the passage of tunnel II.

The subject of construction sequence and the analysis of "unlined" tunnels will be discussed further in Chapter 4.

CHAPTER 3

RESULTS OF ANALYSIS

3.1 GENERAL

The results obtained from a total of 29 different analyses are presented in this chapter. Thirteen of these analyses considered the symmetrical case wherein it was assumed that the two tunnels were advanced together. The unsymmetrical case was considered in eleven analyses. The remaining five analyses were of the single tunnel case and were performed in order to provide data that could be compared to the two tunnel results and thus help illustrate the interaction between two tunnels.

Two tunnel depths were considered: a shallow tunnel with depth of cover equivalent to one tunnel diameter, ($H/D = 1.5$), and a moderately deep tunnel with depth of cover equivalent to five tunnel diameters ($H/D = 5.5$). Three values of pillar width, W , were used in the analysis of the symmetrical case; $W/D = 1.0, 0.5$ and 0.25 . For the unsymmetrical case only one value of pillar width was considered, $W/D = 0.5$.

For the majority of the analyses performed the medium was assumed to be linear-elastic. Young's modulus and Poisson's ratio values selected for the medium were such that, in combination with the corresponding values for the liner and the liner's dimensions, the Compressibility (C) and Flexibility (F) ratios were $C = 0.14$ and $F = 16.6$, respectively.

Where

$$C = \frac{\text{extensional stiffness of medium}}{\text{extensional stiffness of liner}}$$

$$C = \frac{\frac{E_m}{(1 + \nu_m)(1 - 2\nu_m)}}{\frac{E_\ell t}{(1 - \nu_\ell^2)} \cdot \frac{1}{a}}$$

and,

$$F = \frac{\text{flexural stiffness of medium}}{\text{flexural stiffness of liner}}$$

$$F = \frac{\frac{E_m}{(1 + \nu_m)}}{\frac{6 E_\ell I}{(1 - \nu_\ell^2)} \cdot \frac{1}{a^3}}$$

Elasto-plastic behavior was considered in three analyses--one single tunnel case, one symmetrical case, and one unsymmetrical case.

The various analyses are summarized in Tables 3.1, 3.2 and 3.3.

3.2 TWO TUNNELS CONSTRUCTED SIMULTANEOUSLY - THE SYMMETRICAL CASE

3.2.1 MEDIUM STRESSES

It is assumed that the in situ stresses in the undisturbed medium (prior to tunnel excavation) are due to the self weight of the medium. Thus, at any given point in the medium the maximum principal stress is vertical and has a magnitude of $P = \sigma_v = \gamma z$, where γ is the unit weight of the medium and z is the depth of the point below the ground surface. Similarly, the minimum principal stress is horizontal and has a magnitude of $Q = \sigma_H = K_0 \gamma z$, where K_0 is the coefficient of earth pressure at rest. The distribution of in situ principal stresses would thus consist of a set of horizontal contour lines showing a linear increase of magnitude with depth.

Creation of an opening (tunnel) in the medium alters the medium stresses in a region around the opening. Figure 3.1 shows the new distribution

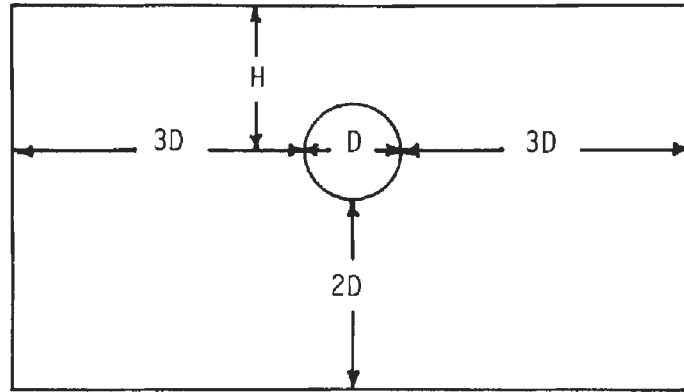


TABLE 3.1
SUMMARY OF SINGLE TUNNEL ANALYSES

Analysis	Lined	H/D
ST1	X	1.5
ST2		1.5
ST3	X	5.5
ST4 ⁺		5.5
ST4EP ⁺⁺		5.5

$$K_0 = 0.5, \quad C = 0.14, \quad F = 16.6$$

$${}^+E_m = 15 \times 10^3 \text{ psi } (103 \times 10^6 \text{ Pa}), \quad \nu_m = 1/3$$

$${}^* \phi = 30^\circ, \quad c = 5 \text{ psi } (34 \times 10^3 \text{ Pa})$$

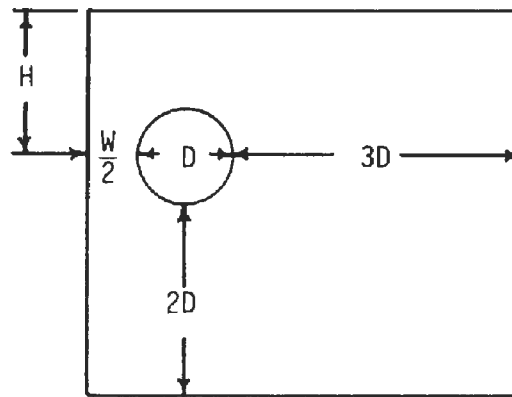


TABLE 3.2 SUMMARY OF SYMMETRICAL ANALYSES

Analysis	Lined	H/D	W/D
TB1	X	1.5	1.0
TB2		1.5	1.0
TB3	X	5.5	1.0
TB4		5.5	1.0
TB5	X	1.5	0.5
TB6		1.5	0.5
TB7	X	5.5	0.5
TB8 ⁺		5.5	0.5
TB8EP* ⁺		5.5	0.5
TB9	X	1.5	0.25
TB10		1.5	0.25
TB11	X	5.5	0.25
TB12		5.5	0.25

$K_o = 0.5, C = 0.14, F = 16.6$

$^+E_m = 15 \times 10^3 \text{ psi } (103 \times 10^6 \text{ Pa}), \nu_m = 1/3$

* $\phi = 30^\circ, c = 5 \text{ psi } (34 \times 10^3 \text{ Pa})$

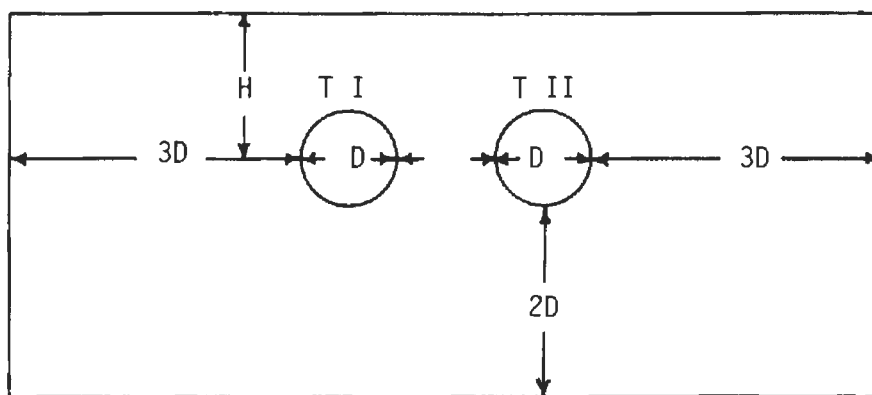


TABLE 3.3 SUMMARY OF UNSYMMETRICAL ANALYSES

Analysis	H/D	Construction sequence
TB13	1.5	Step 1: Excavate T I Step 2: Excavate T II
TB14	1.5	Step 1: Excavate and line T I Step 2: Excavate and line T II
TB15	1.5	Step 1: Excavate and line T I Step 2: Excavate T II
TB16	1.5	Step 1: Excavate T I Step 2: Line T I, excavate and line T II
TB17	1.5	Step 1: Excavate T I Step 2: Line T I, excavate T II
TB30	5.5	same as TB13
TB31	5.5	same as TB14
TB32 ⁺	5.5	same as TB15
TB32EP ^{*+}	5.5	same as TB15
TB33	5.5	same as TB16
TB34	5.5	same as TB17

$$K_D = 0.5, C = 0.14, F = 16.6$$

$${}^+E_m = 15 \times 10^3 \text{ psi } (103 \times 10^6 \text{ Pa}), \nu_m = 1/3$$

$$^* \phi = 30^\circ, c = 5 \text{ psi } (34 \times 10^3 \text{ Pa})$$

$$W/D = 0.5$$

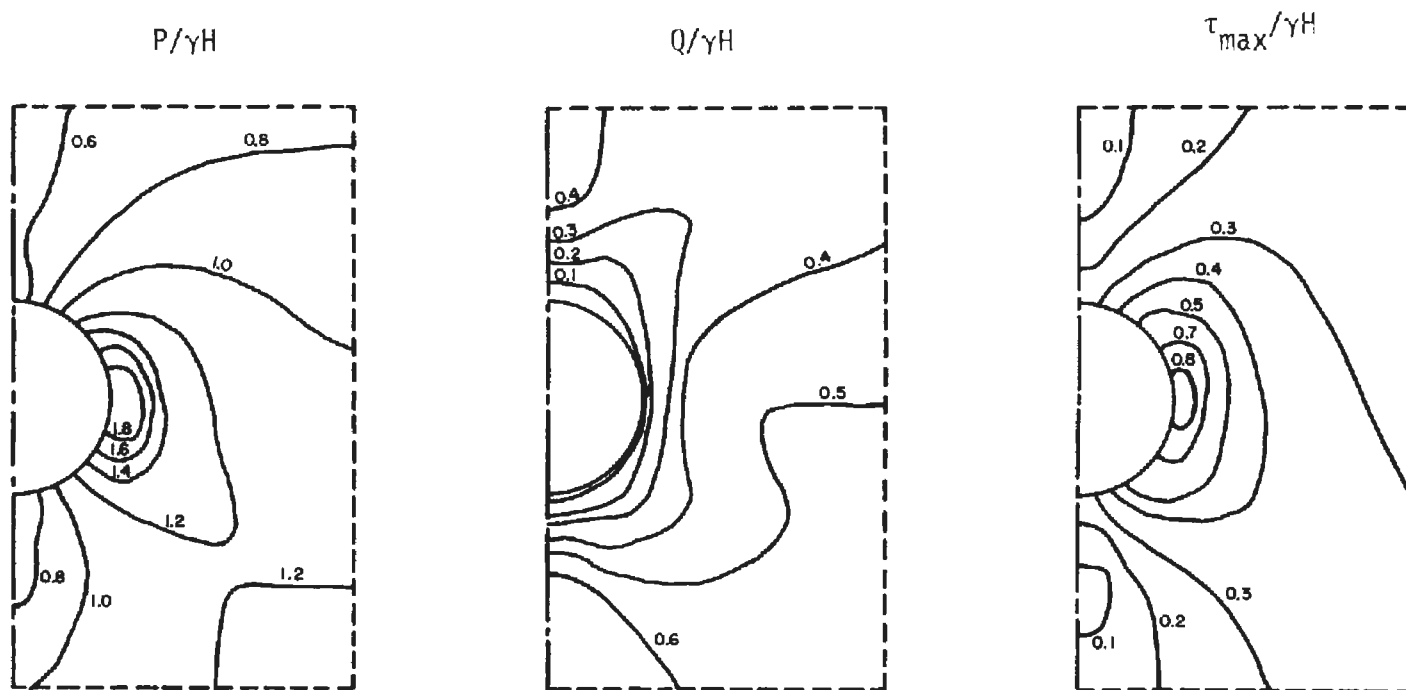


FIGURE 3.1 STRESS DISTRIBUTIONS AROUND SINGLE UNLINED TUNNEL (ST4, H/D = 5.5)

of stresses that occurs around a single unlined tunnel. In this and the following similar figures the distributions of the maximum and minimum principal stresses and the maximum shear stresses in a region around the tunnel are shown by nondimensionalized stress contours (stress at a point divided by γH , where H is depth to tunnel axis). For a single tunnel the stress distributions are symmetrical about a vertical plane through the tunnel axis.

Stress distributions around two parallel unlined tunnels are illustrated in Figs. 3.2, 3.3 and 3.4. Here the stress distributions are symmetrical about a vertical plane through the pillar centerline. Stresses around the right tunnel only are shown. Outside the region bounded by vertical planes through the two tunnel axes the stress distributions are very similar to those for a single tunnel. For $W/D = 1.0$ the distributions are almost identical, but as the pillar width is reduced the differences become more pronounced.

Figures 3.2 through 3.4 illustrate the dissimilarity between the stresses in the pillar and those beyond the outer tunnel springlines. The maximum principal stresses in the pillar are essentially vertical. At the center of the pillar and at the depth of the tunnel axes the vertical stress exceeds the in situ stress that existed at that point by approximately 50 percent when $W/D = 1.0$. Similarly, the vertical stress at this point exceeds the in situ value by approximately 75 and 150 percent when the pillar width is reduced to $W/D = 0.5$ and $W/D = 0.25$, respectively.

Minimum principal stresses in the pillar are oriented approximately horizontal. Note first that when moving from point to point horizontally outward from the opposite springlines the minimum principal stresses are almost identical for each case. At the center of the pillar, on line with the two

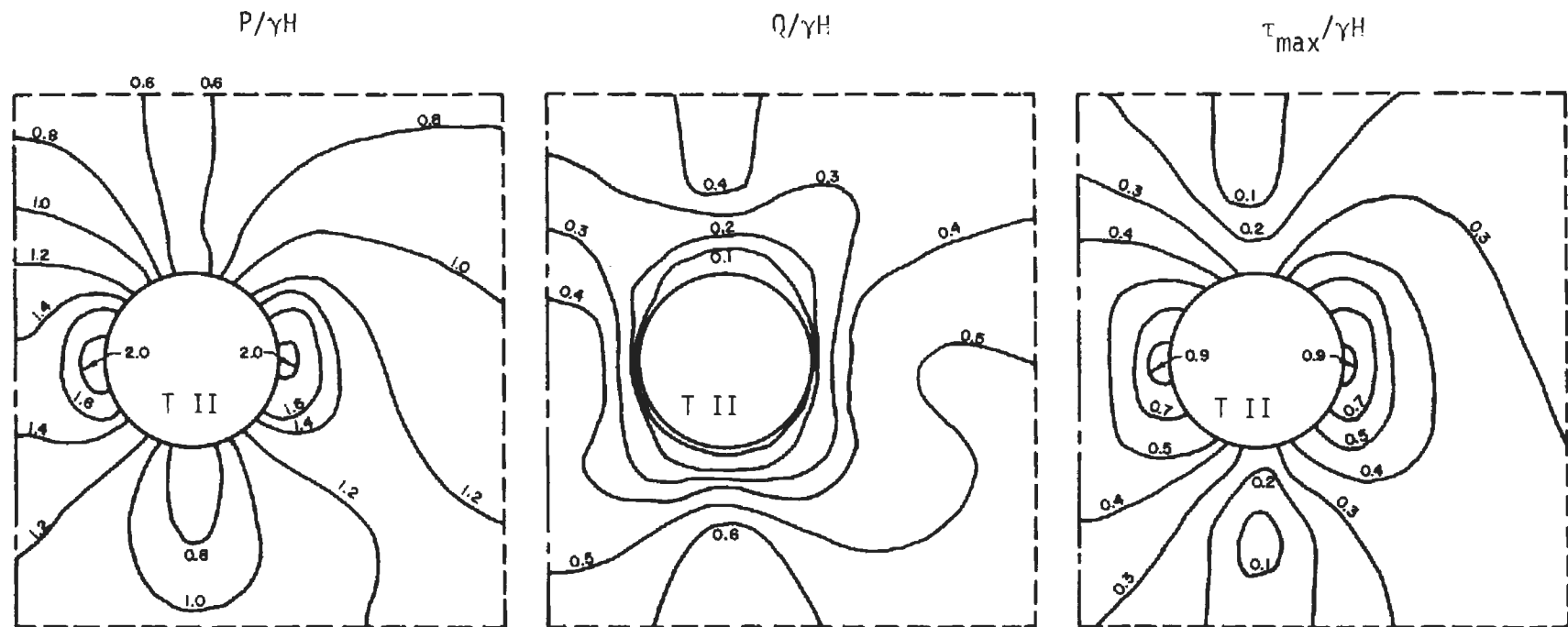


FIGURE 3.2 STRESS DISTRIBUTIONS AROUND TWO PARALLEL UNLINED TUNNELS
(TB4, $H/D = 5.5$, $W/D = 1.0$)

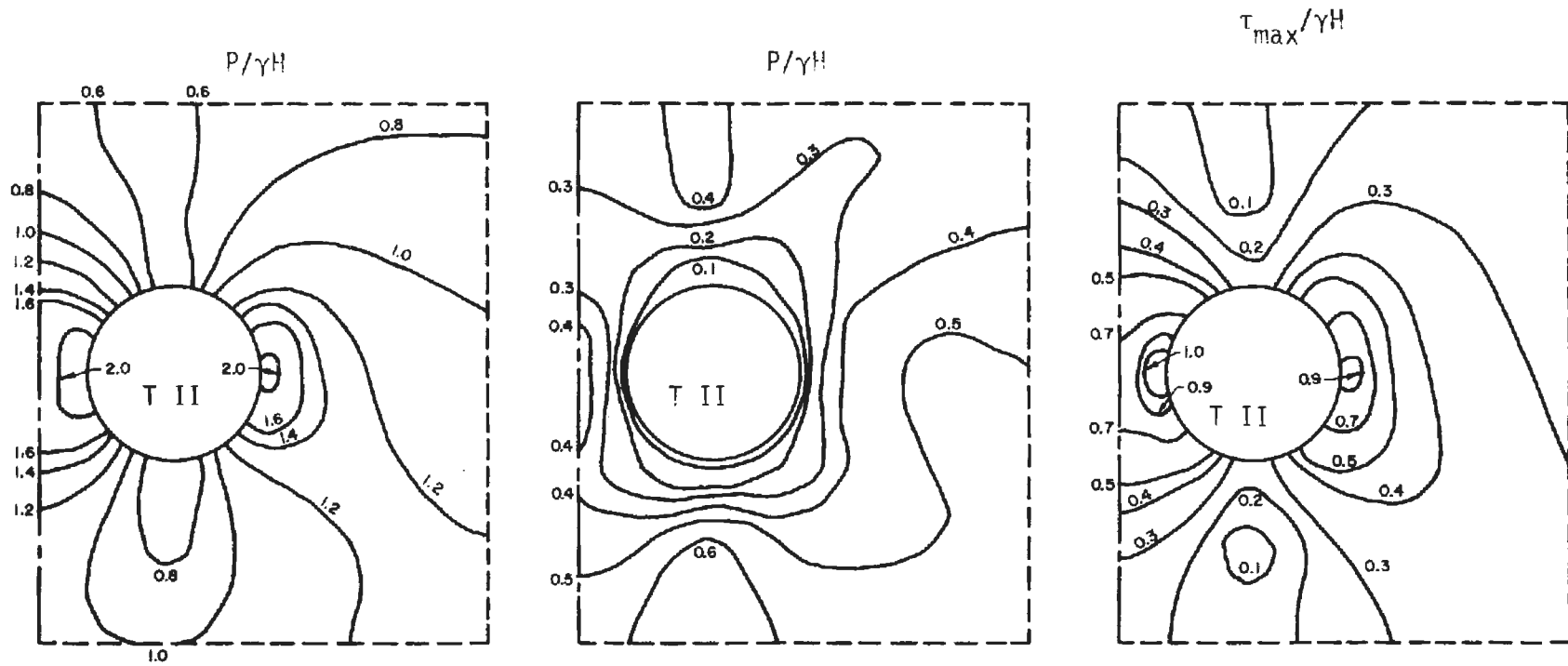


FIGURE 3.3 STRESS DISTRIBUTIONS AROUND TWO PARALLEL UNLINED TUNNELS
(TB8, $H/D = 5.5$, $W/D = 0.5$)

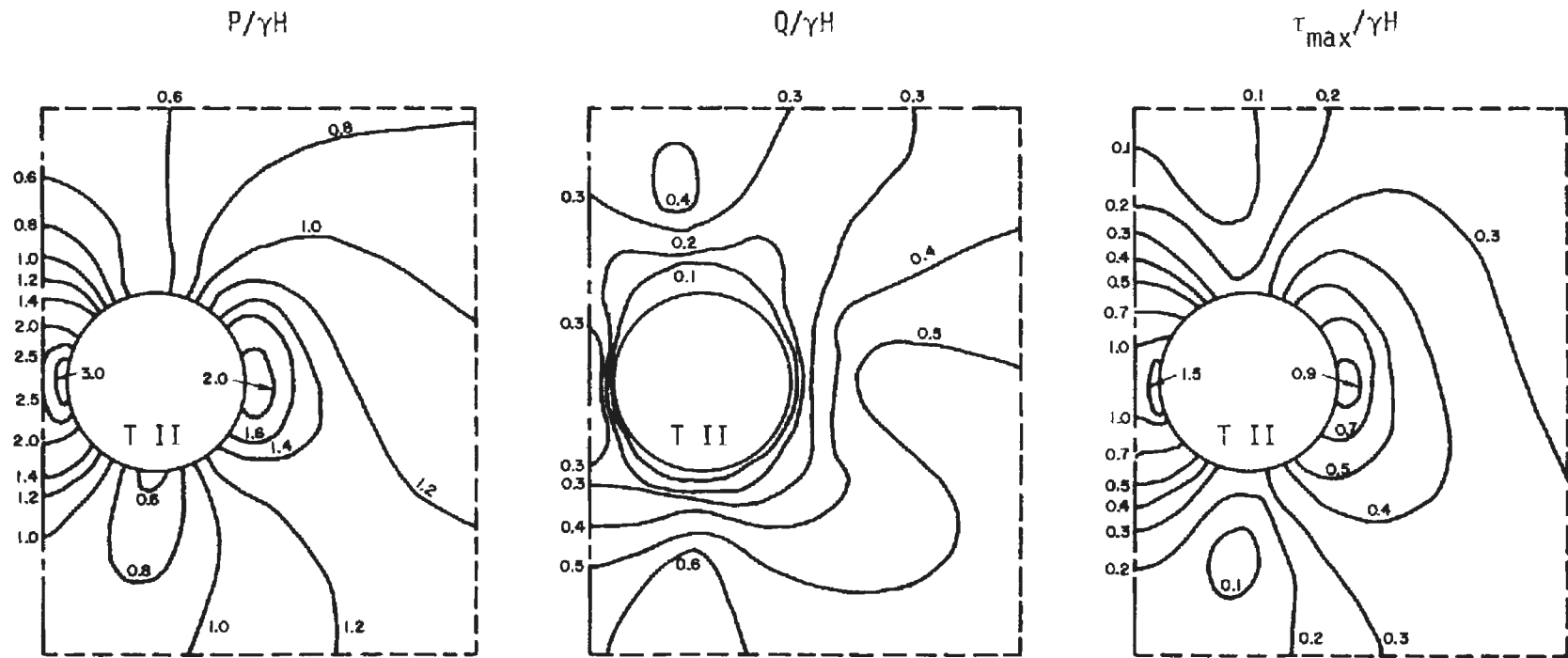


FIGURE 3.4 STRESS DISTRIBUTIONS AROUND TWO PARALLEL UNLINED TUNNELS
(TB12, $H/D = 5.5$, $W/D = 0.25$)

tunnel axes, the horizontal stresses decrease as the pillar width is reduced, although the change is not as great as that associated with the vertical stresses.

The increase of vertical stress and relaxation of horizontal stress indicates a vertical compression and horizontal expansion of the pillar between two parallel unlined tunnels that will be more pronounced the smaller the pillar. This is also suggested by the distributions of maximum shear stress. Figures 3.2 through 3.4 show that these shear stresses in the pillar increase dramatically as the pillar width is reduced.

The stress distributions obtained from one of the analyses for which it was assumed that both tunnels were lined are shown in Fig. 3.5. It was assumed in the lined tunnel analyses that tunnel excavation and liner installation occur instantaneously and simultaneously. For this reason relaxation of the medium surrounding the tunnel is a minimum in these analyses. What stress redistribution does occur is directly related to deformation of the liner. There would be no change in the stress distributions from the in situ state if the liner were perfectly rigid.

The stress distributions from TB11 were selected because they demonstrated the greatest amount of interaction of the lined tunnel analyses (greatest depth and narrowest pillar). It can be seen that there is a considerable difference between the stress distributions in Fig. 3.5 and the corresponding distribution for the unlined case in Fig. 3.4. The vertical stresses in the pillar are only slightly larger than were the in situ stresses at that depth prior to creation of the tunnel. On the other hand the largest horizontal stresses in the pillar are almost double the magnitude of the in

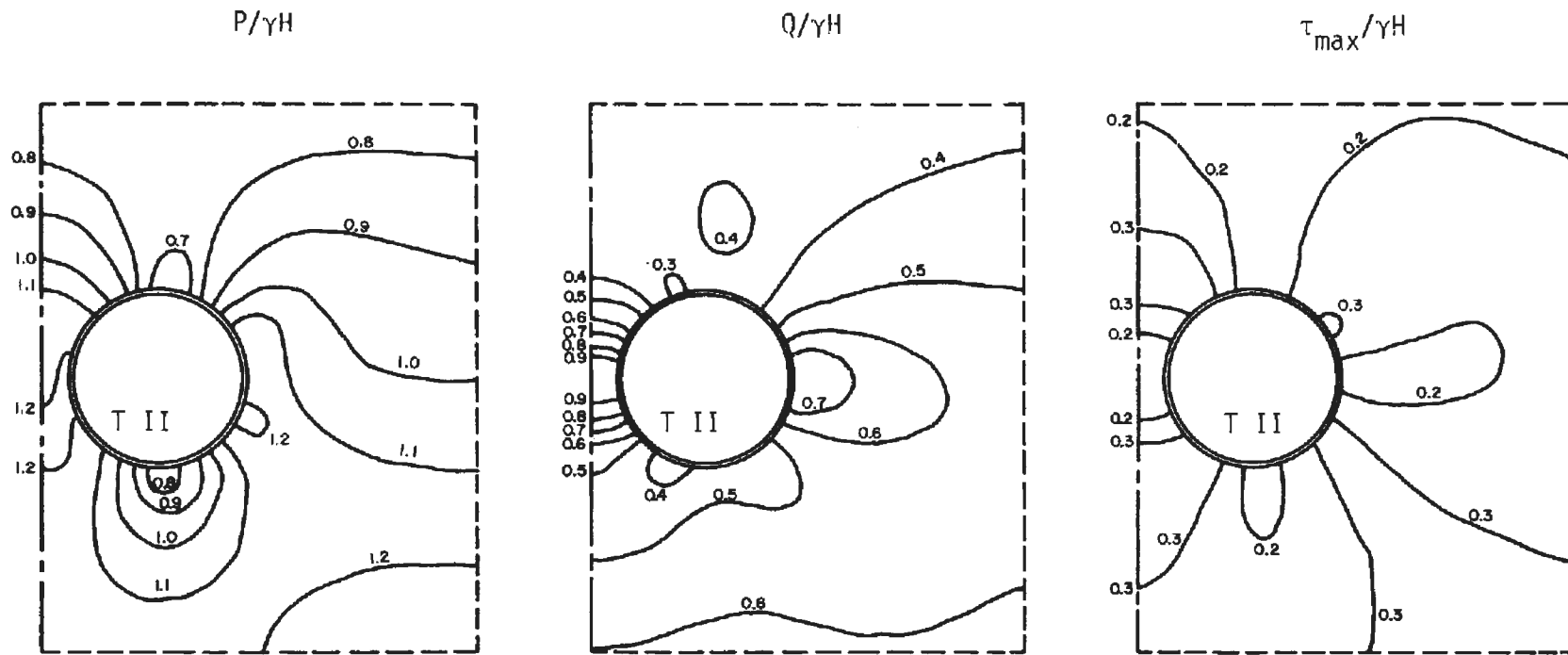


FIGURE 3.5 STRESS DISTRIBUTIONS AROUND TWO PARALLEL LINED TUNNELS (TB11, H/D = 5.5, W/D = 0.25)

situ horizontal stresses. The distribution of maximum shear stresses is also considerably different from that around the unlined tunnel. From Fig. 3.4 it is seen that at the tunnel wall the largest shear stresses occur at the springlines while the smallest shear stresses are located at the crown and invert. Around the lined tunnel the smallest shear stresses occur at the springlines as well as at the crown and invert while the largest shear stresses now occur at points approximately midway between these locations.

The differences between the stress distributions in Figs. 3.4 and 3.5 can be explained by the deformation of the tunnel liner. The liner lends considerable support to the surrounding medium resulting in smaller vertical displacements and thus less vertical compression of the pillar. What deformation does occur results in an inward displacement of the crown and invert and an outward displacement of the springlines. The outward movement of the springlines accounts for the high horizontal stresses at the springlines (Q). The horizontal stresses in the pillar are especially large because the "inner" springlines of the two tunnels are forced towards each other thus causing a horizontal compression of the pillar. Inward displacement at the crown and outward displacement at the springline mobilizes the highest shear stress between these points.

3.2.2 TUNNEL AND SURFACE DISPLACEMENTS

TUNNEL DISPLACEMENTS

Normalized displacements of the unlined and lined tunnel openings for the symmetrical case are plotted in Figs. 3.6 through 3.9. Also shown in

$\frac{\delta/a}{\gamma H/M_c}$
 Scale: 0 2 4

- Single tunnel
- W/D = 1.0
- W/D = 0.5
- △ W/D = 0.25

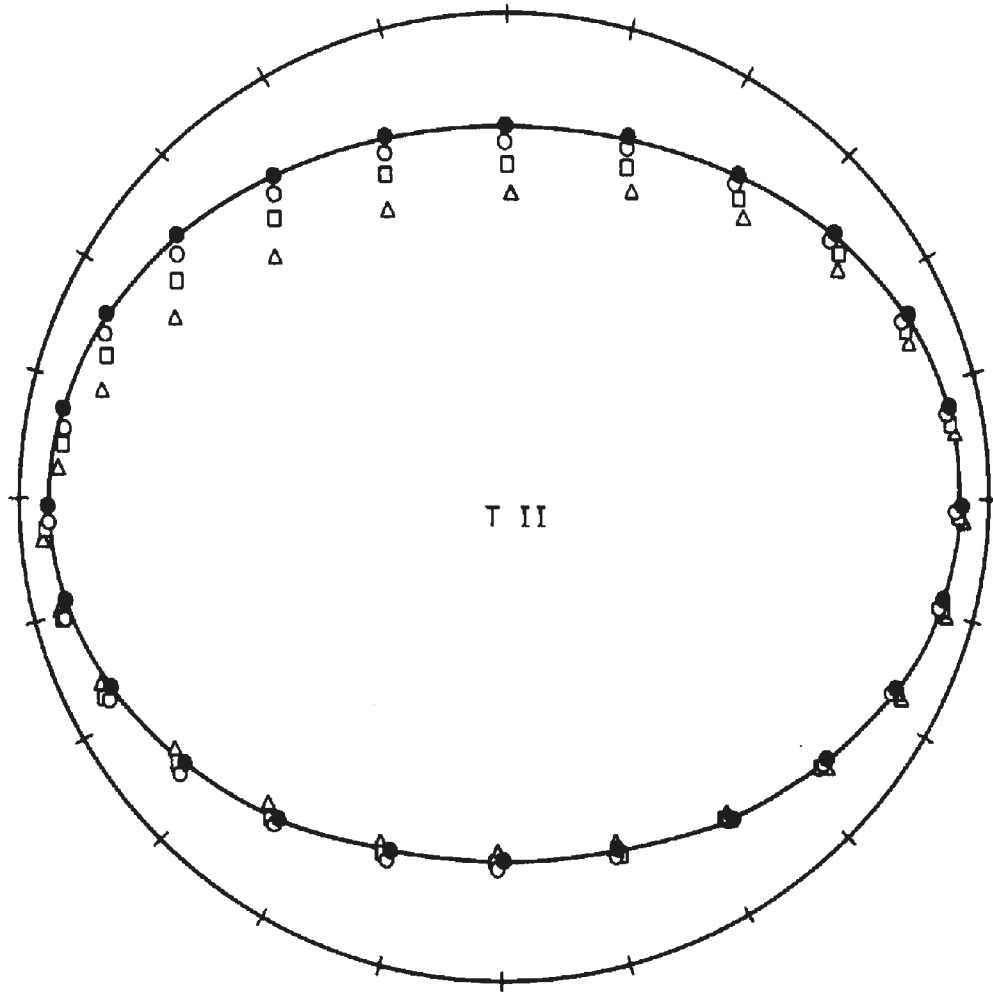


FIGURE 3.6 UNLINED TUNNEL DISPLACEMENTS FOR THE SYMMETRICAL CASE ($H/D = 1.5$)

$$\frac{\delta/a}{\gamma H/M_c}$$
 Scale: 0 2 4

- Single tunnel
- W/D = 1.0
- W/D = 0.5
- △ W/D = 0.25

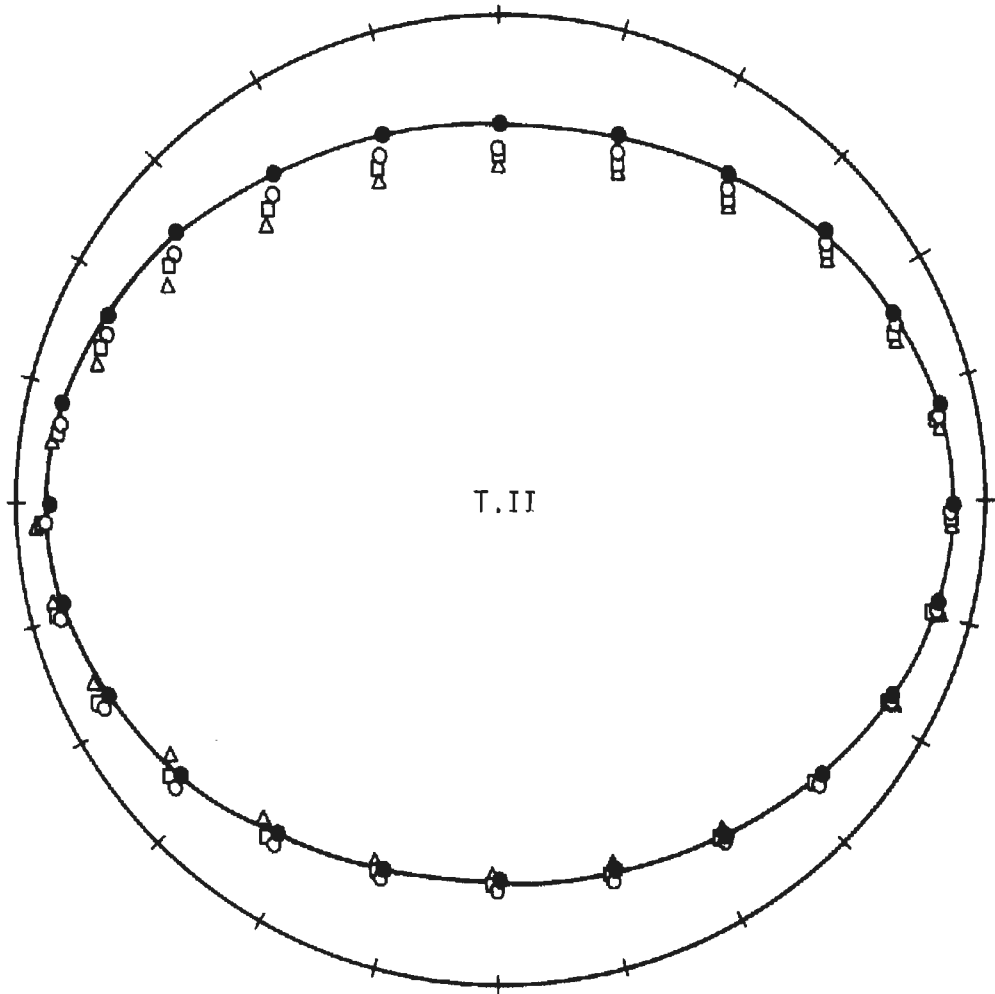


FIGURE 3.7 UNLINED TUNNEL DISPLACEMENTS FOR THE SYMMETRICAL CASE ($H/D = 5.5$)

$\frac{\delta/a}{\gamma H/M_c}$
 Scale: 0 1 2

- Single tunnel
- W/D = 1.0
- W/D = 0.5
- △ W/D = 0.25

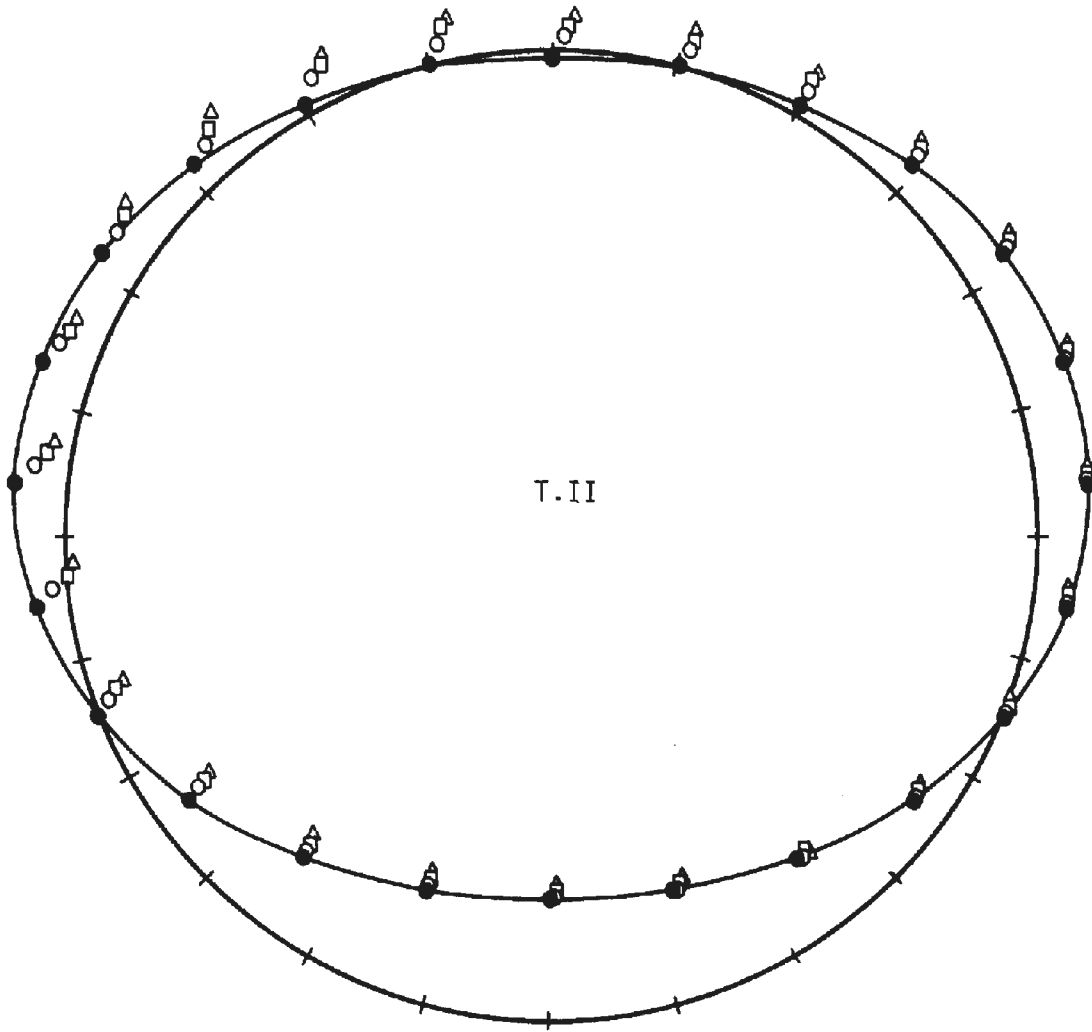
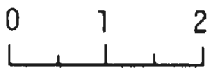


FIGURE 3.8 LINED TUNNEL DISPLACEMENTS FOR
 THE SYMMETRICAL CASE ($H/D = 1.5$)

$\frac{\delta/a}{\gamma H/M_c}$

Scale: 

- Single tunnel
- W/D = 1.0
- W/D = 0.5
- △ W/D = 0.25

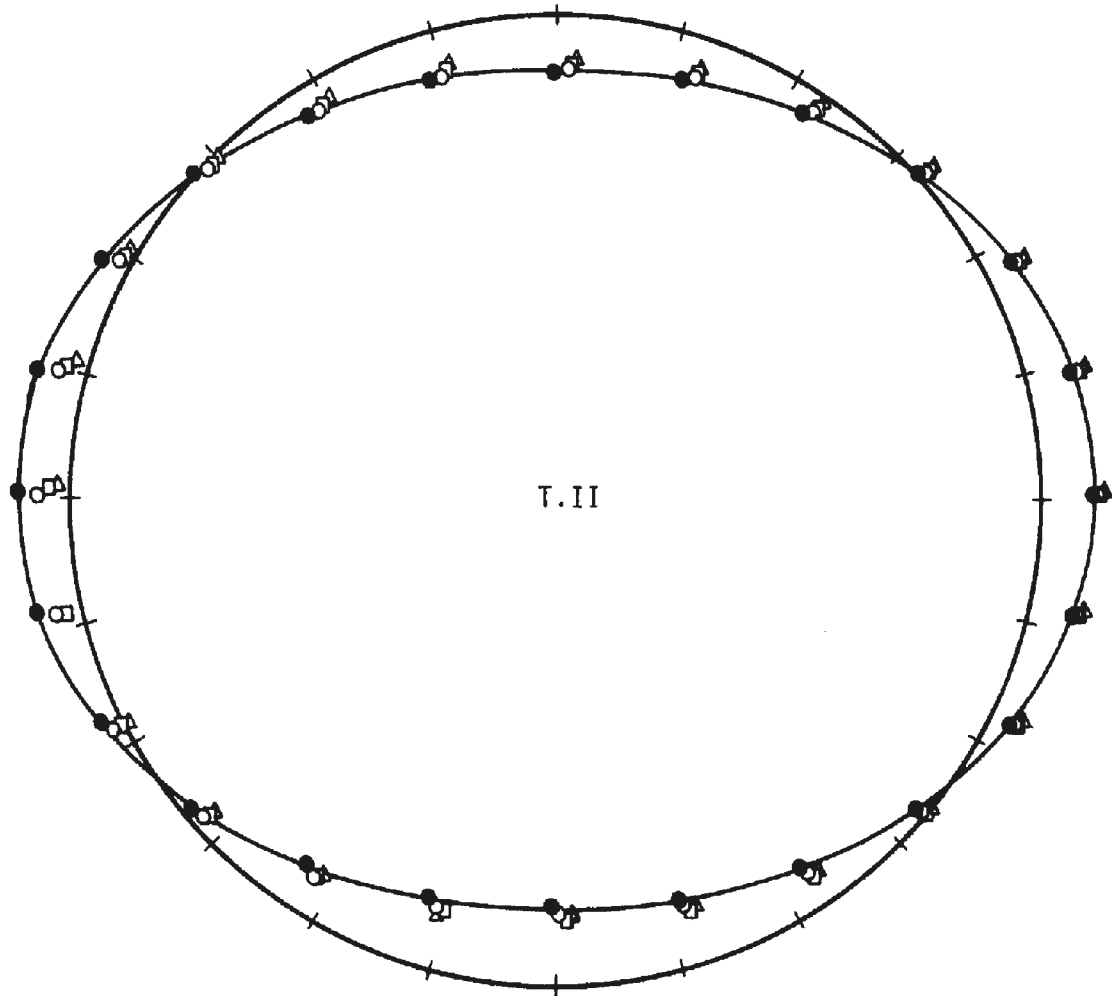


FIGURE 3.9 LINED TUNNEL DISPLACEMENTS FOR THE SYMMETRICAL CASE ($H/D = 5.5$)

these figures are the corresponding single tunnel displacements. Note that because the displacements of the unlined tunnels were so much larger than those of the lined tunnels two different displacement scales were used.

Figures 3.6 and 3.7 show that as the pillar width between two unlined tunnels is reduced, the downward displacements of the upper half of the tunnels increase. This is a result of the vertical compression of the pillar which is greater for a narrow pillar than a wide pillar. Above the springlines there is little difference between the displacements for $W/D = 1.0$ and those for a single tunnel when the tunnels are located at a shallow depth. However, for deep tunnels this difference is more pronounced, indicating that the minimum pillar width at which the two tunnels can be said to act independently of each other increases with depth of the tunnels. Pillar width seems to have its greatest effect on the vertical displacement component. The greatest variation of horizontal displacements occurs on the pillar side of the tunnel where there is slightly less inward displacement as the pillar width is reduced. Pillar width has almost no effect on displacements in the lower right-hand quadrant of the tunnels.

Figure 3.8 gives the displacements of the shallow ($H/D = 1.5$) lined tunnels. At this depth the weight of overburden is not sufficient to prevent the upward rise of the liner. This effect is more pronounced for two parallel tunnels than for a single tunnel. It is also clear that the upward displacement is greater for a narrow pillar than for a wide pillar and that the pillar springline of the liner moves upward more than the far springline.

Displacements of the deep ($H/D = 5.5$) lined tunnels are given in Fig. 3.9. At this depth the weight of overburden is great enough to prevent

the rise of the liner and a more symmetrical deformed liner shape results. At this depth the interaction of two parallel lined tunnels is indicated primarily by the horizontal displacements of the liner next to the pillar. This effect is also observed for the shallow tunnels (Fig. 3.8). Under the K_0 condition assumed, a tunnel liner will be forced outward at the springlines until sufficient passive pressure is built up to balance the vertical pressure. This reaction is indicated by the single tunnel displacements in Figs. 3.8 and 3.9. These figures also indicate that when two parallel lined tunnels are constructed simultaneously with a pillar width of approximately one tunnel diameter or less they will interact so as to yield smaller outward displacement of the pillar springlines than would result for a single tunnel. In addition, the necessary passive pressure at the two inner springlines is mobilized with less displacement of each springline as the pillar width is reduced.

SURFACE DISPLACEMENTS

Displacements of the ground surface over the shallow unlined tunnels are shown in Fig. 3.10. Because of the vertical compression of the pillar the surface displacements are generally greater than those that would be indicated by simple superposition of the settlement profiles of the two single tunnels. The differences are greater for the smaller pillar widths. Also note that as the width of the pillar decreases it becomes less evident from the shape of the settlement profiles that there are two tunnels and not just one.

Figure 3.11 gives the surface displacements for the deep ($H/D = 5.5$) unlined tunnels. It is clear from these plots that the lateral distance from

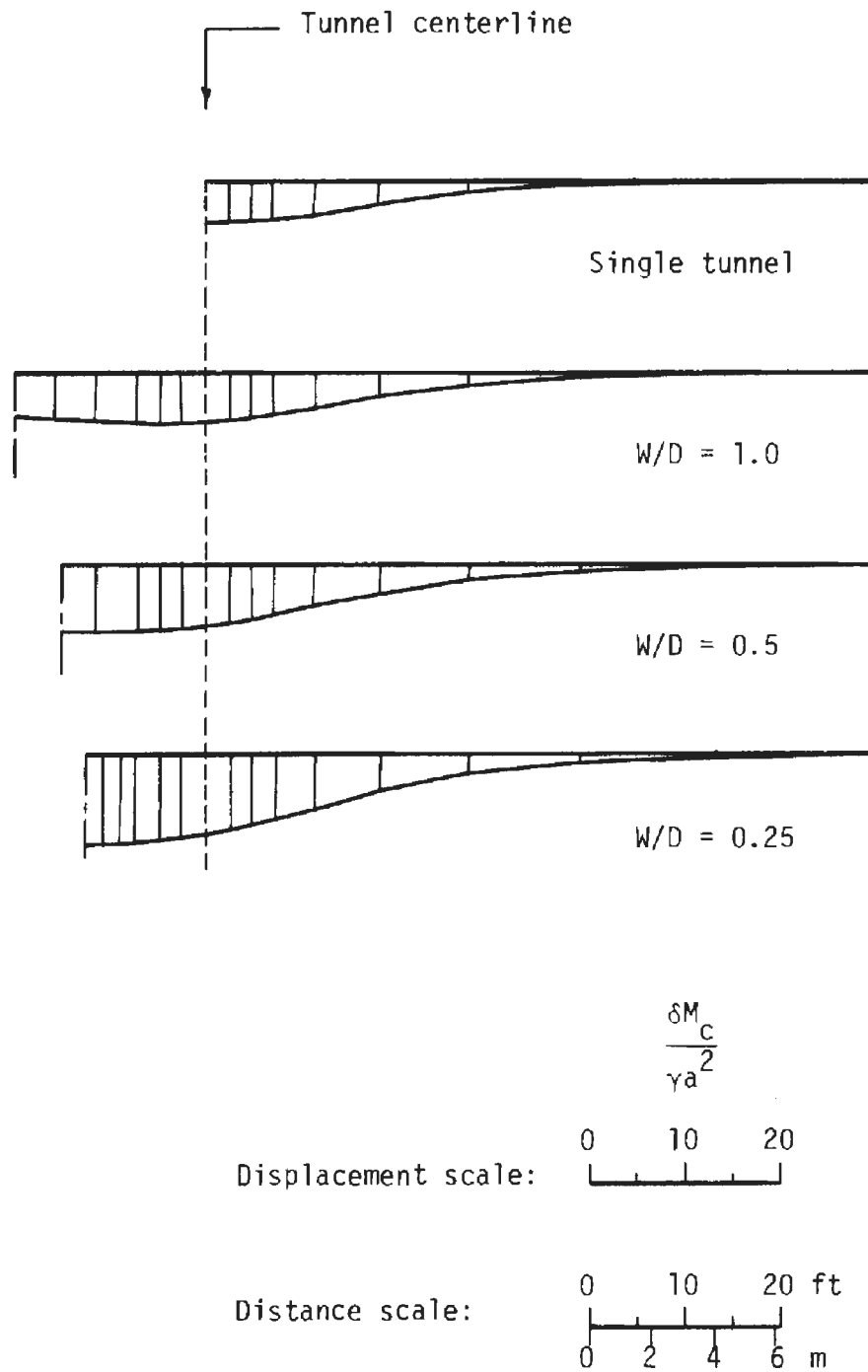


FIGURE 3.10 SURFACE DISPLACEMENT FOR UNLINED TUNNELS (H/D = 1.5)

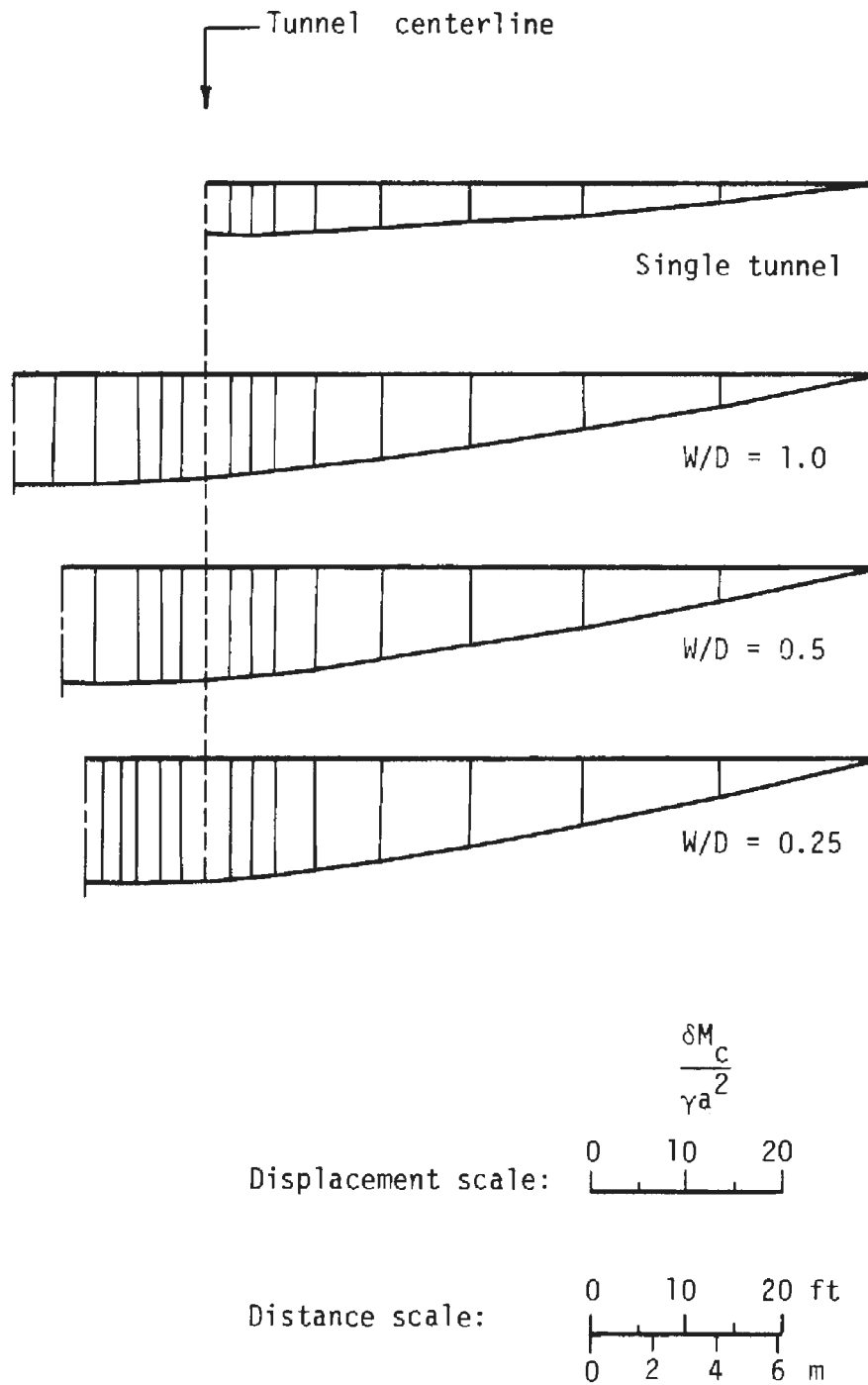


FIGURE 3.11 SURFACE DISPLACEMENTS FOR UNLINED TUNNELS ($H/D = 5.5$)

the tunnels to the finite element mesh boundaries was too small. The fixed boundary displacement condition has forced the surface displacements to go to zero and thus has distorted the shape of the settlement profiles away from the tunnels. The displacements in the vicinity of the tunnel centerline should be little affected by this, however. These profiles also indicate that settlements over the tunnels are greater than what would be indicated by superposition. Because of the great depth at which these tunnels are located, the contributions of each tunnel to the vertical medium displacements have overlapped to such an extent by the time they reach the surface that there is no indication from the shape of the settlement profiles that more than one tunnel exists.

The ground surface displacements obtained from the lined tunnel analyses are shown in Figs. 3.12 and 3.13 for the shallow and deep tunnels respectively. These displacements are very small and thus an expanded scale has been used. Figure 3.12 shows that the ground surface over the shallow lined tunnels has been forced upward. Maximum displacements occur above the pillar for the two tunnel case and are approximately the same for all pillar widths. For the single tunnel case the maximum displacements occur at locations outside the tunnel springlines which Fig. 3.8 shows as having moved upward and outward while the crown remained almost stationary. Figure 3.13 illustrates that there has been a small amount of surface subsidence over the deep lined tunnels.

3.2.3 LINER FORCES AND MOMENTS

The distributions of normalized liner forces and moments are given in Figs. 3.14 through 3.19 for the shallow ($H/D = 1.5$) and deep ($H/D = 5.5$)

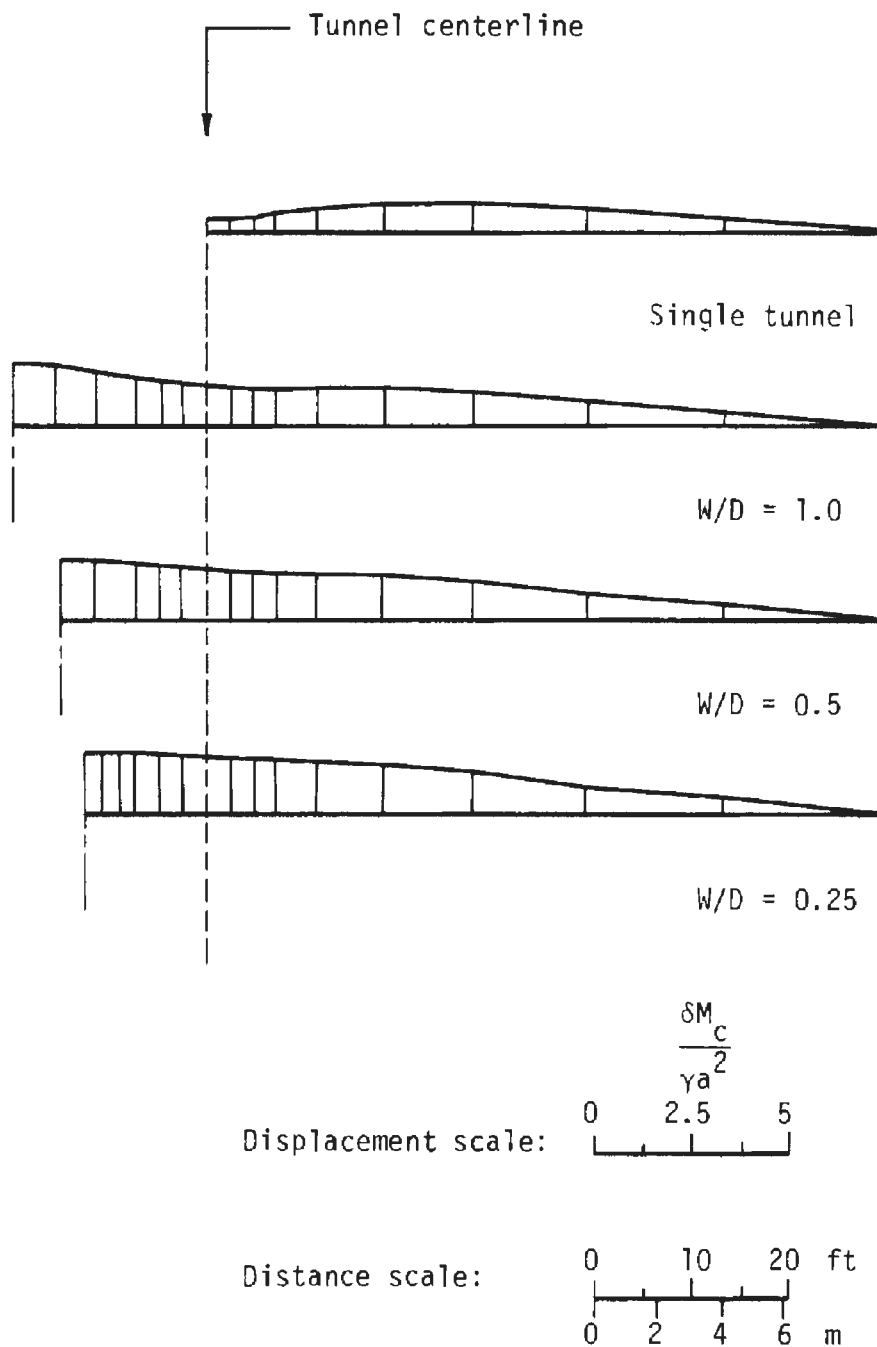


FIGURE 3.12 SURFACE DISPLACEMENTS FOR LINED TUNNELS ($H/D = 1.5$)

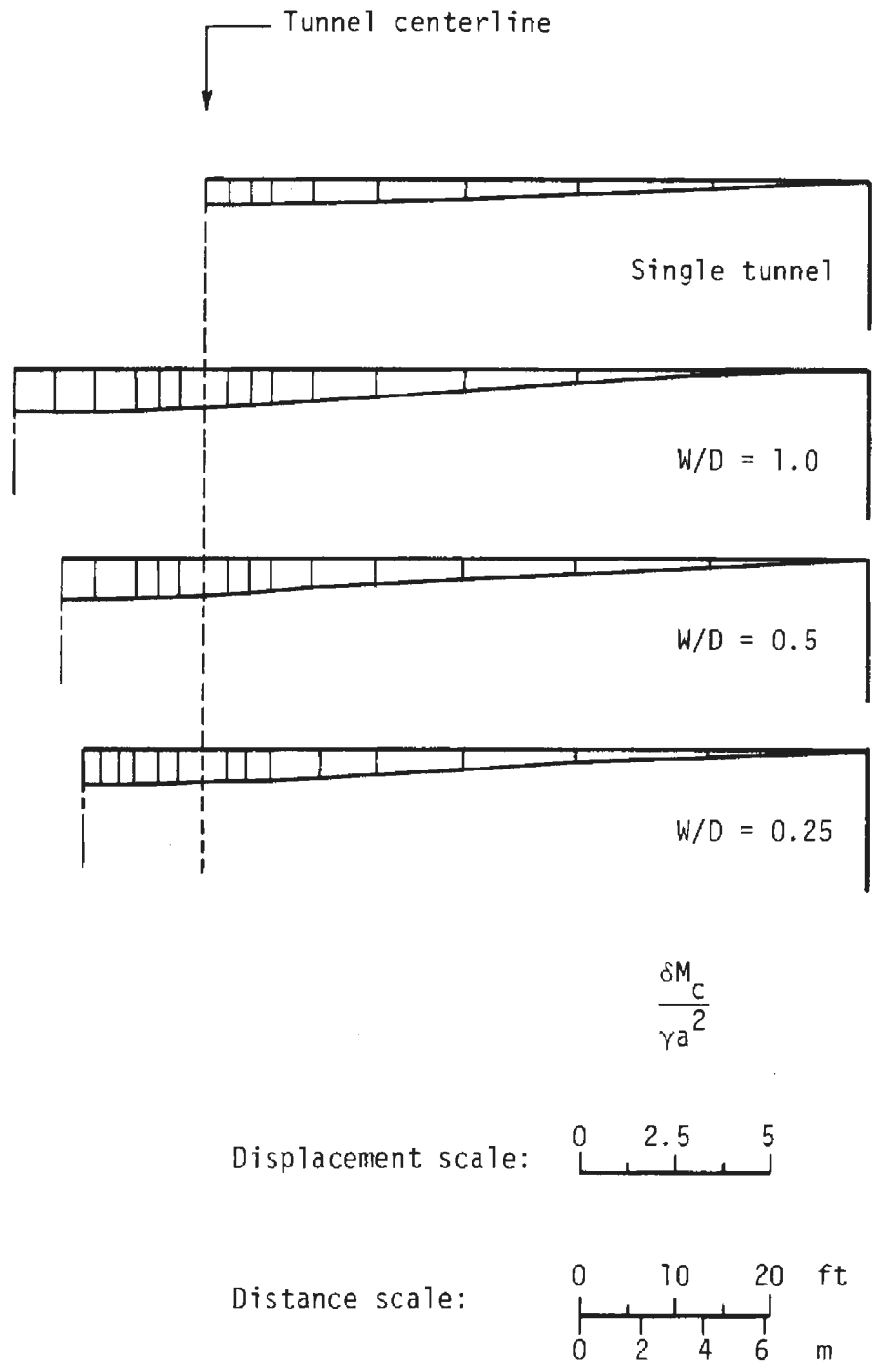


FIGURE 3.13 SURFACE DISPLACEMENTS FOR LINED TUNNELS ($H/D = 5.5$)

Scale: 0 0.5 1.0 T/γHa

———— Single tunnel
———— W/D = 1.0
———— W/D = 0.5
----- W/D = 0.25

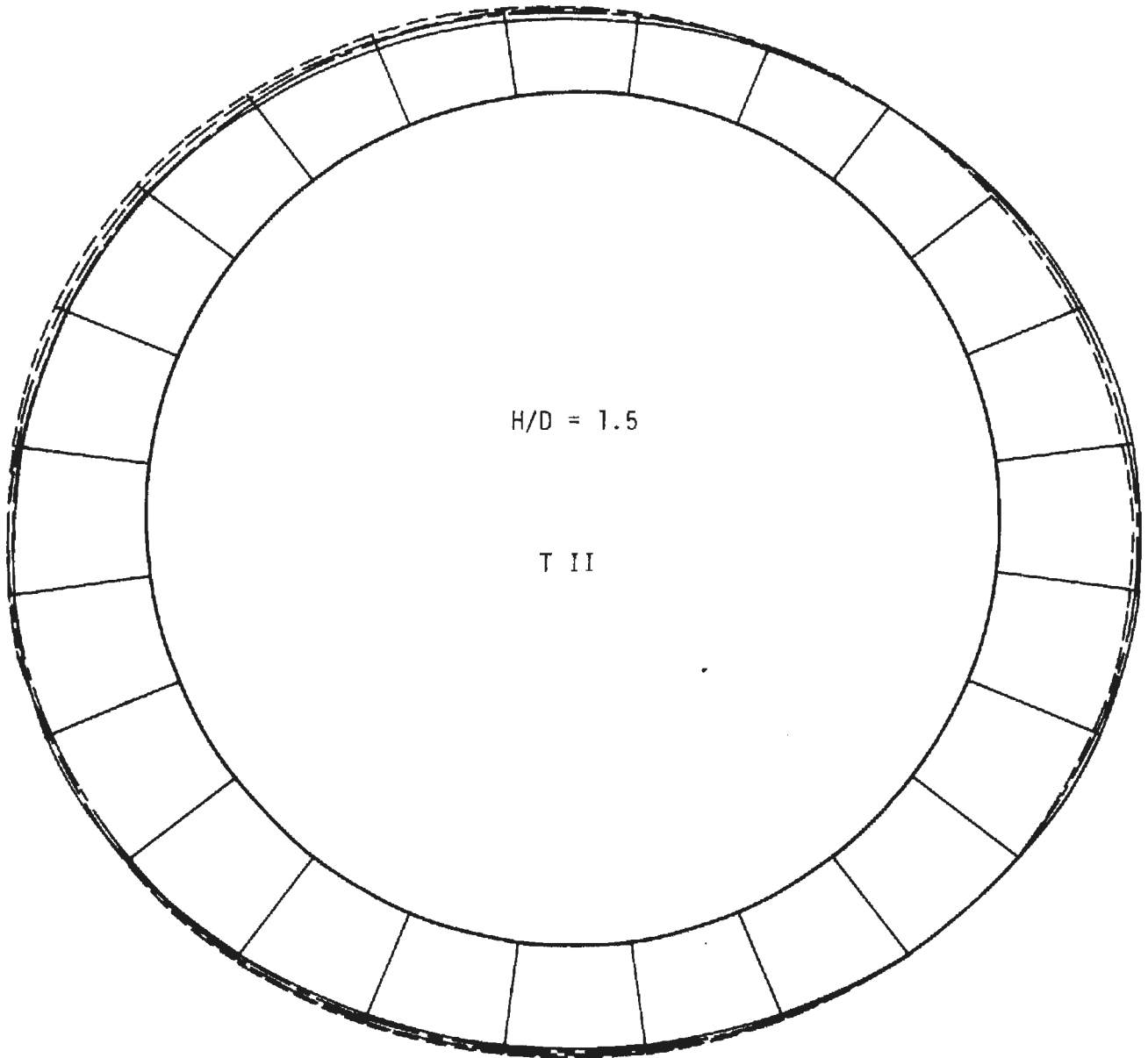


FIGURE 3.14 DISTRIBUTIONS OF LINER THRUST FOR THE SHALLOW TUNNELS

Scale: 0 .005 .01 $M/\gamma H a^2$

- Single tunnel
- $W/D = 1.0$
- $W/D = 0.5$
- $W/D = 0.25$

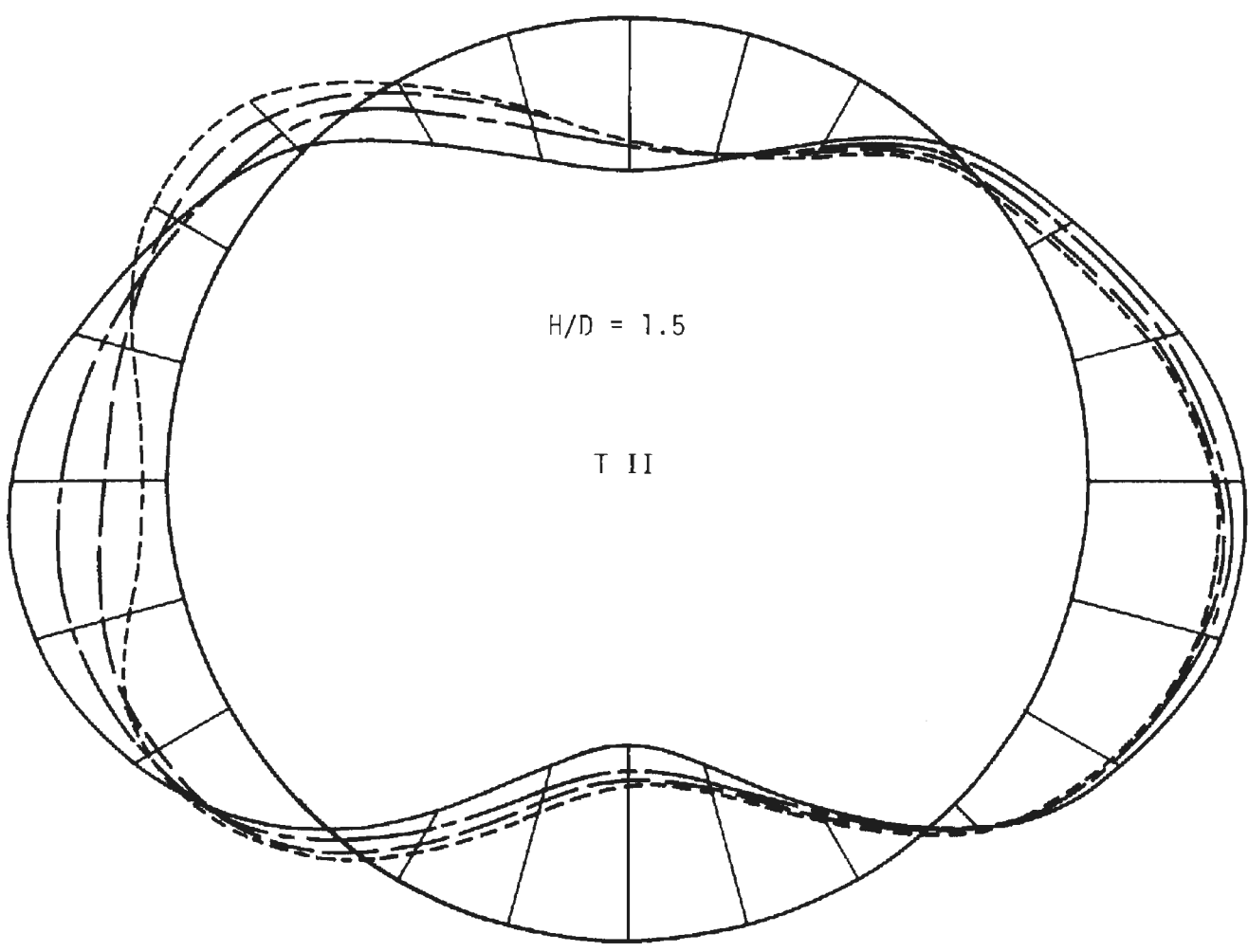


FIGURE 3.15 DISTRIBUTIONS OF LINER MOMENTS FOR THE SHALLOW TUNNELS

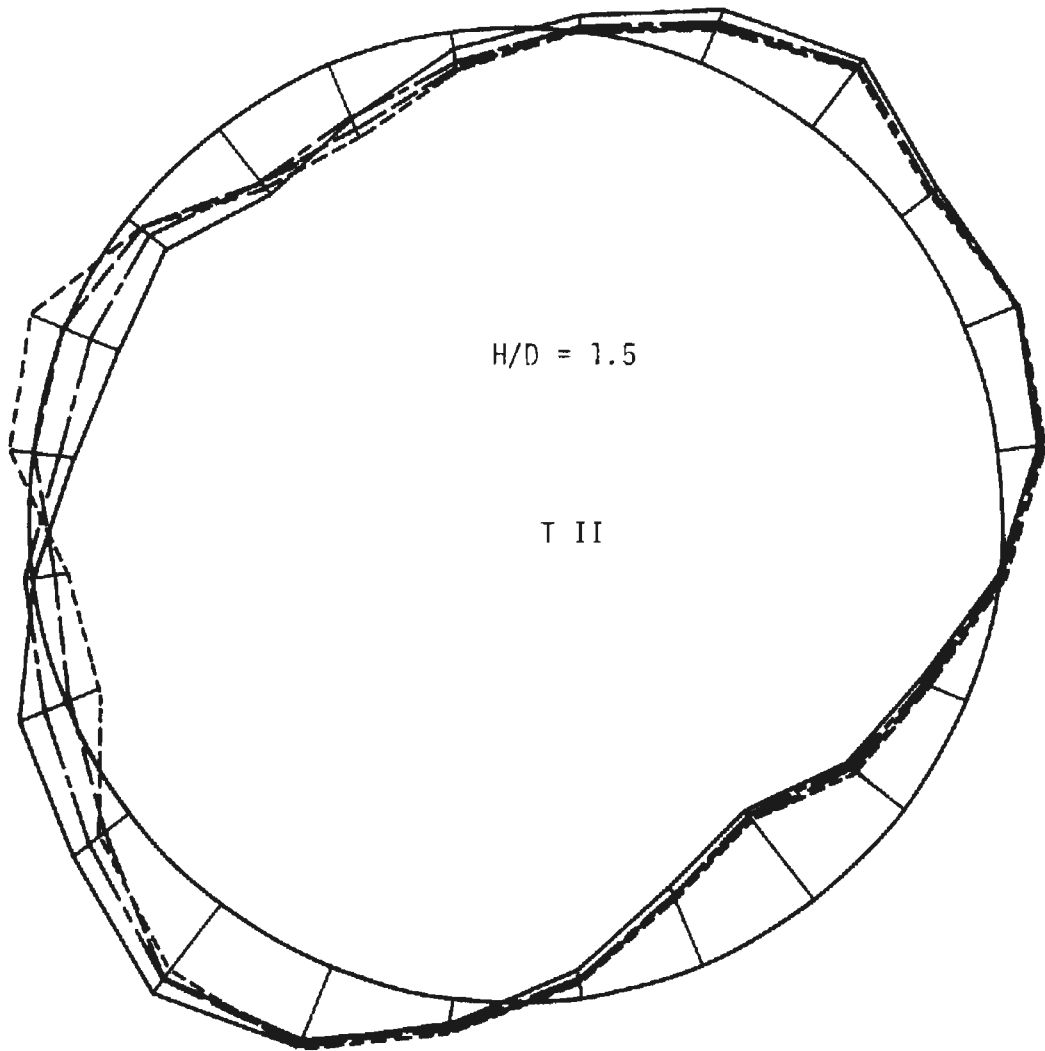


FIGURE 3.16 DISTRIBUTIONS OF LINER SHEAR FOR THE SHALLOW TUNNELS

Scale: 0 0.5 1.0 $T/\gamma H a$

———— Single tunnel
- - - - - $W/D = 1.0$
- - - - - $W/D = 0.5$
- - - - - $W/D = 0.25$

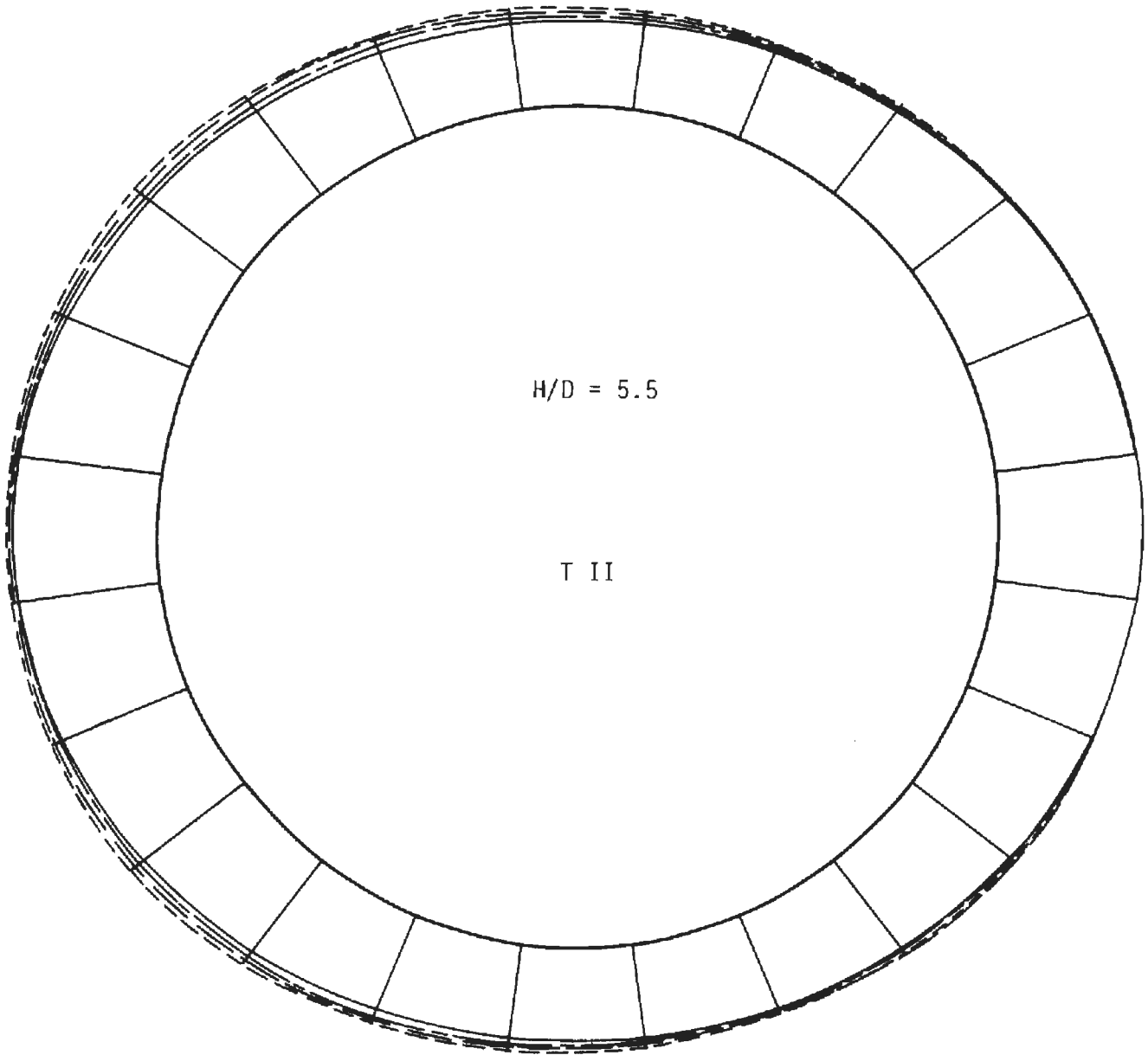


FIGURE 3.17 DISTRIBUTIONS OF LINER THRUST FOR THE DEEP TUNNELS

Scale: 0 .005 .01 $M/\gamma H a^2$

———— Single tunnel
——— W/D = 1.0
- - - - W/D = 0.5
- - - - W/D = 0.25

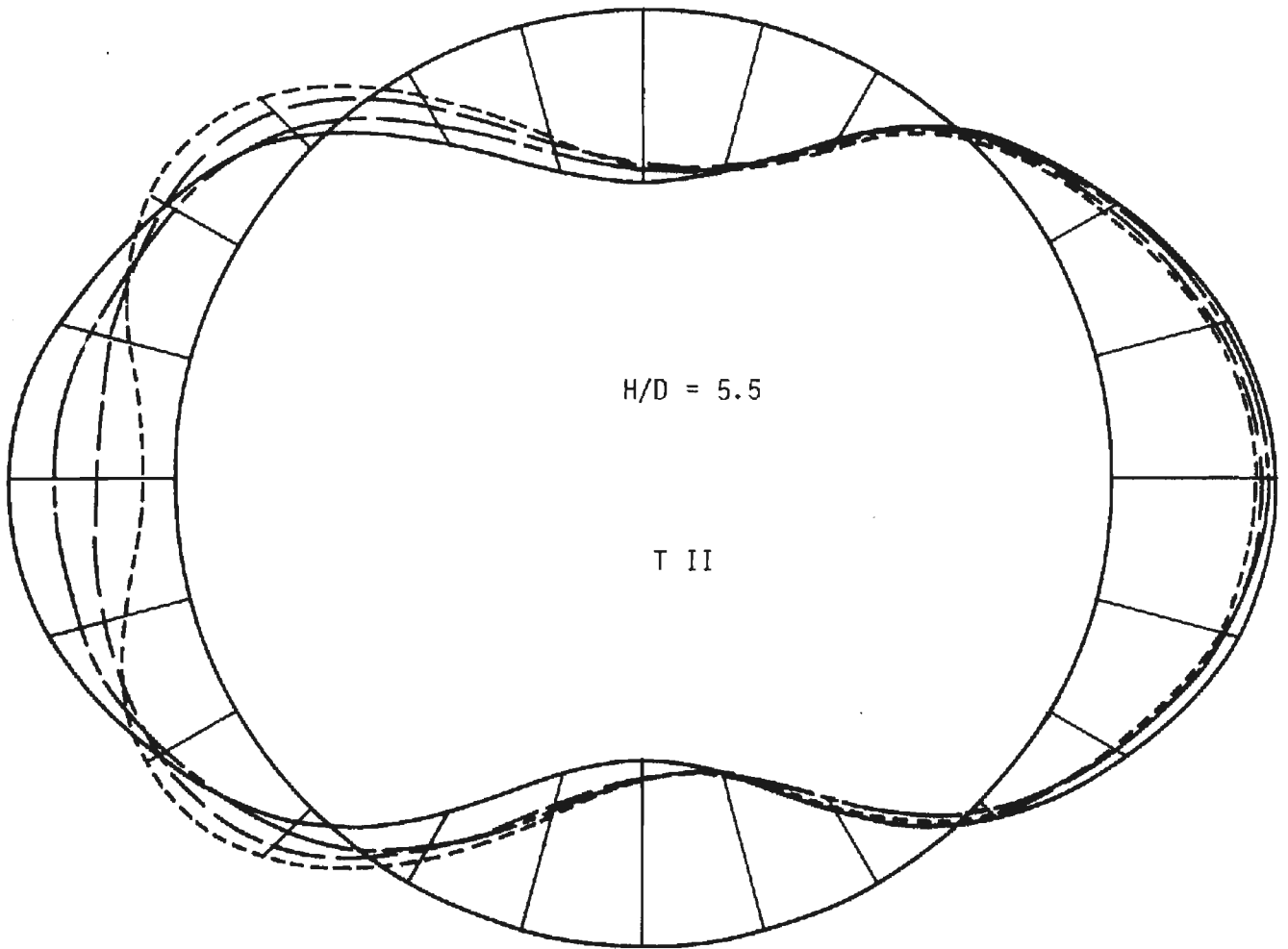


FIGURE 3.18 DISTRIBUTIONS OF LINER MOMENTS FOR THE DEEP TUNNELS

Scale: 0 .02 .04 $V/\gamma H a$

- Single tunnel
- $W/D = 1.0$
- $W/D = 0.5$
- $W/D = 0.25$

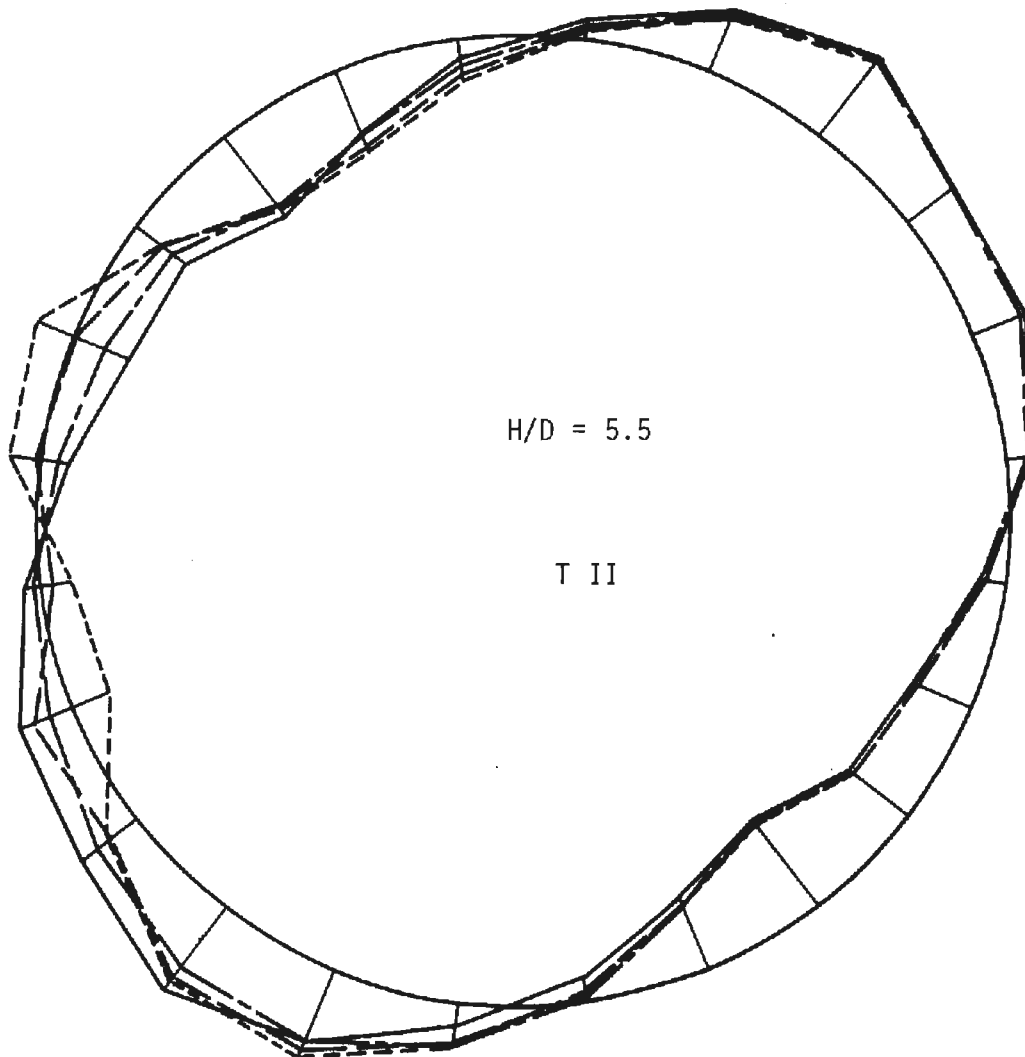


FIGURE 3.19 DISTRIBUTIONS OF LINER SHEAR FOR THE DEEP TUNNELS

tunnels. Liner thrust and bending moment data obtained were such that smooth curves could easily be drawn through the normalized data points. However, the transverse shear force data were rather erratic, possibly due to the manner in which the beam elements were arranged to form the liner in the finite element mesh. Rather than attempt to artificially smooth these data out, it was decided to simply connect the data points with straight lines.

It can be seen from these figures that in most instances the differences between the two tunnel values and the single tunnel values are not as great as might have been expected. The moment distributions exhibit the greatest variation, but the general trend is toward smaller bending moments, due primarily to the reduced displacements of the left springline.

Table 3.4 lists the maximum liner force and moment coefficient values. Maximum thrust values were located at the liner springlines. Maximum bending moment values were located at the invert. Maximum shear force values were located at points approximately mid-way between the invert and springline. Although the figures indicate that, at several points around the liner, force

TABLE 3.4
MAXIMUM LINER FORCE AND MOMENT COEFFICIENTS FOR THE SYMMETRICAL CASE

	$T/\gamma H a$		$M/\gamma H a^2$		$V/\gamma H a$	
	Shallow	Deep	Shallow	Deep	Shallow	Deep
Single tunnel	.849	.871	-.0105	-.0099	-.0237	-.0218
W/D = 1.0	.834	.866	-.0091	-.0088	-.0220	-.0214
W/D = 0.5	.837	.870	-.0086	-.0088	-.0214	-.0205
W/D = 0.25	.853	.905	-.0083	-.0087	-.0211	-.0205

and moment values for two tunnels exceed those for a single tunnel, Table 3.4 shows that this is not the case as far as maximum force and moment values are concerned. In all but one case the interaction between two parallel tunnels constructed simultaneously has been such as to reduce the maximum forces and moments to values less than those for a single tunnel. For the one exception, two deep tunnels separated by a pillar width of $W/D = 0.25$, the maximum thrust coefficient exceed that for a single tunnel by less than 4 percent.

3.3 SECOND TUNNEL CONSTRUCTED ADJACENT TO AN EXISTING TUNNEL - THE UNSYMMETRICAL CASE

3.3.1 MEDIUM STRESSES

The distributions of medium stresses obtained from the unsymmetrical analyses in which both tunnels were either unlined or lined (TB13, TB30, TB14, TB31) were essentially identical to those distributions obtained from the corresponding analyses for the symmetrical case.

For analyses TB17 and TB34, the medium stresses were similar to those found for two unlined tunnels. The construction sequence for these analyses was such that on the first step of the analysis tunnel I was excavated but left unlined. At the end of this step the distributions of medium stresses were identical to those for a single unlined tunnel. A liner was then placed in tunnel I, but since the surrounding medium was already in equilibrium no interaction occurred and there was no change in the medium stresses. Finally tunnel II was excavated and left unlined. The creation of this second opening altered the stresses around tunnel I, but only slightly since the liner in tunnel I was relatively rigid and thus effective in resisting deformations.

Because of the restraining effect of the liner the final stress distributions differed from those around two unlined tunnels such that the minimum principal stresses were slightly larger, while the maximum principal stresses and the maximum shear stresses were smaller around the lined tunnel I, especially in the pillar.

The distributions of stresses obtained from analysis TB32 are given in Fig. 3.20. In this analysis tunnel I was excavated and lined on the first step. On the second step tunnel II was excavated, but left unlined. The medium stresses around tunnel I are similar to those found when both tunnels were lined, and the stresses around tunnel II bear some resemblance to those stresses found when both tunnels were unlined. It is evident, however, that each tunnel has had an effect on the other and that interaction between the two tunnels has taken place resulting in new stress distributions.

A similar effect is observed for the stresses in the medium surrounding the two tunnels of analysis TB33. Figure 3.21 shows that although both tunnels were lined in this analysis the stress distributions are almost mirror images of those in Fig. 3.20. This occurs because the liner of tunnel I was not installed until after all medium displacements associated with the creation of this opening had occurred. Tunnel II was lined immediately upon excavation.

The distributions of medium stresses obtained from analysis TB15 are given in Fig. 3.22. TB15 is the shallow tunnel ($H/D = 1.5$) equivalent of analysis TB32 for deep tunnels ($H/D = 5.5$). The influence of the ground surface can be seen by comparing Figs. 3.22 and 3.20. Although there are many similarities in form of the distributions for the shallow and deep cases,

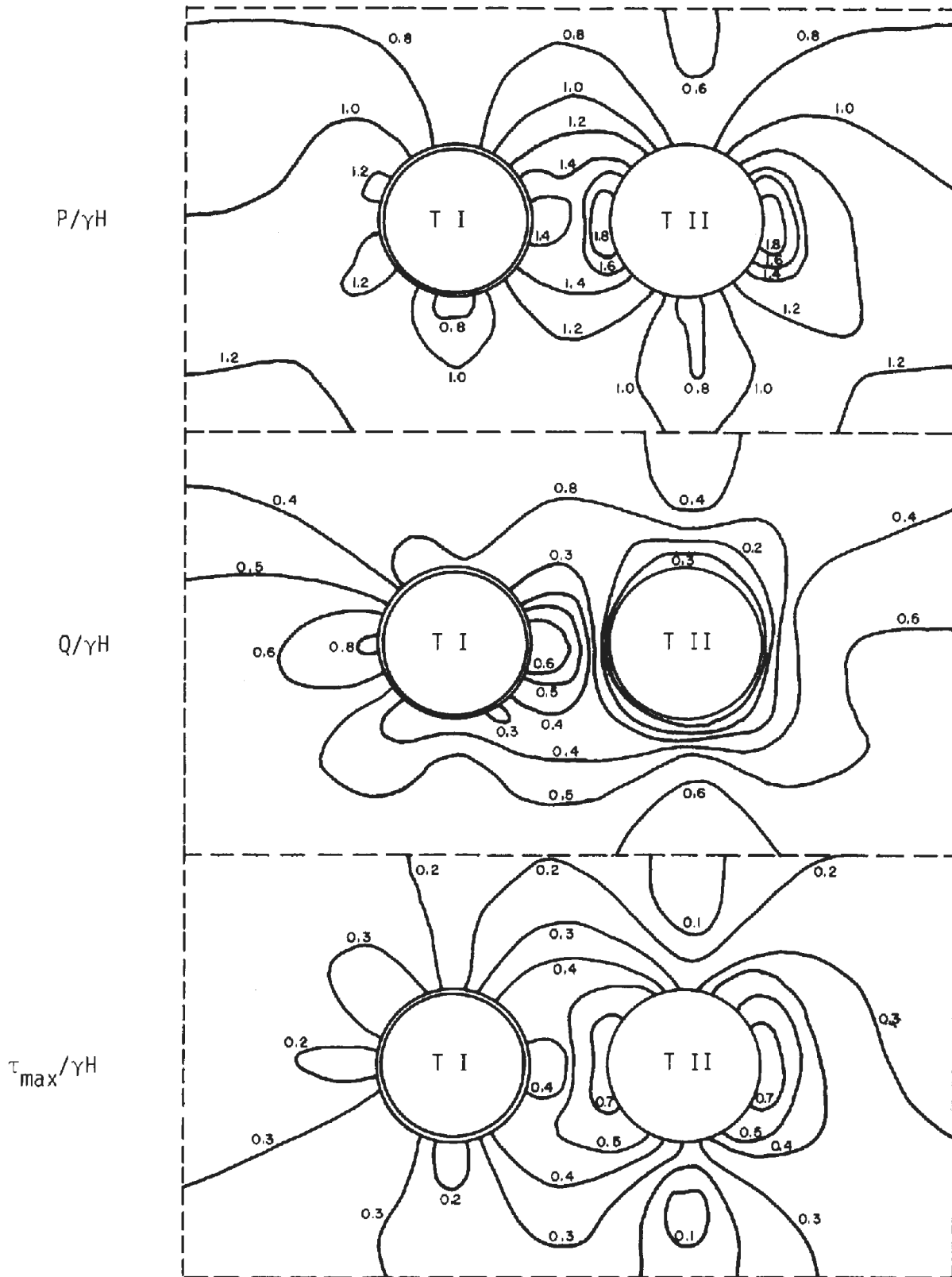


FIGURE 3.20 STRESS DISTRIBUTIONS FROM UNSYMMETRICAL ANALYSIS
TB32 ($H/D = 5.5$, $W/D = 0.5$)

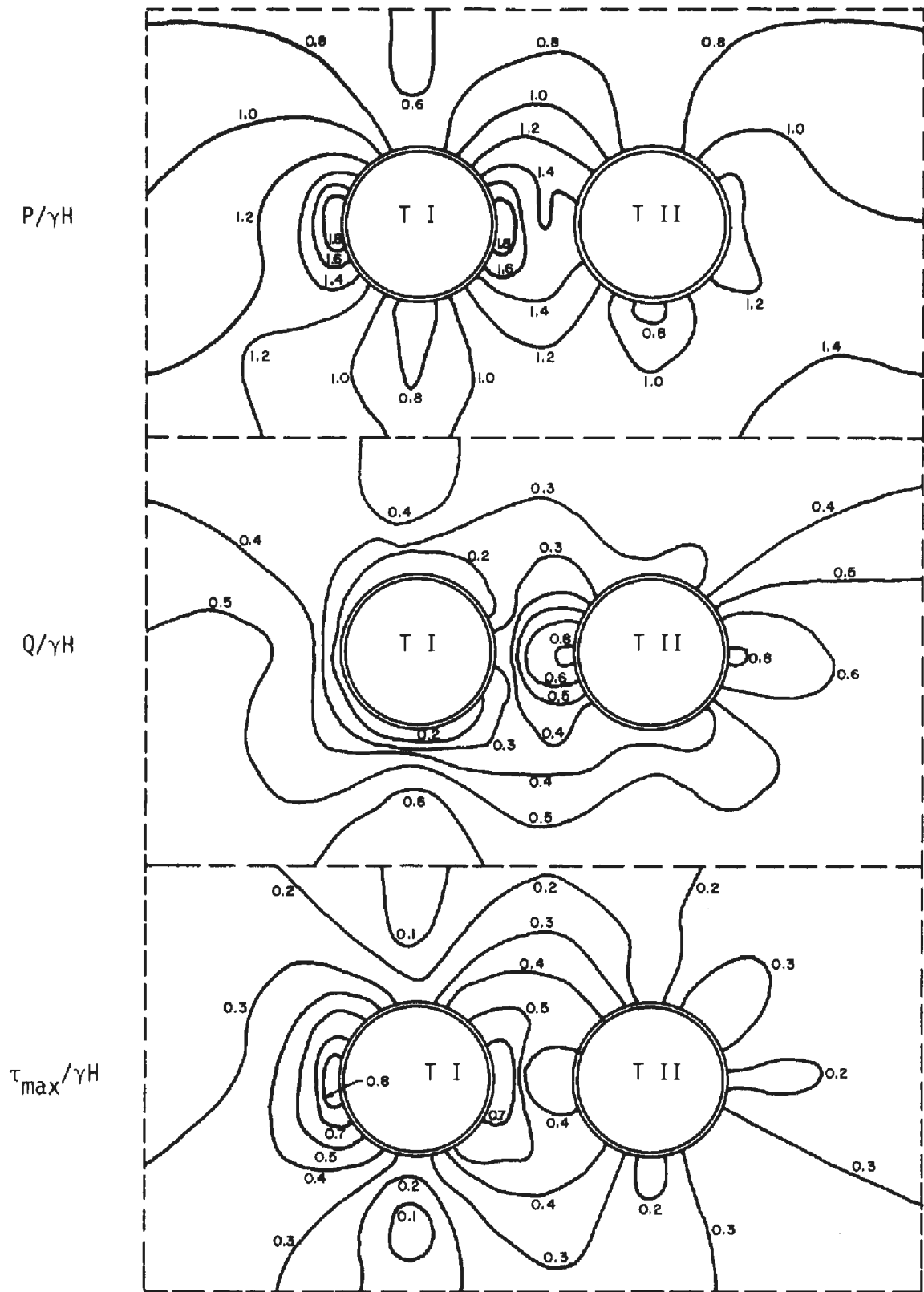


FIGURE 3.21 STRESS DISTRIBUTIONS FROM UNSYMMETRICAL ANALYSIS TB33 ($H/D = 5.5$, $W/D = 0.5$)

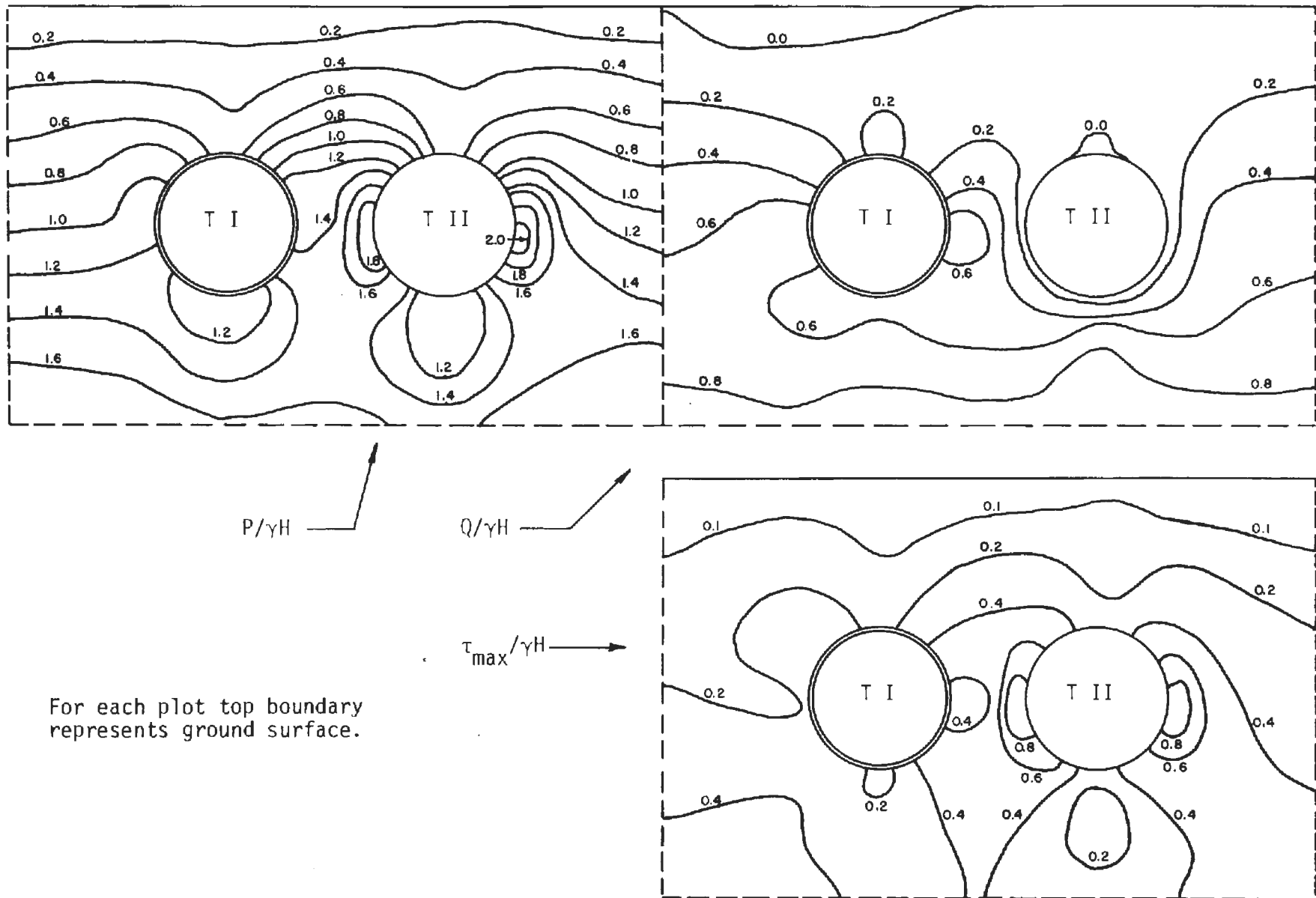


FIGURE 3.22 STRESS DISTRIBUTIONS FROM UNSYMMETRICAL ANALYSIS TB15 ($H/D = 1.5$, $W/D = 0.5$)

there is a greater range of normalized stress magnitudes associated with the shallow tunnels. This is because the stress increase with depth over a given vertical distance (e.g., one tunnel diameter) is more pronounced near the ground surface than at great depth. Figure 3.22 illustrates the presence of two small regions of tensile minimum principal stress, one at the ground surface and the other at the crown of the unlined tunnel. Similar tensile stress regions were observed for all shallow tunnel analyses that considered unlined tunnels. These stresses were always of very small magnitude, usually less than 1.0 psi (7×10^3 Pa) and never greater than 2.0 psi (14×10^3 Pa). The tensile stresses above the crown of the unlined tunnel are oriented in a nearly radial direction and act in combination with relatively small circumferential stresses. Figure 3.22 shows only one zone of tensile stresses at the ground surface. There were usually two such zones observed, symmetrically located to the left and right of the unlined tunnels. These tensile stresses are undoubtedly the result of the lateral (horizontal) component of the surface displacements.

3.3.2 TUNNEL AND SURFACE DISPLACEMENTS

TUNNEL DISPLACEMENTS

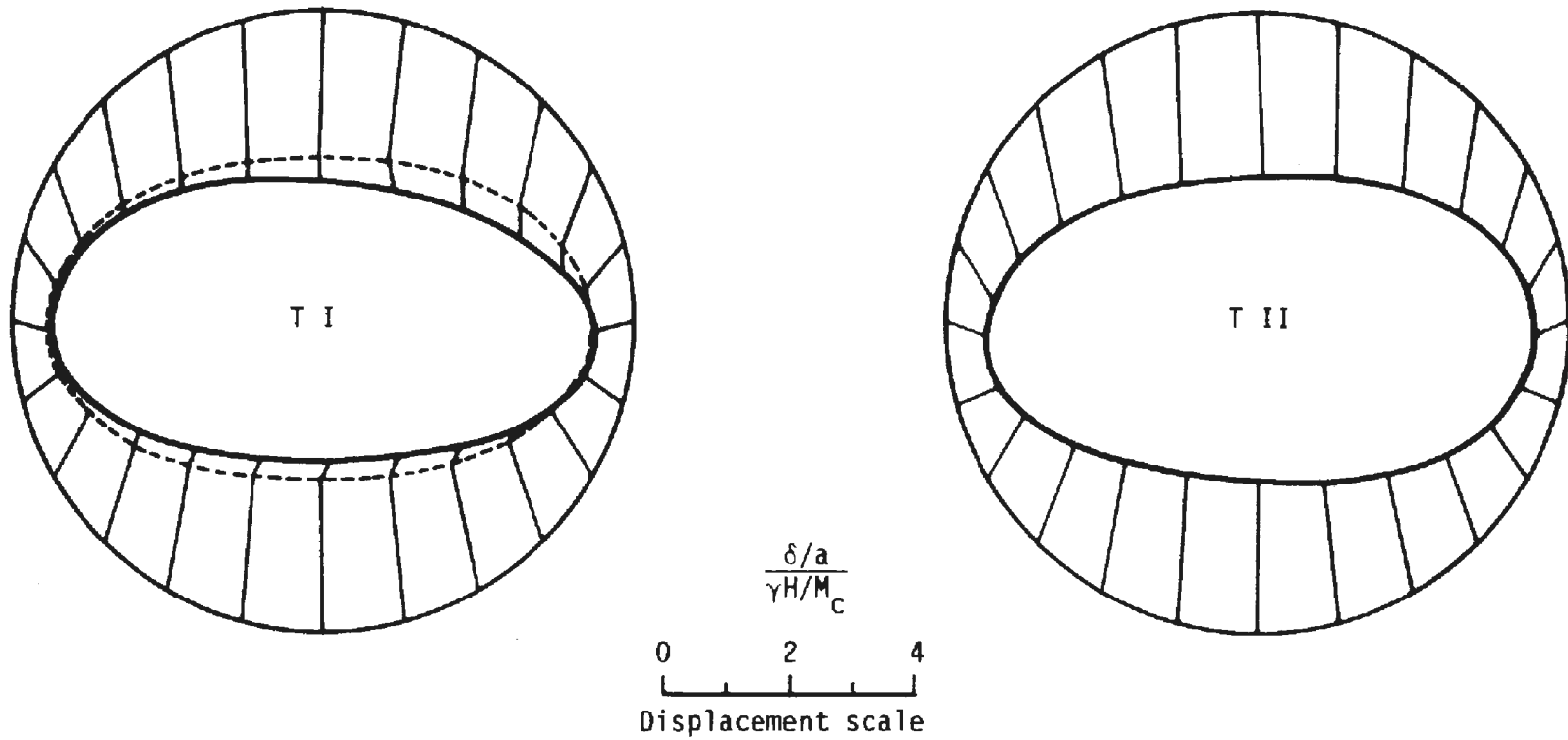
Displacements of the tunnel openings for the unsymmetrical analyses TB13 through TB17 (shallow tunnels) and TB30 through TB34 (deep tunnels) are given in Figs. 3.23 through 3.27 and Figs. 3.28 through 3.32, respectively. In order to clearly show the displacements of the lined tunnels a rather large displacement scale was necessary. Since the displacements of the unlined openings were several times greater than the liner displacements the shapes of the deformed openings are rather severely distorted. It must be kept in mind

that the displacements are measured in fractions of an inch while the tunnels are 20 ft (6 m) in diameter. In all analyses the left tunnel, designated T1, was excavated first, followed by the right tunnel, designated TII. Displacements due to the excavation of tunnel I are shown by the dashed curve, while displacements resulting from the excavation of the second tunnel are shown by the continuous curves. Thus, displacements given by the dashed curves are equivalent to those for single tunnels.

Figure 3.23 gives the displacements for the shallow case when both tunnels remain unlined. Upon excavation of the second tunnel, both the crown and invert of the first tunnel move further inward. In addition, a lateral translation of the entire opening toward tunnel II is indicated. The right springline of tunnel I is also displaced downward, reflecting the vertical compression of the pillar.

Displacements for the shallow case when both tunnels are lined immediately upon excavation are given in Fig. 3.24. Installation of the liner simultaneously with excavation results in a buoyancy effect in two-dimensional, plane strain, elastic analyses. Thus, in Fig. 3.24 it can be seen that for a single tunnel at shallow depth the crown is forced downward ($K_0 = 1/2$) only a small distance, whereas the invert and springlines exhibit a significantly larger upward movement. When the second tunnel and liner are installed the combined effect of both tunnels contributes to a rise of the second tunnel crown and a general upward translation of tunnel I. As the left springline of tunnel II is forced outward, this displacement is transmitted through the pillar causing an inward displacement of the right springline of the first tunnel.

----- Initial displacements (excavation of tunnel I)
—— Final displacements

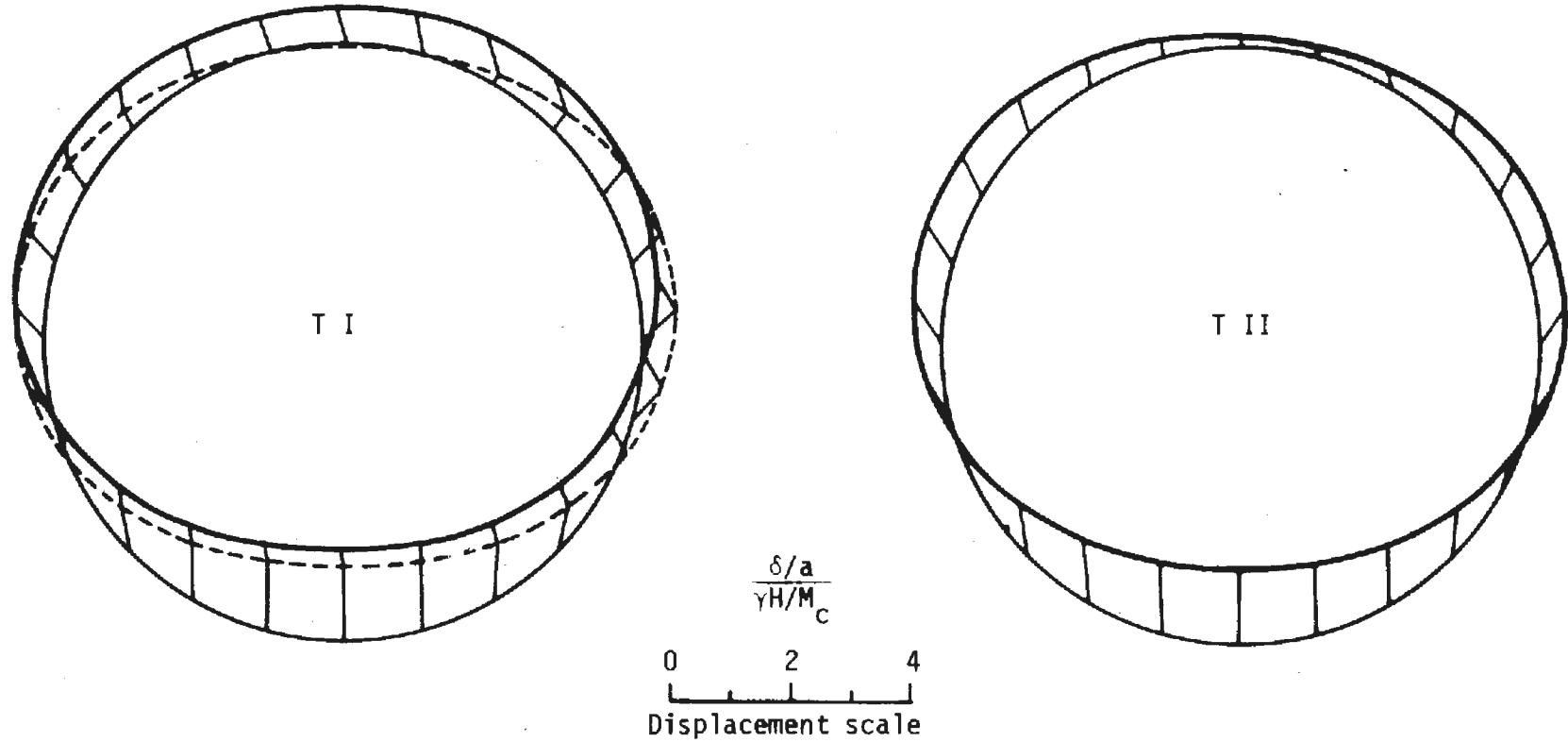


3-39

FIGURE 3.23 TUNNEL DISPLACEMENTS FOR TB13 (H/D = 1.5)

----- Initial displacements (excavation of tunnel I)

———— Final displacements



3-40

FIGURE 3.24 TUNNEL DISPLACEMENTS FOR TB14 (H/D = 1.5)

Plotted in Fig. 3.25 are the tunnel displacements for the shallow tunnel analysis TB15. For this analysis the left tunnel was excavated and lined in one step. Upon excavation of the right tunnel (unlined) the resulting medium displacements caused a small additional inward movement of the liner crown and invert and a general lateral translation of the liner to the right. The presence of the liner in tunnel I had an effect on the displacements of tunnel II. The liner, in effect, strengthened the pillar, thus restricting vertical compression of the pillar. Note that there has been almost no vertical movement of the second tunnel's left springline and that the crown has experienced approximately 20 percent less inward displacement than was the case when both tunnels were unlined (Fig. 3.23).

Figure 3.26 shows the tunnel displacements for analysis TB16 ($H/D = 1.5$). In this analysis tunnel I was not lined until all displacements had already occurred (dashed line). Tunnel II on the other hand was lined simultaneously with excavation. The pattern of displacements observed for this analysis are similar in all major respects to that obtained from analysis TB14. Here, however, all liner displacements are due solely to the creation of the second tunnel. As a result, the liner here experiences smaller displacements than in the former situation. The invert displacements are approximately 80 percent less in fact. In terms of the final shape of the lined opening, however, tunnel II in Fig. 3.26 has undergone significantly more displacement than that in Fig. 3.24, due to the large displacements that occurred before the liner was installed.

For analysis TB17 the liner in tunnel I was not installed until after all displacements had occurred. This is the only difference between the

----- Initial displacements (excavation of tunnel I)

———— Final displacements

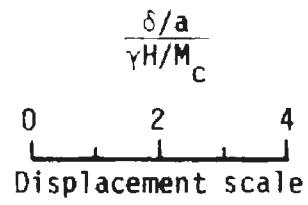
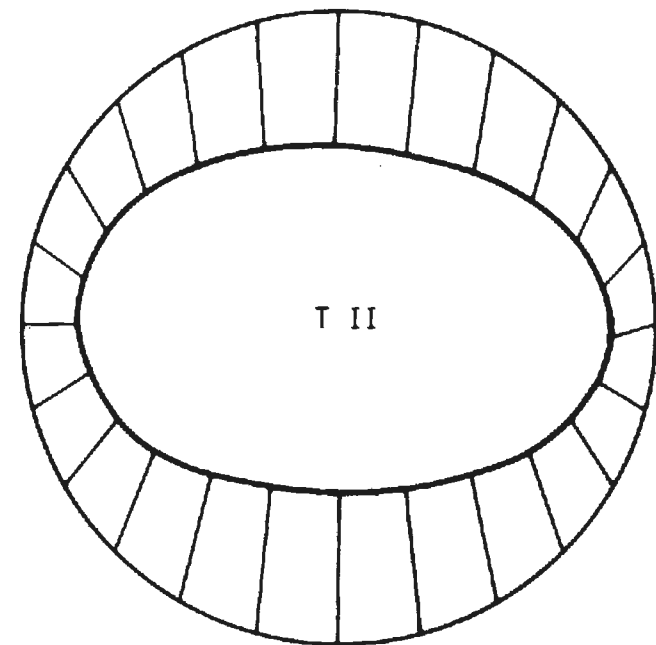
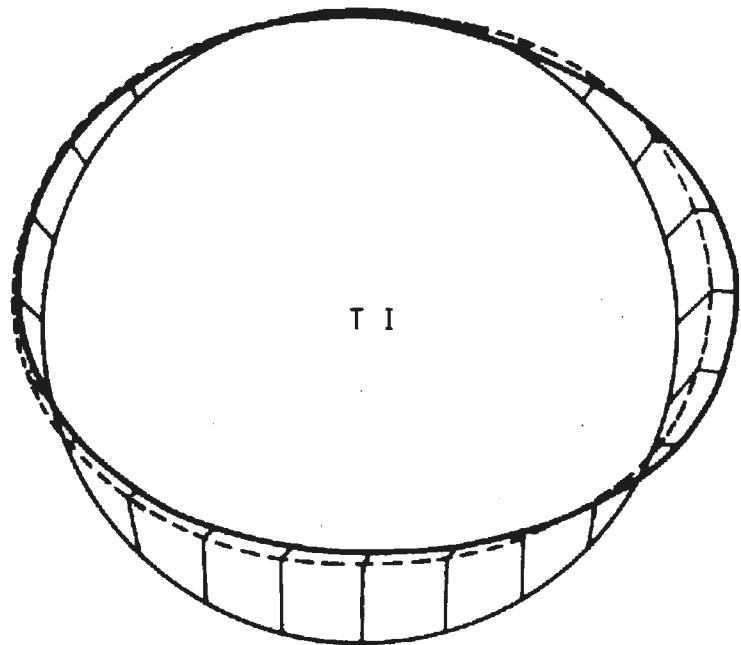


FIGURE 3.25 TUNNEL DISPLACEMENTS FOR TB15 (H/D = 1.5)

----- Initial displacements (excavation of tunnel I)
———— Final displacements

3-43

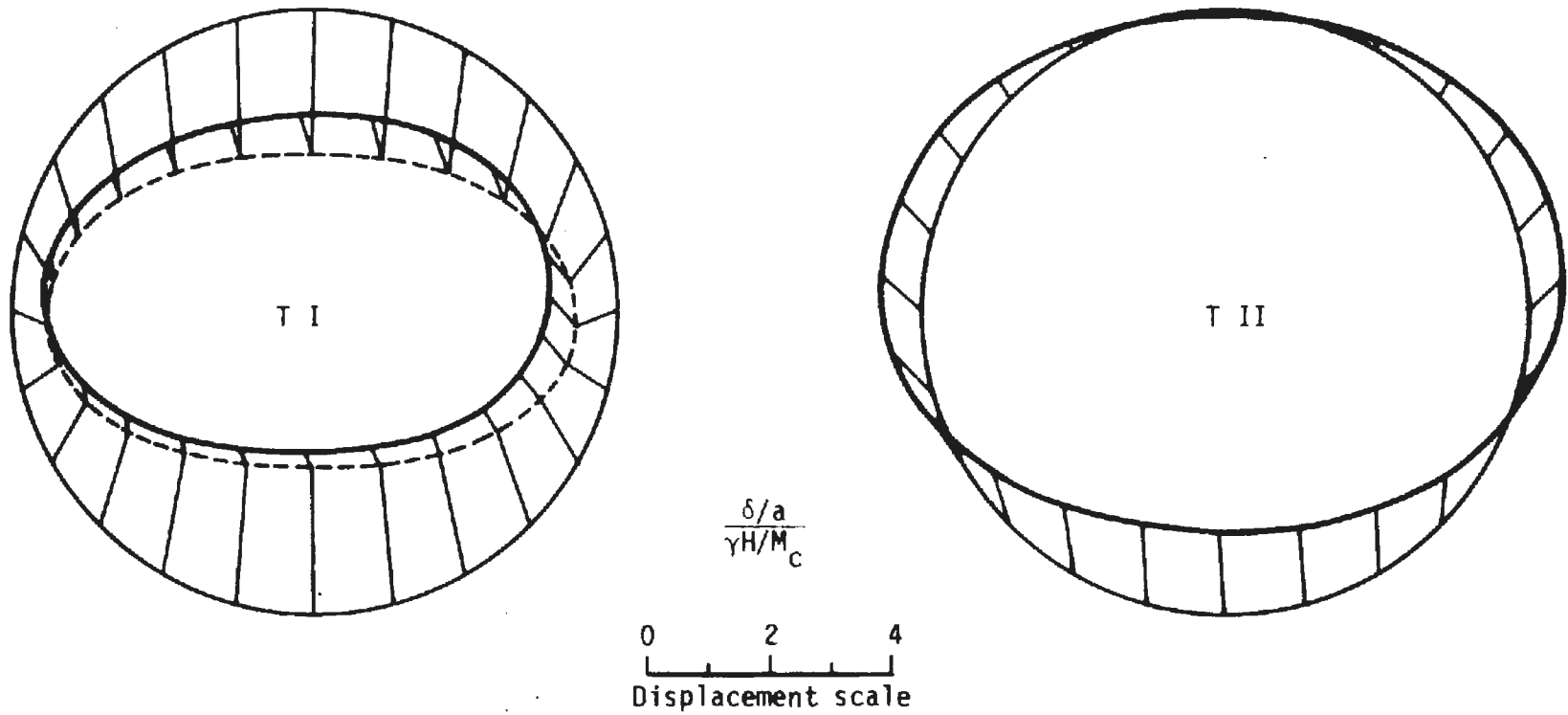


FIGURE 3.26 TUNNEL DISPLACEMENTS FOR TB16 (H/D = 1.5)

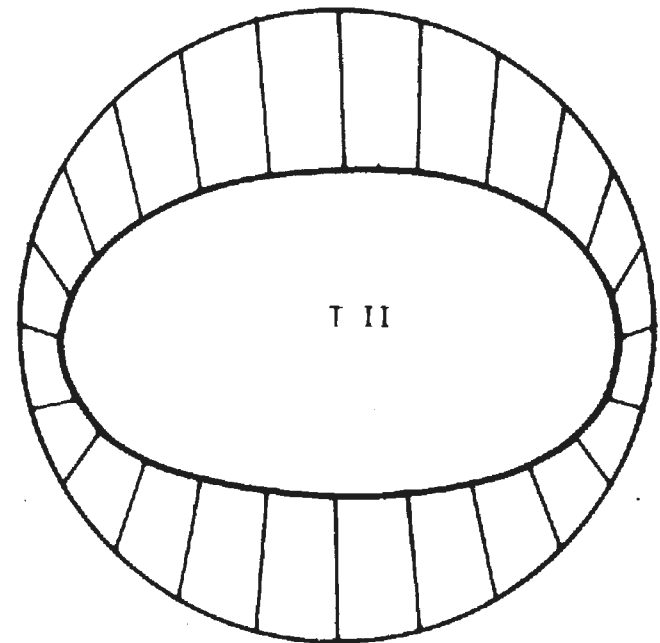
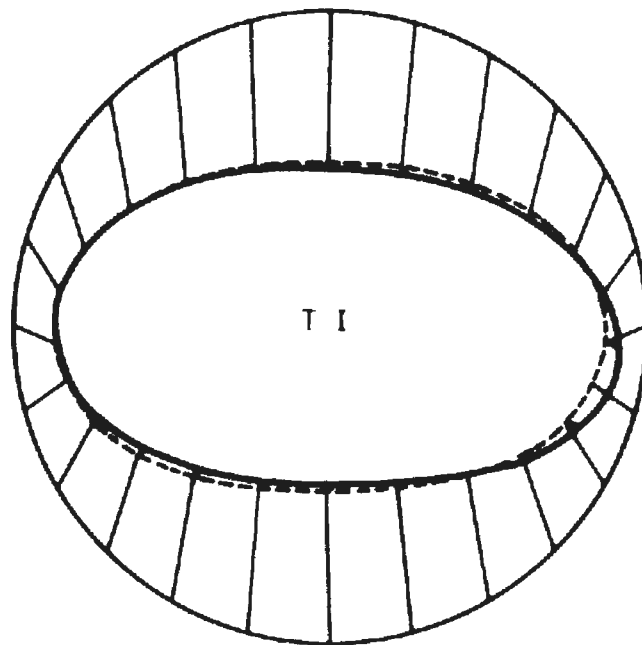
construction sequences of analyses TB17 and TB15, in which the tunnel I liner was installed simultaneously with excavation. In both analyses the second tunnel remained unlined. The tunnel displacements obtained from TB17 are given in Fig. 3.27. As mentioned previously, in analysis TB15 the liner in tunnel I appeared to act so as to help support the pillar and thus restrict the displacements in the second tunnel to values smaller than would have occurred had both tunnels been unlined. This sort of behavior is not indicated by Fig. 3.27 for TB15.

Tunnel displacements from the analyses of deep tunnels ($H/D = 5.5$) are given in Figs. 3.28 through 3.32. All displacements have been normalized with respect to tunnel depth. Thus, the displacement patterns exhibited by both shallow and deep tunnels are similar in most respects. However, since the increase of stress with depth was considered in these analyses normalization of the data with respect to depth does not result in identical plots for tunnels at different depths. The most significant difference, between the displacement curves for the shallow and deep analyses with identical construction sequences are associated with the displacements in the vertical direction. It was observed from the shallow tunnel analyses that when a liner was installed simultaneously with excavation there was a relatively large upward displacement of the invert, a somewhat smaller rise of the springlines, and a slight rise, or at best a small downward movement, of the crown. This pattern was not observed in the deep tunnel analyses. At the greater depth the downward pressure at the crown and the upward pressure at the invert are more nearly in balance. Thus, both the crown and invert move inward, with the displacement of the invert only slightly exceeding that of the crown, while the springlines experience almost no vertical displacement.

----- Initial displacements (excavation of tunnel I)

———— Final displacements

3-45



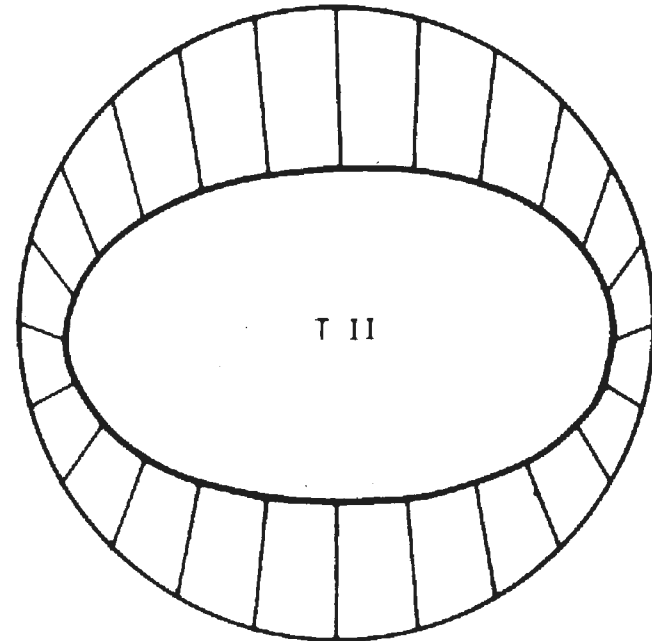
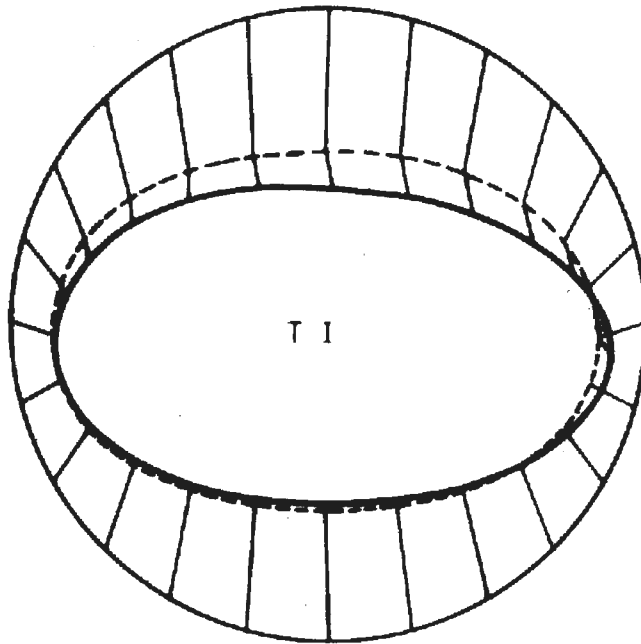
$$\frac{\delta/a}{\gamma H/M_c}$$

0 2 4
Displacement scale

FIGURE 3.27 TUNNEL DISPLACEMENTS FOR TB17 (H/D = 1.5)

----- Initial displacements (excavation of tunnel I)

———— Final displacements



$$\frac{\delta/a}{\gamma H/M_c}$$

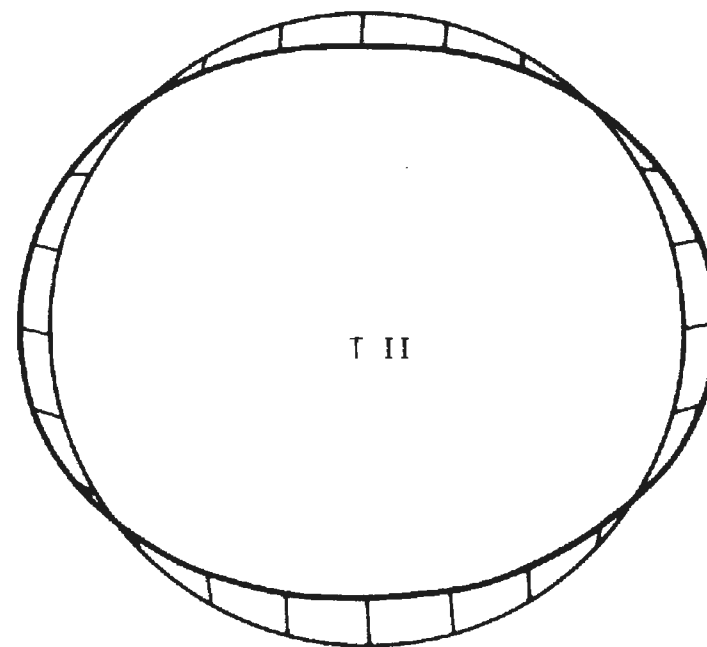
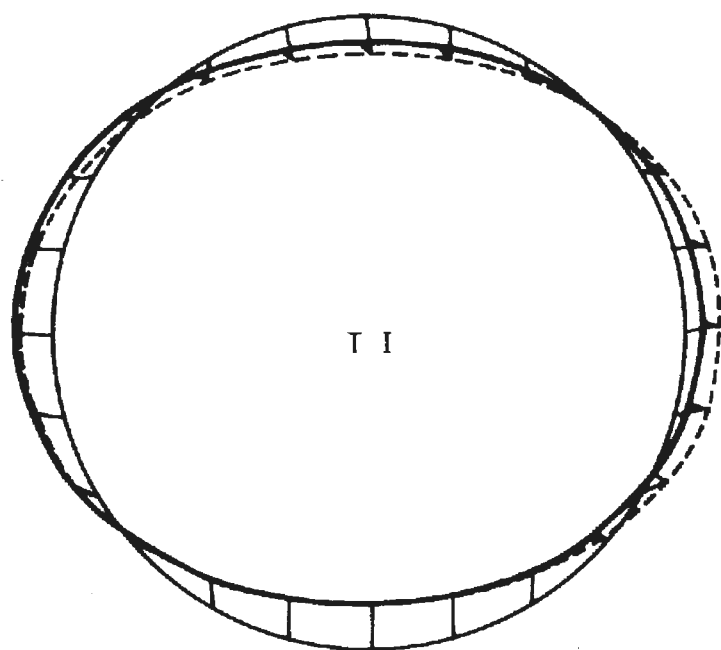
0 2 4
Displacement scale

FIGURE 3.28 TUNNEL DISPLACEMENTS FOR TB30 (H/D = 5.5)

----- Initial displacements (excavation of tunnel I)

———— Final displacements

3-47



$$\frac{\delta/a}{\gamma H/M_c}$$

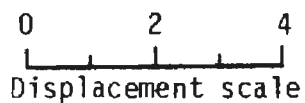
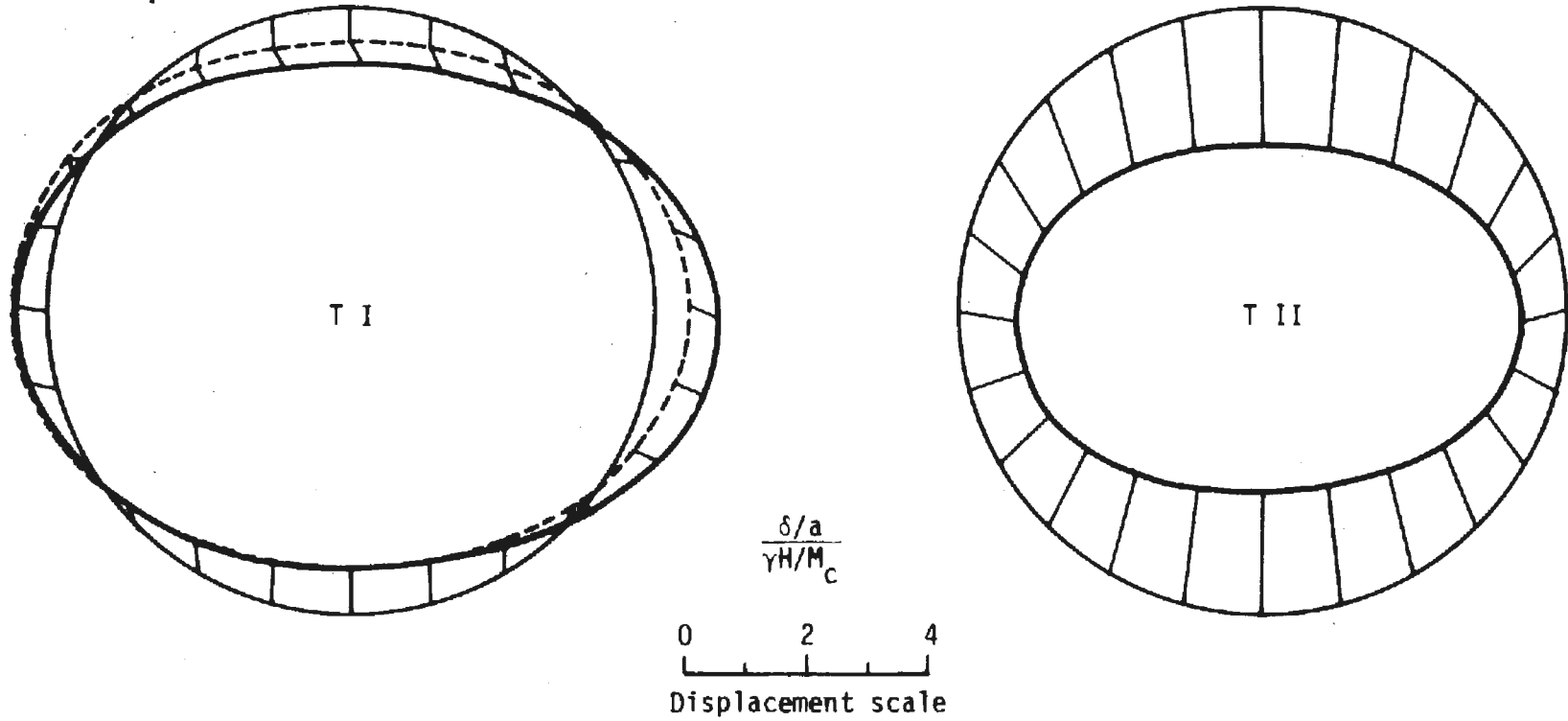


FIGURE 3.29 TUNNEL DISPLACEMENTS FOR TB31 (H/D = 5.5)

----- Initial displacements (excavation of tunnel I)

———— Final displacements



3-48

FIGURE 3.30 TUNNEL DISPLACEMENTS FOR TB32 (H/D = 5.5)

----- Initial displacements (excavation of tunnel I)
———— Final displacements

3-49

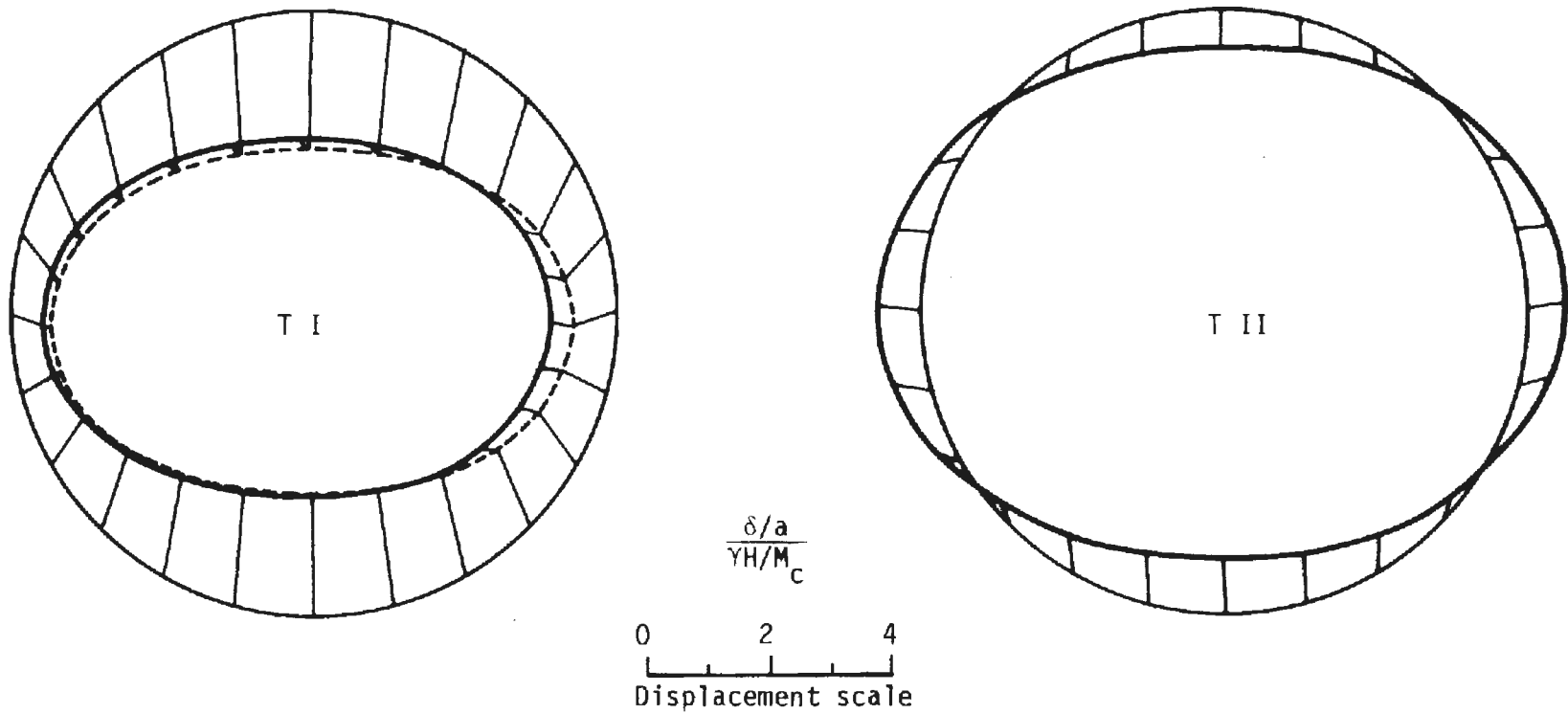
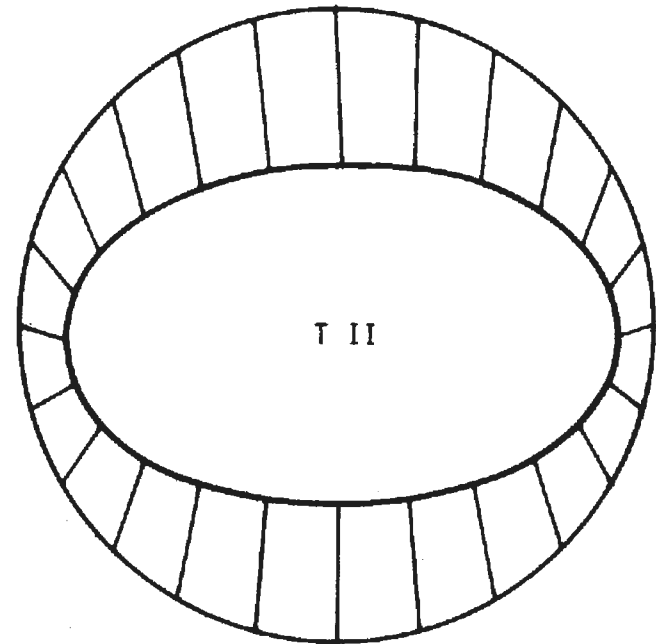
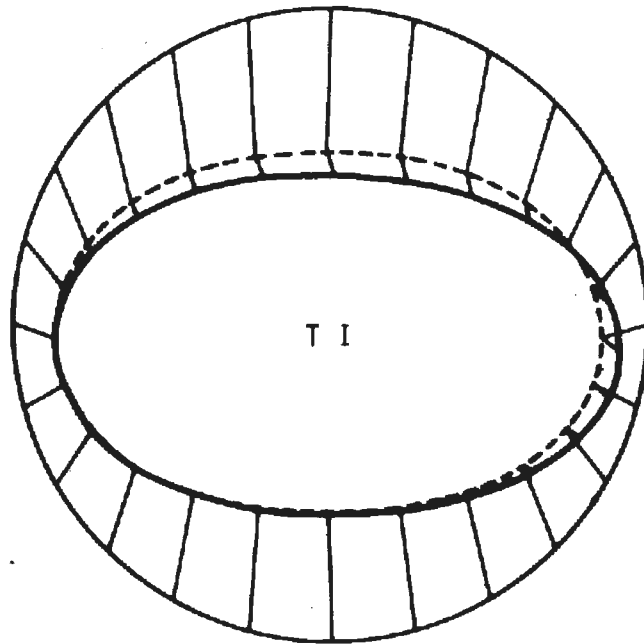


FIGURE 3.31 TUNNEL DISPLACEMENTS FOR TB33 (H/D = 5.5)

----- Initial displacements (excavation of tunnel I)

———— Final displacements

3-50



$$\frac{\delta/a}{\gamma H/M_c}$$

0 2 4
Displacement scale

FIGURE 3.32 TUNNEL DISPLACEMENTS FOR TB34 (H/D = 5.5)

SURFACE DISPLACEMENTS

Normalized displacements of the ground surface obtained from the unsymmetrical analyses of shallow tunnels ($H/D = 1.5$) are given in Fig. 3.33. Two displacement profiles are shown for each analysis. One shows the initial displacements due to excavation of the first tunnel and the other shows the total final displacements that exist after both tunnels have been excavated.

Initial displacements in analyses TB13, TB16 and TB17 were identical because they all assumed the first tunnel to be unlined. Final displacements for TB13 and TB17 were the largest observed for the shallow tunnel analyses. In TB17 a liner was installed in tunnel I before tunnel II was excavated, thus the final displacements, especially directly above tunnel I, are smaller than those in TB13 in which both tunnels remained unlined throughout the analysis. In analysis TB16 both tunnels were lined on the step when the second tunnel was excavated. Because of the displacements of these tunnel liners the ground surface was pushed up from the position it had assumed after the excavation of tunnel I.

In analyses TB14 and TB15 tunnel I was lined simultaneously with excavation. Thus, the profile of surface heave observed from the shallow, single lined tunnel is also observed as the initial displacements in these two analyses. In TB14 the second tunnel was also lined immediately upon excavation and it can be seen that additional surface heave was the result. The second tunnel was left unlined in analysis TB15. This resulted in a final, net surface settlement over the region to the right of a point above the first tunnel centerline. It had no significant effect on surface movement to the left of the first tunnel, however.

3-52

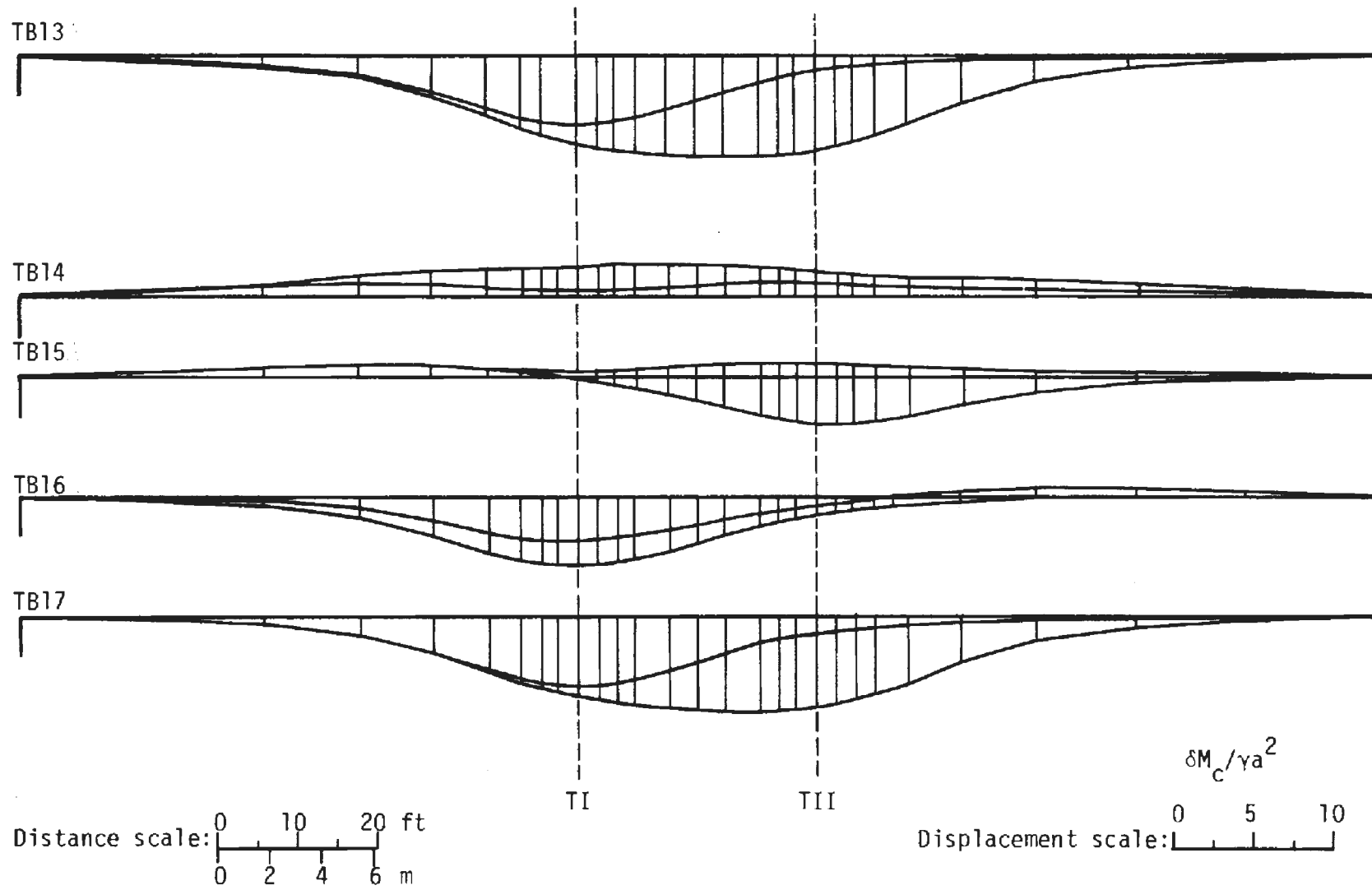


FIGURE 3.33 SURFACE DISPLACEMENTS FOR THE SHALLOW TUNNELS ($H/D = 1.5$) - UNSYMMETRICAL CASE

Figure 3.34 gives the surface displacements for the deep tunnel analyses. The various displacement profiles are given in the same order, with respect to construction sequence assumed, as in Fig. 3.33. Thus, the only difference between the corresponding analyses is the depth of the tunnels. It can be seen that, as with the symmetrical analyses of deep tunnels, the lateral extent of the finite element mesh was not sufficient to give the complete settlement trough. Although the displacements in the region above the tunnels are reliable, those near the mesh boundaries are undoubtedly distorted.

Surface displacements over the lined tunnels all take the form of settlement rather than heave as was observed for the shallow tunnels. These displacements can all be directly related to the displacements of the liners at depth.

3.3.3 LINER FORCES AND MOMENTS

Liner forces and moments from the unsymmetrical analyses are summarized in Tables 3.5, 3.6 and 3.7 in the form of dimensionless coefficients. Also shown in these tables are the coefficients obtained from the single tunnel analyses. Values are given for points located every 45° around the liner circumference.

The thrust coefficient values in Table 3.5 show that liner thrusts for analyses TB14 and TB31, in which both tunnels were lined simultaneously with excavation, differ only slightly from those obtained for the single tunnels. This parallels what was observed from the symmetrical analyses. When the first tunnel is lined immediately upon excavation and then a second, unlined tunnel is excavated along side, the result is an increase in thrust in

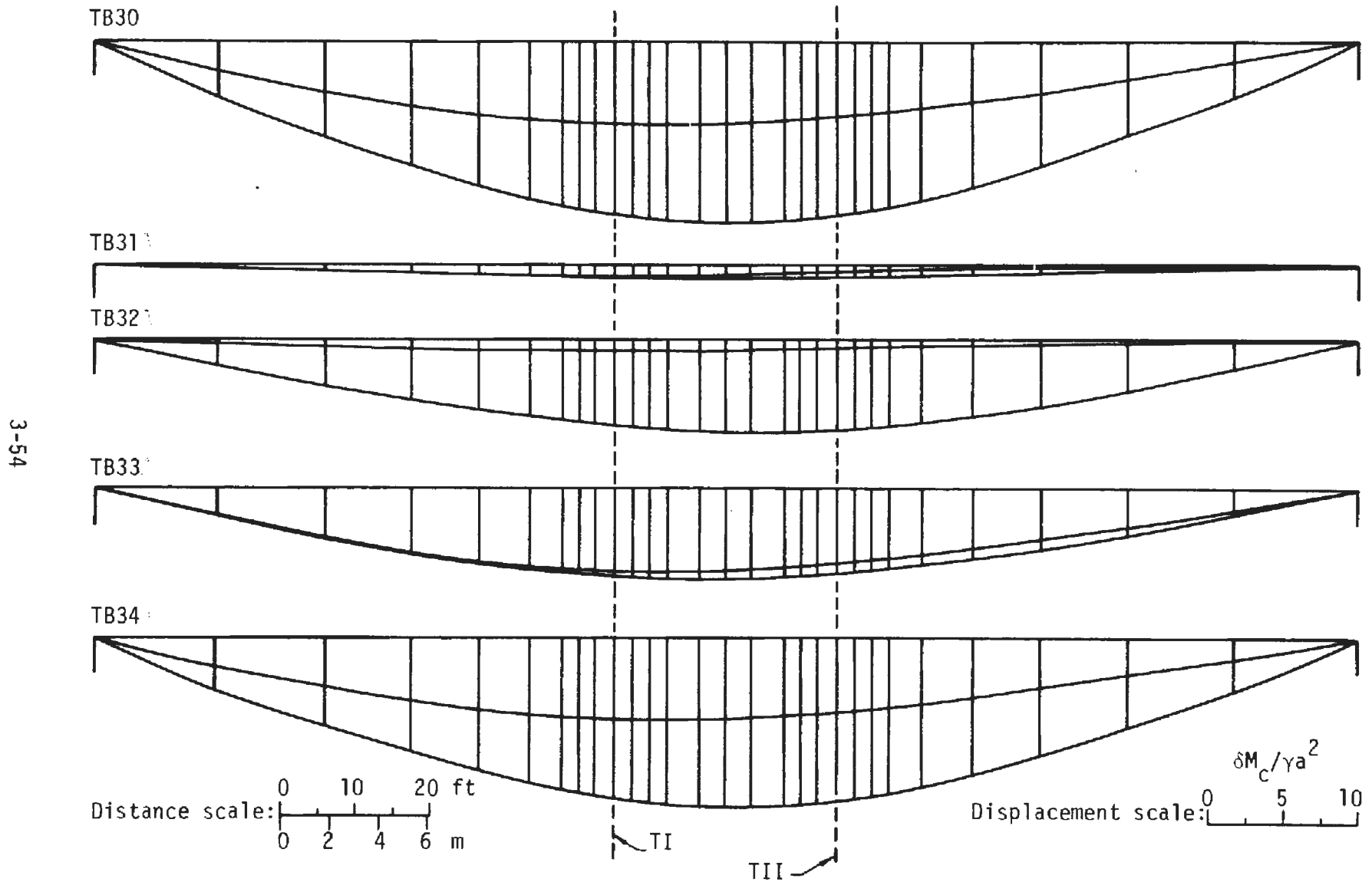


FIGURE 3.34 SURFACE DISPLACEMENTS FOR THE DEEP TUNNELS ($H/D = 5.5$) - UNSYMMETRICAL CASE

TABLE 3.5

THRUST COEFFICIENTS ($T/\gamma H a$) FROM THE LINED TUNNEL ANALYSES - UNSYMMETRICAL CASE

	θ (degrees)*	ST1	TB14		TB15	TB16		TB17
		Single tunnel	Tunnel I	Tunnel II	Tunnel I	Tunnel I	Tunnel II	Tunnel I
H/D = 1.5	0	.836	.786	.808	.984	-.002	.863	.203
	45	.591	.627	.573	.616	.059	.626	.074
	90	.435	.469	.454	.493	.046	.449	.023
	135	.591	.562	.620	.618	-.017	.625	.051
	180	.836	.781	.803	.849	-.018	.908	.051
	225	.768	.745	.748	.751	-.001	.795	.020
	270	.631	.645	.638	.599	.040	.627	.007
	315	.768	.761	.767	.807	.033	.787	.110
		ST3	TB31		TB32	TB33		TB34
	θ (degrees)*	Single tunnel	Tunnel I	Tunnel II	Tunnel I	Tunnel I	Tunnel II	Tunnel I
H/D = 5.5	0	.865	.873	.869	1.018	.045	.899	.194
	45	.677	.741	.696	.702	.095	.709	.079
	90	.523	.571	.558	.498	.061	.522	.008
	135	.677	.692	.722	.708	.033	.708	.050
	180	.865	.861	.865	.912	.028	.936	.081
	225	.725	.732	.762	.731	.029	.753	.030
	270	.574	.616	.607	.541	.061	.571	.000
	315	.725	.779	.742	.753	.097	.748	.088

* θ is measured counter-clockwise from the right springline.

TABLE 3.6

MOMENT COEFFICIENTS ($M/\gamma H a^2$) FROM THE LINED TUNNEL ANALYSES - UNSYMMETRICAL CASE

θ (degrees)*	ST1	TB14		TB15	TB16		TB17
	Single tunnel	Tunnel I	Tunnel II	Tunnel I	Tunnel I	Tunnel II	Tunnel I
0	.0084	.0037	.0079	.0139	-.0066	.0093	.0031
45	.0005	.0017	-.0012	-.0039	.0018	.0004	-.0038
90	-.0081	-.0057	-.0070	-.0084	.0029	-.0088	.0003
135	.0005	-.0012	.0018	.0011	-.0016	-.0015	.0008
180	.0084	.0069	.0058	.0093	-.0013	.0114	.0011
225	.0018	.0022	.0009	.0021	-.0005	.0002	-.0007
270	-.0105	-.0090	-.0087	-.0128	.0020	-.0111	-.0018
315	.0018	.0031	.0011	.0012	.0019	.0009	.0002
θ (degrees)*	ST3	TB31		TB32	TB33		TB34
	Single tunnel	Tunnel I	Tunnel II	Tunnel I	Tunnel I	Tunnel II	Tunnel I
0	.0089	.0049	.0088	.0154	-.0059	.0102	.0036
45	.0009	.0002	-.0002	-.0020	.0017	.0007	-.0018
90	-.0092	-.0084	-.0085	-.0118	.0016	-.0104	-.0021
135	.0009	.0002	.0013	.0018	-.0011	-.0008	.0004
180	.0089	.0083	.0066	.0109	-.0003	.0117	.0021
225	.0012	.0008	.0013	.0014	-.0010	-.0004	-.0006
270	-.0099	-.0092	-.0090	-.0125	.0012	-.0108	-.0019
315	.0012	.0026	.0000	-.0007	.0019	.0003	-.0009

* θ is measured counter-clockwise from the right springline.

TABLE 3.7

SHEAR COEFFICIENTS ($V/\gamma H\alpha$) FROM THE LINED TUNNEL ANALYSES - UNSYMMETRICAL CASE

	θ (degrees)*	ST1	TB14		TB15	TB16		TB17
		Single tunnel	Tunnel I	Tunnel II	Tunnel I	Tunnel I	Tunnel II	Tunnel I
H/D = 1.5	0	.004	.009	.006	.008	-.002	.004	.003
	45	.014	.008	.013	.019	-.007	.014	.004
	90	.000	.004	-.004	.006	.004	.003	-.006
	135	-.014	-.012	-.011	-.014	.003	-.017	.000
	180	-.004	-.009	-.003	-.003	.000	-.005	.002
	225	.020	.017	.016	.021	-.003	.024	.001
	270	.000	-.002	.001	.003	-.004	-.002	.000
	315	-.020	-.013	-.019	-.027	.010	-.021	-.004
<hr/>								
	θ (degrees)*	ST3	TB31		TB32	TB33		TB34
		Single tunnel	Tunnel I	Tunnel II	Tunnel I	Tunnel I	Tunnel II	Tunnel I
H/D = 5.5	0	.001	.001	.001	.001	-.001	.001	.000
	45	.017	.013	.016	.026	-.006	.018	.006
	90	.000	.003	-.002	-.005	.003	.002	-.004
	135	-.017	-.016	-.014	-.020	.001	-.021	-.003
	180	.001	-.001	-.001	.000	-.000	-.001	.001
	225	.018	.017	.015	.021	-.001	.022	.002
	270	.000	-.003	.002	.003	-.004	-.001	.001
	315	-.018	-.014	-.018	-.026	.007	-.019	-.005

* θ is measured counter-clockwise from the right springline.

the pillar side of the liner to a level significantly above that for a single tunnel (TB15 and TB32). Maximum liner thrust for this excavation sequence is approximately equal to that due to the full overburden pressure ($T = \gamma H a$). For analyses TB16 and TB33 the first tunnel was not lined until all displacements had occurred, while the second tunnel was lined simultaneously with excavation. This led to very small thrusts in tunnel I. In fact, for the shallow case tensile forces were found to exist in the invert and right springline. Thrusts in the tunnel II liner approximated those for the single tunnel case everywhere except in the left (pillar side) springline where they were slightly higher. For analyses TB17 and TB34, in which the construction sequence was similar to that for TB16 and TB33 except that the second tunnel was unlined, low thrust values were again observed. Maximum thrusts were located around the right springline, adjacent to the pillar.

Moment coefficients are given in Table 3.6. In general, the liner moments are relatively small. In no instance do they exceed two percent of $\gamma H a^2$. The largest moments occur in those liners that were installed immediately upon excavation and that were later influenced by an adjacent unlined tunnel (TB15 and TB32). The general trend is to negative moments in the crown and invert and positive moments at the springlines. This pattern was reversed for tunnel I in analyses TB16 and TB33, however, due to the displacements imposed on these liners by the adjacent lined tunnels. The smallest moments were observed in the tunnel I liners of analyses TB17 and TB34. However, as will be discussed in Chapter 4, magnitude and sign are of little significance when moments alone are considered. What is important is the combined contribution of both bending moments and thrusts to liner stresses.

Shear force coefficients for the eight, equally spaced points around the liners are given in Table 3.7. It is evident that the shear forces are everywhere very small. The maximum shear invariably exists in combination with high thrust values or at points where bending moments and thrusts are more significant in affecting liner integrity.

3.4 ELASTO-PLASTIC ANALYSES

Three elasto-plastic analyses were performed in this study, one each for the single tunnel, symmetrical two tunnel and unsymmetrical two tunnel cases.

In a previous study [1] utilizing an axisymmetric finite element analysis it was shown that the plastic zone around an advancing tunnel begins to form at a point ahead of the tunnel face. The radius of the plastic zone around the excavated tunnel increases from a minimum value at the face to a maximum value at some distance behind the face. The maximum radius, R , and the distance behind the face at which it occurs are both influenced by the in situ stresses, the properties of the medium, the stiffness of the liner, and the point of liner installation. If the tunnel is left unlined the maximum radius of the plastic zone corresponds to that given by a two-dimensional, plane-strain analysis. It was found that the point at which the maximum radius occurred was located a distance of approximately $3R$ behind the face. If a liner is installed a short distance behind the face ($<3R$) a smaller plastic

zone results. The maximum radius of this reduced plastic zone, $R_L < R$, is achieved only a short distance behind the leading end of the liner.

With the type of two-dimensional analysis used in this study only two sequences of excavation and liner installation were possible. These were as follows:

1. Excavate and line the tunnel on separate steps of the analysis.
2. Excavate and line the tunnel on the same step of the analysis.

When the first option is used all medium displacements occur, and the plastic zone is fully developed, before the liner is installed. This corresponds to the case where the liner is installed at a distance greater than $3R$ behind the face. Unless the medium exhibits time-dependent behavior or additional events occur (passage of a second tunnel) the liner will remain unstressed and undeformed.

The second option approximates the case where the liner is installed right at the tunnel face. Actually, the approximation is not very good in an elasto-plastic analysis because the two-dimensional analysis cannot account for displacements and plastic yielding that occur ahead of the face. Unless the liner considered is very flexible the two-dimensional analysis will drastically underestimate the amount of plastic yielding.

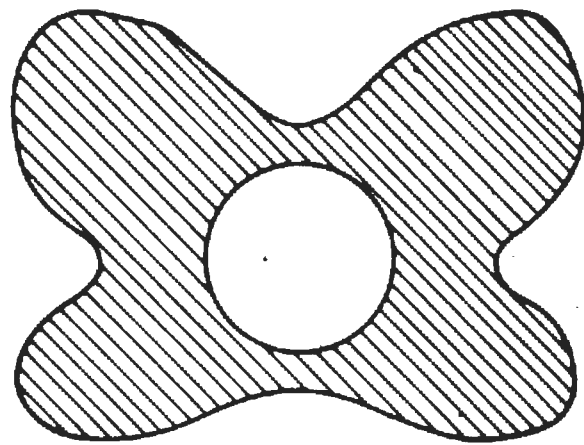
Thus, the two options that are available can only approximate two extreme conditions. The general practice of installing a liner a short distance behind the face can not be realistically considered with the standard two-dimensional, plane-strain analysis.

The elasto-plastic analyses performed here (see Tables 3.1, 3.2 and 3.3) were reruns of certain of the elastic analyses with the medium properties

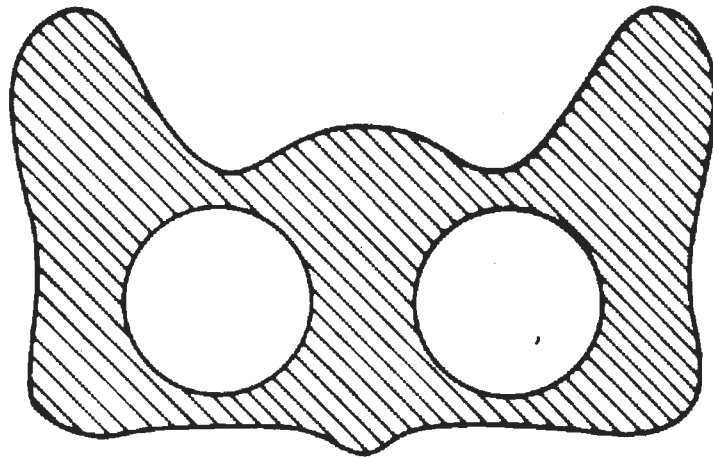
modified to reflect elasto-plastic behavior. For the single tunnel analysis the tunnel was left unlined because no yielding would have occurred had the tunnel been lined. The same applies to the symmetrical analysis of two parallel tunnels. For the unsymmetrical analysis it was assumed that the first tunnel was lined simultaneously with excavation while the second tunnel was unlined.

Plastic zones that formed around the tunnels are shown in Fig. 3.35. These zones correspond roughly to the regions of highest shear stress. For the single tunnel (ST4EP) and symmetrical case (TB8EP) analyses the regions of plastic yielding are symmetrical about vertical planes through the tunnel and pillar centerlines, respectively. In the unsymmetrical analysis (TB32EP) the first tunnel was lined simultaneously with excavation. The liner provided sufficient support to the medium to prevent yielding initially. When the second tunnel, which was left unlined, was excavated the medium surrounding it yielded. This induced additional displacement of the liner and the two small zones of yielding on the left side of the liner. Increased horizontal passive pressures exerted by the outward deflecting right springline of the liner helped keep the stress difference small in a region right next to the springline. As a result the medium there did not yield.

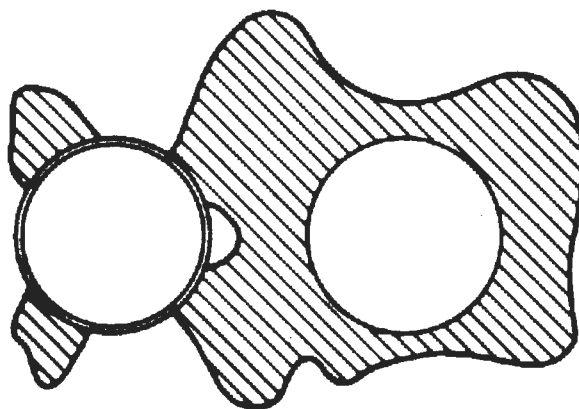
Plastic yielding around the unlined tunnels resulted in increased displacements of the tunnel openings and corresponding increases in the surface settlements. Displacements of the tunnel openings obtained from the linear-elastic and elasto-plastic analyses are compared for the single tunnel, symmetrical case, and unsymmetrical case in Figs. 3.36a, 3.36b and 3.37, respectively. The plots for the two tunnel analyses show only the total, final



ST4EP



TB8EP



TB32EP

FIGURE 3.35 PLASTIC ZONES

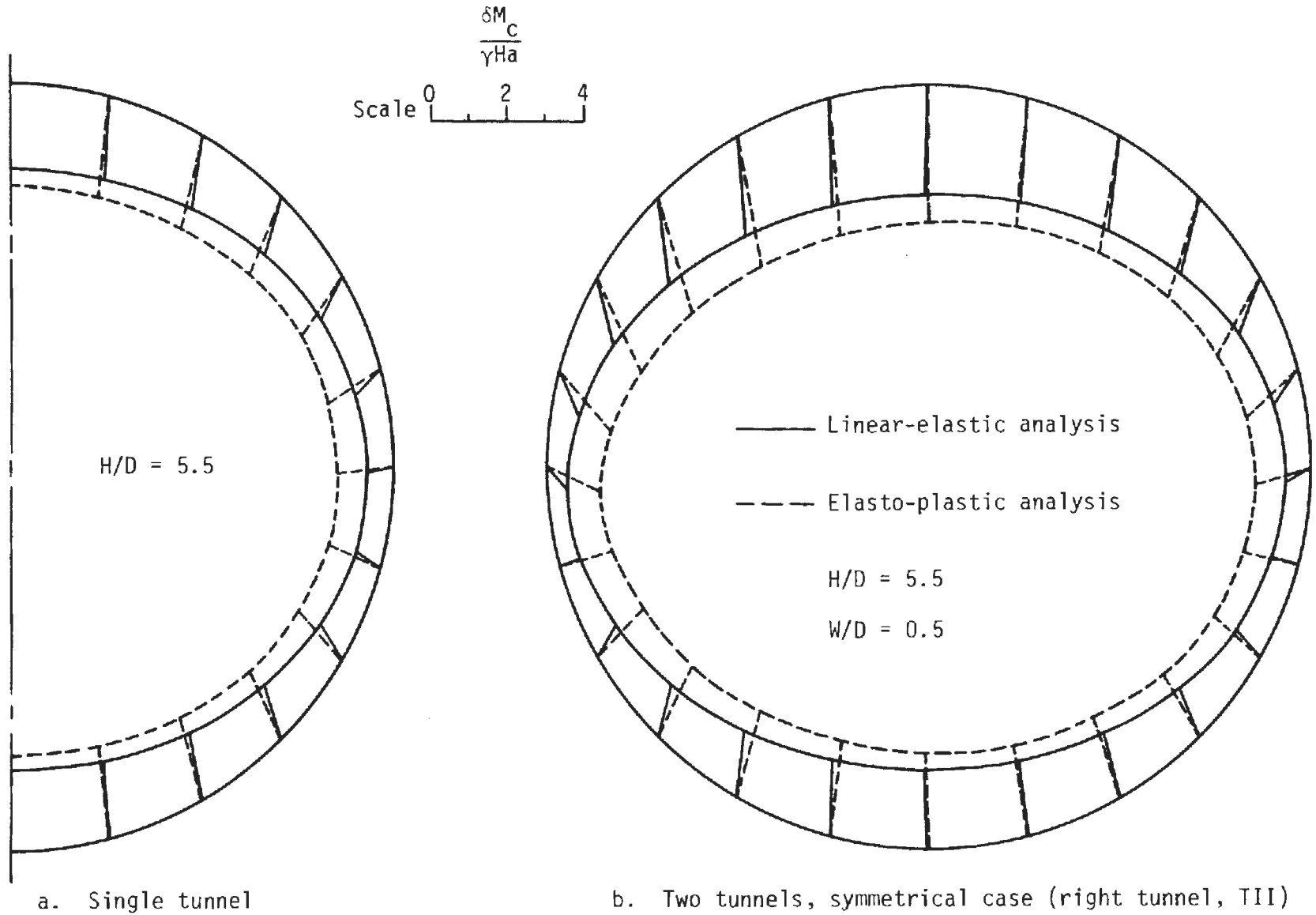


FIGURE 3.36 LINEAR-ELASTIC AND ELASTO-PLASTIC TUNNEL DISPLACEMENTS FOR SINGLE TUNNEL (ST4, ST4EP) AND SYMMETRICAL CASE (TB8, TB8EP)

----- Elasto-Plastic analysis (TB32EP)
————— Linear-Elastic analysis (TB32)

3-64

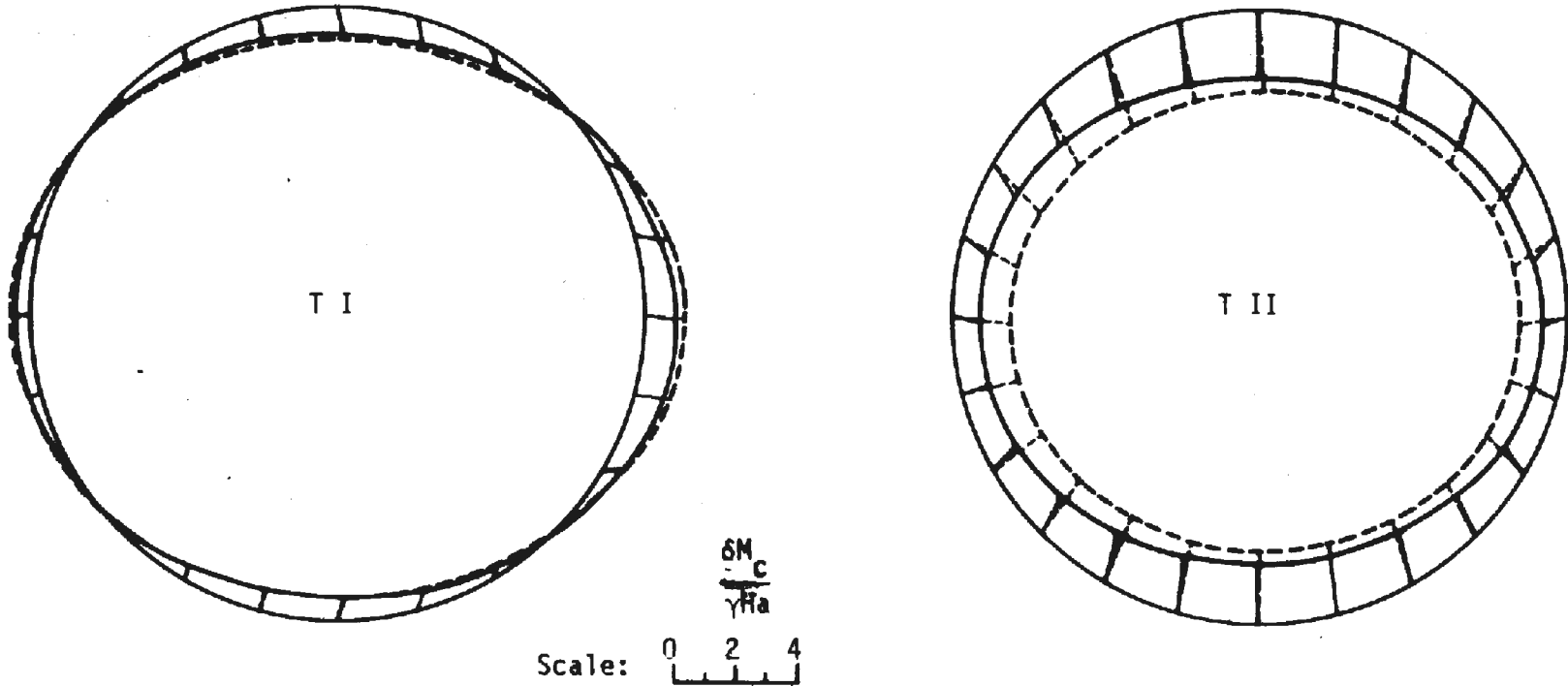


FIGURE 3.37 LINEAR-ELASTIC AND ELASTO-PLASTIC TUNNEL DISPLACEMENTS FOR THE UNSYMMETRICAL CASE

displacements experienced as a result of the creation of both tunnel openings. Similar comparisons for the vertical displacements of the medium are shown in Figs. 3.38 and 3.39. In these figures the non-dimensionalized displacements have been plotted for the ground surface and for four additional depths between the surface and the tunnels. These plots illustrate the attenuation and lateral spreading of the vertical displacements that occurs with increasing distance above the tunnels.

Of the three elasto-plastic analyses only TB32EP considered a lined tunnel. In this unsymmetrical analysis of the two tunnel problem, tunnel I was excavated and lined in one step. Although the medium had been assigned elasto-plastic stress-strain properties, support provided to the surrounding medium by the liner prevented the formation of a plastic zone. Thus, at the end of the first construction step of the analysis the distributions of forces and moments in the liner corresponded to those found at the end of the same step in elastic analysis TB32. Since, at this stage of the analysis, only one tunnel exists, the forces and moments also correspond to those given by the elastic single tunnel analysis ST3 (see Figs. 3.17, 3.18, 3.18 and Tables 3.5, 3.6, 3.7). In the next step of the analysis tunnel II was excavated, simulating the passage of a second, parallel, unlined tunnel. As a result of the creation of this second opening a considerable amount of plastic yielding occurred (Fig. 3.35). The passage of this second tunnel disturbed the equilibrium of the first tunnel causing a change in the force and moment distributions around its liner. The changes in liner thrusts and moments induced by the passage of the second tunnel are shown in Figs. 3.40 and 3.41, respectively. These changes are shown for both the linear-elastic analysis, TB32, and the elasto-plastic analysis, TB32EP.

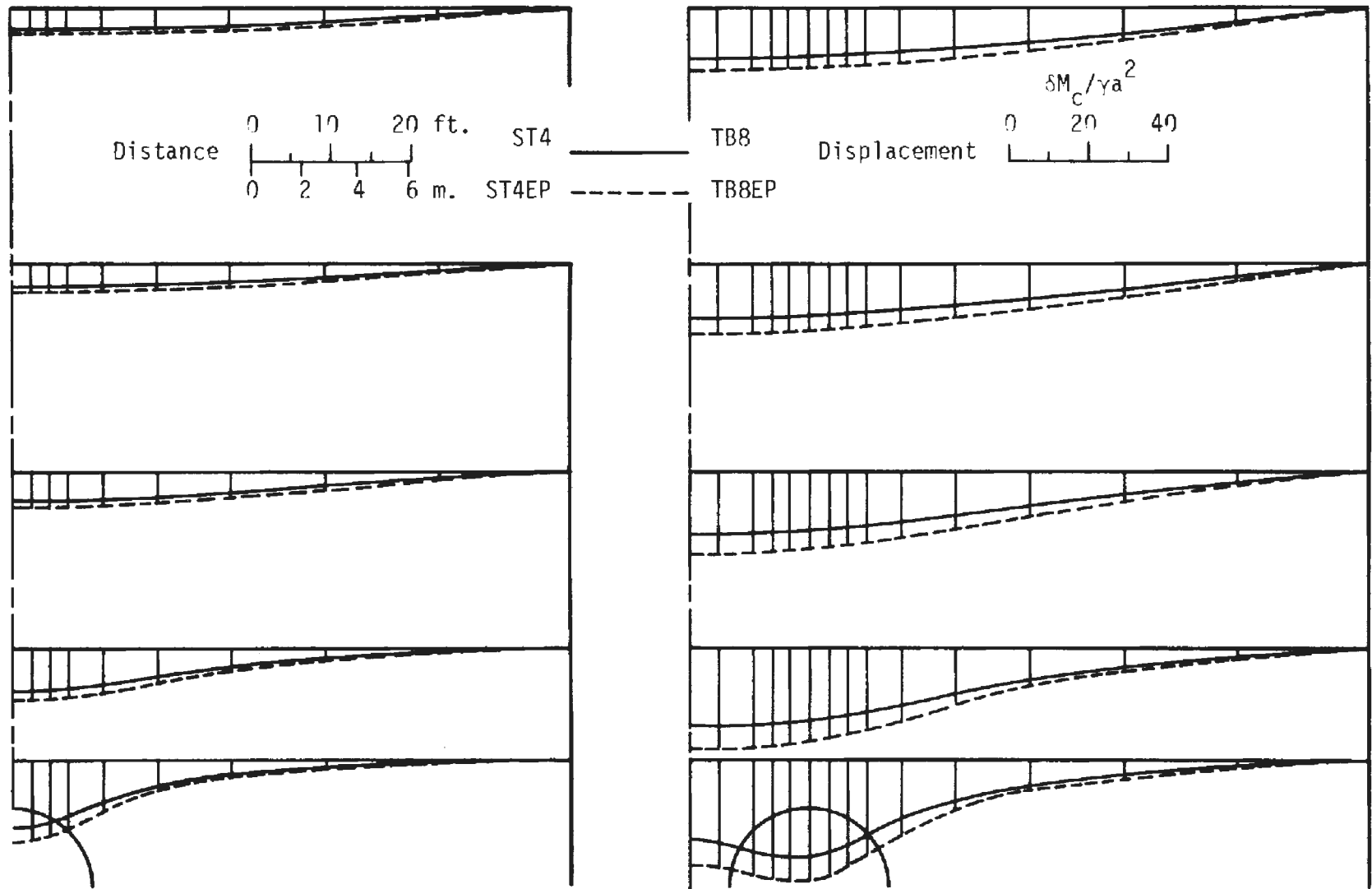


FIGURE 3.38 VARIATION OF VERTICAL GROUND DISPLACEMENTS WITH DEPTH - SINGLE TUNNEL AND SYMMETRICAL CASE LINEAR-ELASTIC AND ELASTO-PLASTIC ANALYSES

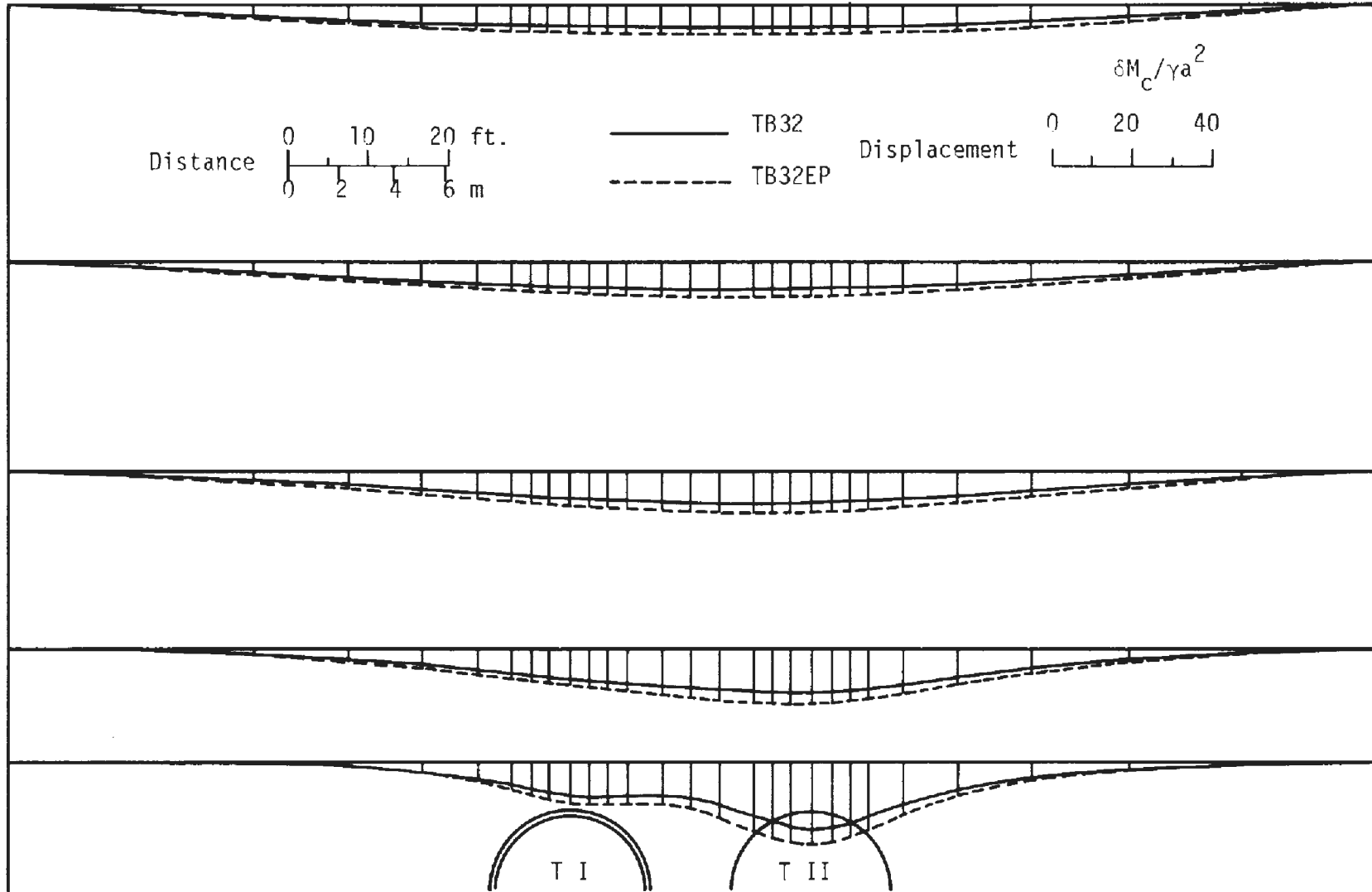


FIGURE 3.39 VARIATION OF VERTICAL GROUND DISPLACEMENTS WITH DEPTH - UNSYMMETRICAL CASE LINEAR-ELASTIC AND ELASTO-PLASTIC ANALYSES

Figure 3.40 shows that the passage of the second tunnel resulted in a thrust increase around the springlines of the tunnel I liner and a slight thrust reduction around the crown and invert. The changes in liner thrust were relatively small at all locations away from the pillar. The maximum thrust increase occurred at the right (pillar) springline. The linear-elastic analysis gave a thrust value at this point that was 20 percent larger than the single tunnel case value. For the elasto-plastic analysis the thrust increase at this same point was slightly smaller, amounting to 16 percent of the single tunnel value.

The changes in liner moments due to the passage of tunnel II are given in Fig. 3.41. This figure shows that the greatest changes occur on the right side of the liner, the side closest to tunnel II. It is also clear that the changes observed in the elasto-plastic analysis are significantly larger than those from the elastic analysis. Passage of the second tunnel caused additional positive moments at the right springline amounting to 70 percent of the single tunnel moment at that location in the elastic analysis and 150 percent in the elasto-plastic analysis. Percentage figures are essentially meaningless for expressing the additional moments that occur approximately 45° to either side of the right springline since the moments are approximately zero at these locations before the second tunnel passes.

Changes to the distribution of liner shear forces are not shown. These were relatively small for the elastic analysis. In the elasto-plastic analysis rather substantial shear forces were mobilized as a result of the extreme fluctuations in the moment distribution. However, relative to the great magnitudes of the thrusts and moments even these shears appear small. They could have only a minor influence on liner behavior.

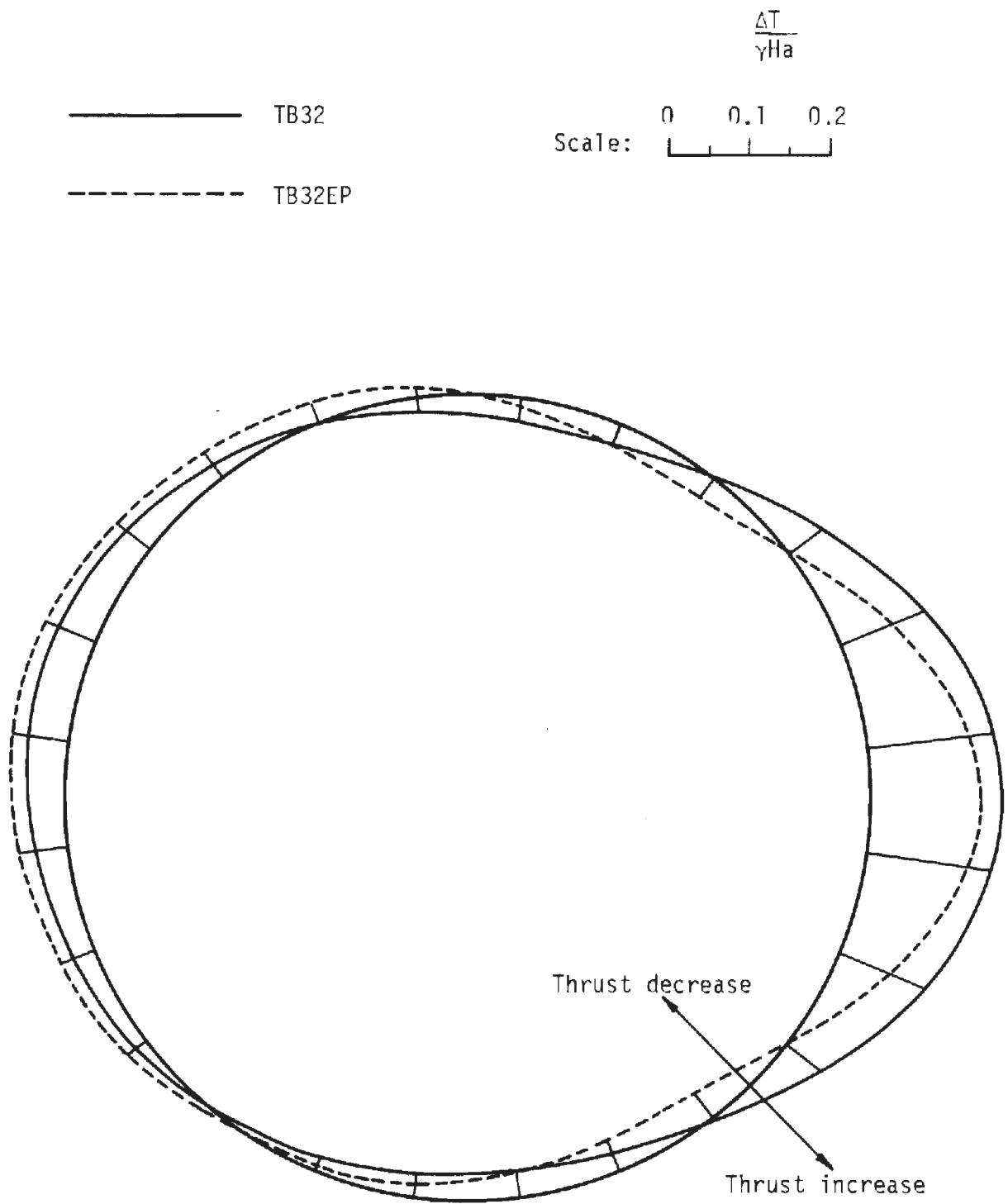


FIGURE 3.40 DISTRIBUTION OF LINER THRUST CHANGES (TUNNEL I)
DUE TO PASSAGE OF TUNNEL II (TB32, TB32EP)

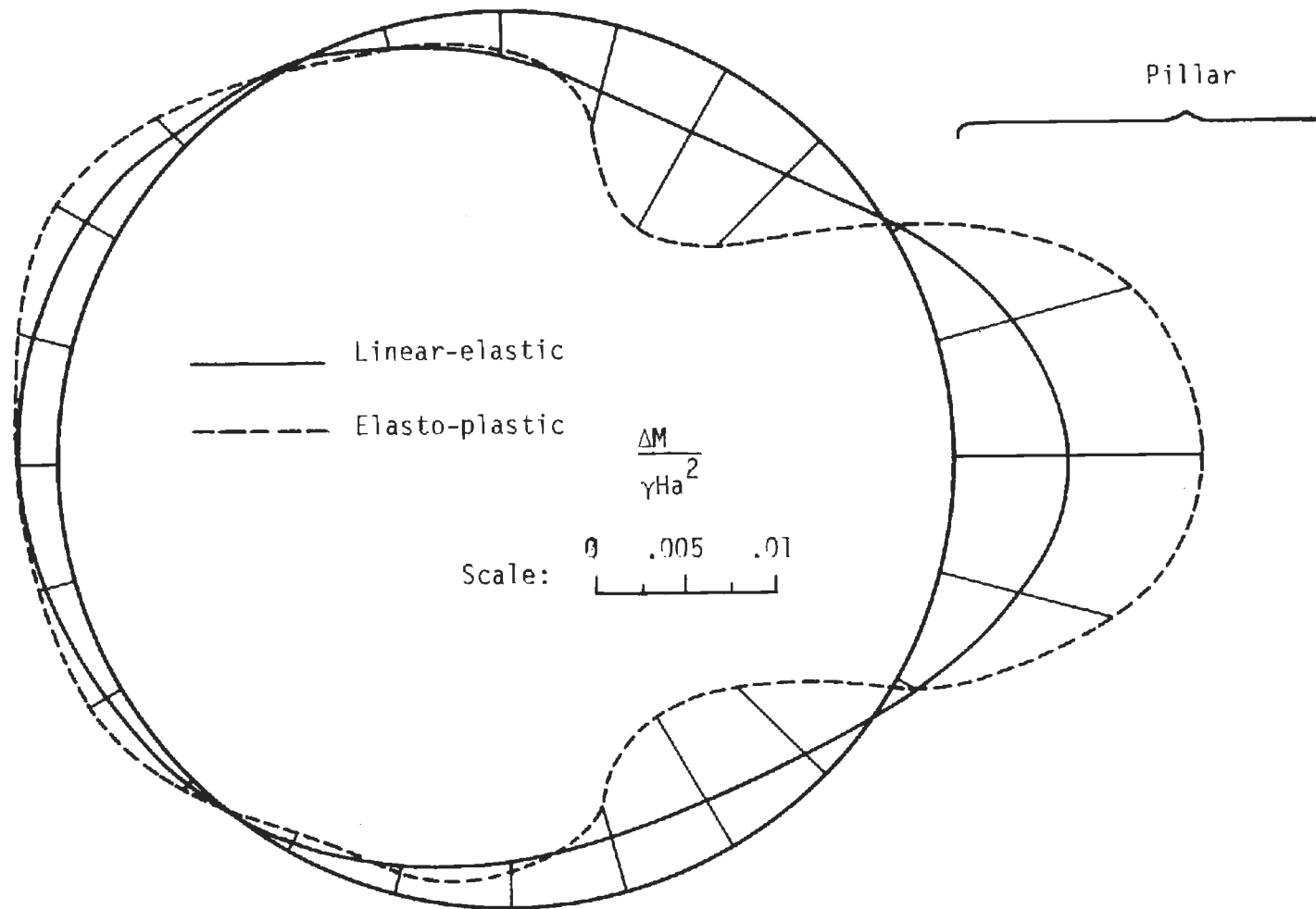


FIGURE 3.41 DISTRIBUTION OF CHANGES IN BENDING MOMENTS IN LINER OF TUNNEL I DUE TO PASSAGE OF TUNNEL II (TB32, TB32EP)

CHAPTER 4

DISCUSSION OF RESULTS

4.1 GENERAL

In most analytical and numerical investigations into the behavior of underground openings many simplifying assumptions must be invoked in order to reduce what is a highly complex problem to a manageable form that allows solution. The investigation described in this report is no different from many others in this respect and consequently the results obtained must be evaluated with the underlying assumptions in mind.

Two simplifications made in this investigation are especially significant. First, what is in reality a three-dimensional problem has been reduced to two-dimensions. Second, while most geologic materials exhibit both instantaneous and time-dependent behavior when disturbed by the excavation of a tunnel, only the instantaneous response has been considered.

In the two-dimensional analyses it was necessarily assumed that liner installation occurred either simultaneously with excavation or at a point far behind the face.

Simultaneous excavation and liner installation rarely occurs in practice (nor does the equivalent condition of liner placement prior to excavation). This type of analysis is an approximation to the construction sequence in which the liner is installed right at, or possibly just behind, the tunnel face. The approximation leads to a conservative solution with respect to liner forces and moments, but an undoubtedly unconservative prediction of surface settlements. The analyses provide no information as to face

stability or the behavior of the medium ahead of the face in general. It is necessarily assumed, therefore, that the face remains stable. Because the analyses do not consider time-dependent behavior, nothing is learned about the long term behavior of the tunnels. However, there should be little change with time since the medium disturbance (change from initial equilibrium) is reduced to a minimum when the liner is installed at the face.

A number of analyses considered what were called unlined tunnels. It should be pointed out that these tunnels were unlined only with respect to the instantaneous response of the medium. Because the analyses did not consider time-dependent behavior, it was not necessary to assume that the tunnels were left entirely unlined. There are many tunnels in which internal supports are installed a considerable distance behind the face or in which a gap exists between the liner and the surrounding ground. In many such cases it is reasonable to expect that all, or a major portion, of the instantaneous response (displacements) of the medium associated with the advance of the face occurs before the liner becomes effective in providing support. The load on the liner in such cases is initially either zero or of only a very small magnitude. Unless the medium exhibits time-dependent behavior or some external event such as the passage of a second tunnel influences the medium surrounding the tunnel, the load on the liner remains very small. To approximate these conditions in this investigation a number of analyses were performed in which it was assumed that the liner was installed at a point behind the face where the instantaneous response of the medium had already occurred. Since time-dependent behavior was not considered there was no need to include a liner in the analyses unless the passage of a second tunnel was to be considered.

It was necessarily assumed in the "unlined" tunnel analyses that the unsupported section of tunnel between the face and the liner remained stable. Thus, for the elastic analyses it must be assumed that the shear strength of the medium around the opening exceeds the maximum shear stress. If the stresses exceed the strength the results from the elastic analyses do not apply. A similar restriction must be placed on the elasto-plastic analyses. In these analyses it was assumed that once the maximum shear strength of the medium was reached the shear strength remained at this peak value. If the medium should exhibit a loss of strength after the peak value was reached the results obtained from these analyses would not apply.

The lined tunnel analyses, in which it is assumed that no medium displacements occur prior to medium-liner interaction, yield upper bound values for liner forces, moments and displacements. The "unlined" tunnel analyses provide no useful information as to liner behavior. These analyses imply that the liner remains undisturbed. This may approximate the conditions of the liner just after being installed some distance behind the face, but it is not likely to be the ultimate condition.

The lined tunnel analyses give a distorted view of medium stresses and displacements because they do not take into consideration the relaxation that the medium experiences before the liner begins to act as a support (relaxation occurring both ahead of and behind the face). These analyses give stress changes and displacements that are less than would normally be expected. The "unlined" tunnel analyses give medium stresses and displacements that are reasonable for the case in which the liner is installed after the instantaneous displacements, but before significant time-dependent displacements of the medium occur.

4.2 SURFACE SETTLEMENTS

In studying settlement data from actual tunnels previous researchers [8,9,10] have found that in many, but not all, cases the Gaussian error function or normal probability curve can be a useful device for fitting a curve through the available data points. Such a curve is shown in Fig. 4.1. The displacement, s , at any point is given by the relation:

$$s = S_{\max} \exp \left[-\frac{x^2}{2i^2} \right] \quad (4.1)$$

where S_{\max} is the displacement at the center of the settlement trough, x is the horizontal distance from the center to the point considered, and i is the horizontal distance to the point of inflection of the curve (a measure of trough width). The width of the settlement trough, and thus i , is a function of the size and depth of the tunnel and the material properties of the medium.

After studying settlement data from tunnels in a wide variety of soil types, Peck [8] presented a chart of $(H/2a)$ vs (i/a) which was divided into different zones on the basis of soil type (Fig. 4.2b). Cording and Hansmire [10] suggested that the relationship between settlement trough width and tunnel depth could be expressed as a vertical angle β , measured to a line drawn from the tunnel springline to the point defining the trough width, w , at the ground surface (Fig. 4.2a). Several β values are shown in Fig. 4.2b for comparison with Peck's zones.

Points labeled 1 and 2 in Fig. 4.2b represent the relationships between tunnel radius, tunnel depth and settlement trough width for the unlined, single tunnel finite element analyses. Point 1 was obtained directly from the

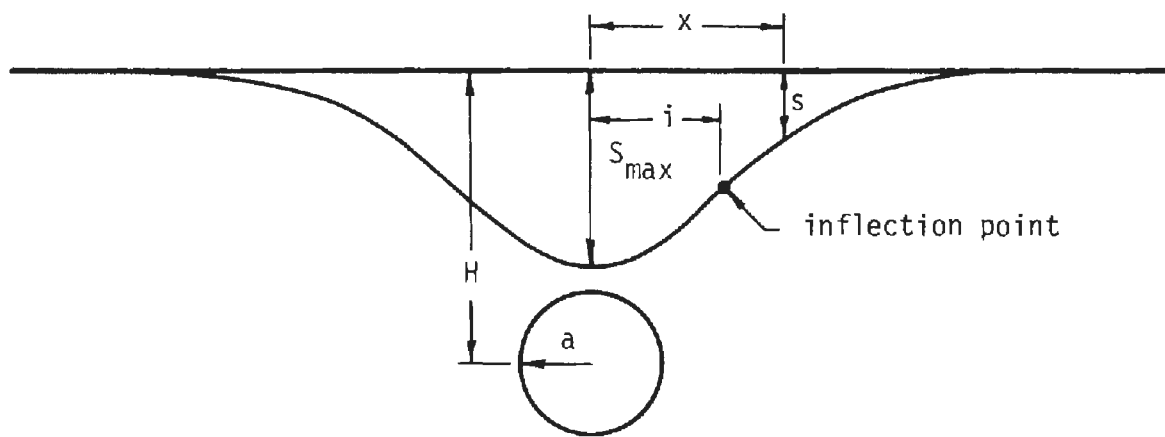


FIGURE 4.1 SHAPE OF SETTLEMENT TROUGH AS CALCULATED FROM GAUSSIAN ERROR FUNCTION

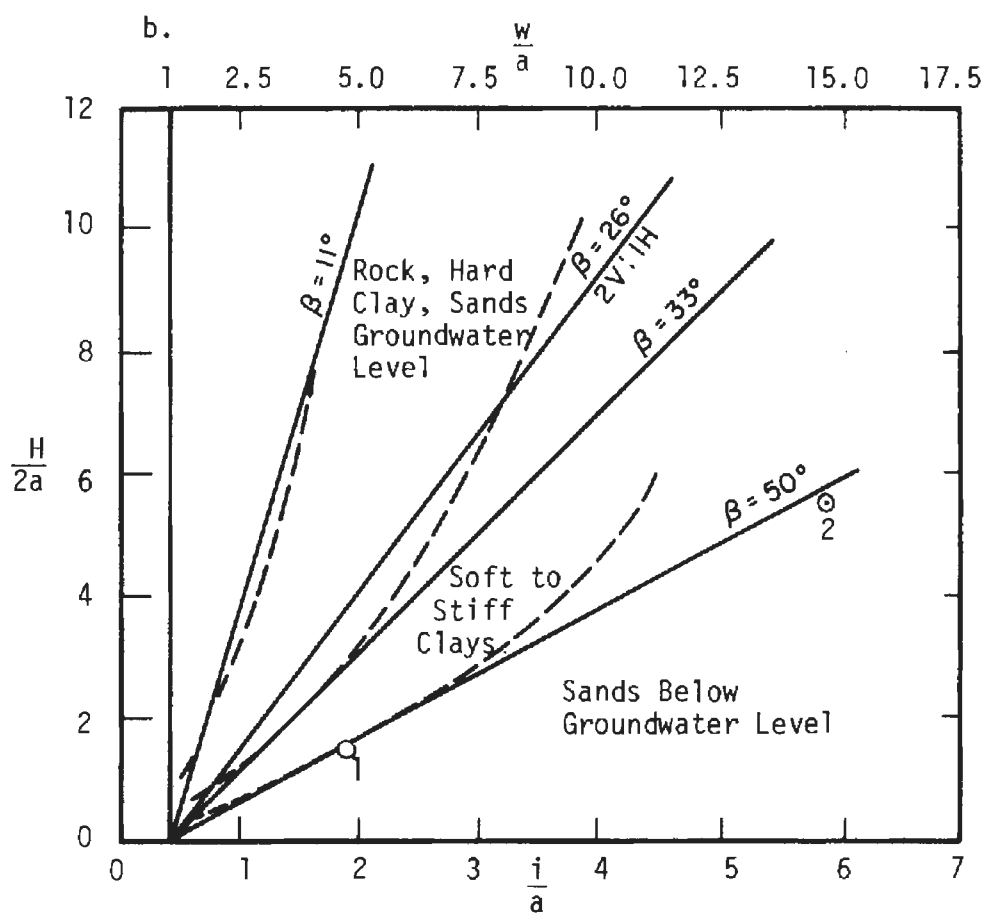
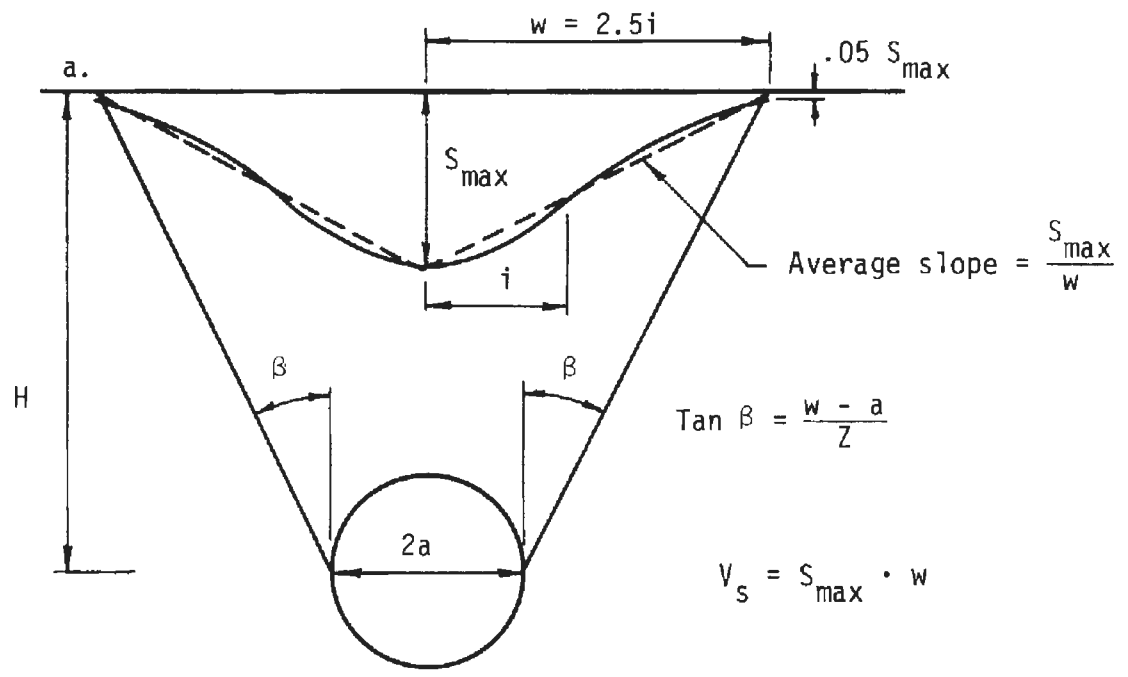


FIGURE 4.2 RELATIONSHIP BETWEEN β AND WIDTH OF SETTLEMENT TROUGH (MODIFIED AFTER CORDING AND HANSMIRE [10])

settlement curve provided by the finite element analysis of the shallow tunnel case. A value of $\beta = 51$ degrees was calculated for this case. Point 2 could not be obtained directly from the finite element data because the surface displacements for the deep tunnel case were distorted by the finite element mesh boundary conditions. However, since the material properties assigned to the medium in both shallow and deep tunnel cases were the same, it was assumed that β was the same for both cases. Thus, the position estimated for point 2 is the intersection of the $H/2a = 5.5$ line and the $\beta = 51$ degrees line.

The solid curves in Fig. 4.3 represent surface settlements obtained from the finite element analyses of unlined single tunnels. Displacements have been normalized with respect to S_{\max} , which is the maximum vertical displacement obtained in each case. Horizontal distance, x , from a vertical line through the tunnel centerline has been normalized with respect to a , the tunnel radius. The settlement curves are symmetrical about the $x/a = 0$ point.

The dashed curve in Fig. 4.3a is the normal probability curve equivalent of the finite element settlement trough for the shallow tunnel case. The two curves are equivalent in that they enclose equal areas. The dashed curve in Fig. 4.3b is a portion of the normal probability curve calculated from Eq. 4.1; the value of i being taken from point 2 in Fig. 4.2b. On the basis of the relationship between the solid and dashed curves in part a of Fig. 4.3 the position of the "true" settlement curve (had a wider mesh been used) for the deep tunnel case can be said to lay somewhere between the solid and dashed curve of Fig. 4.3b.

Figure 4.3a shows a reasonably good agreement between the settlement trough obtained from the finite element analysis and the normal probability

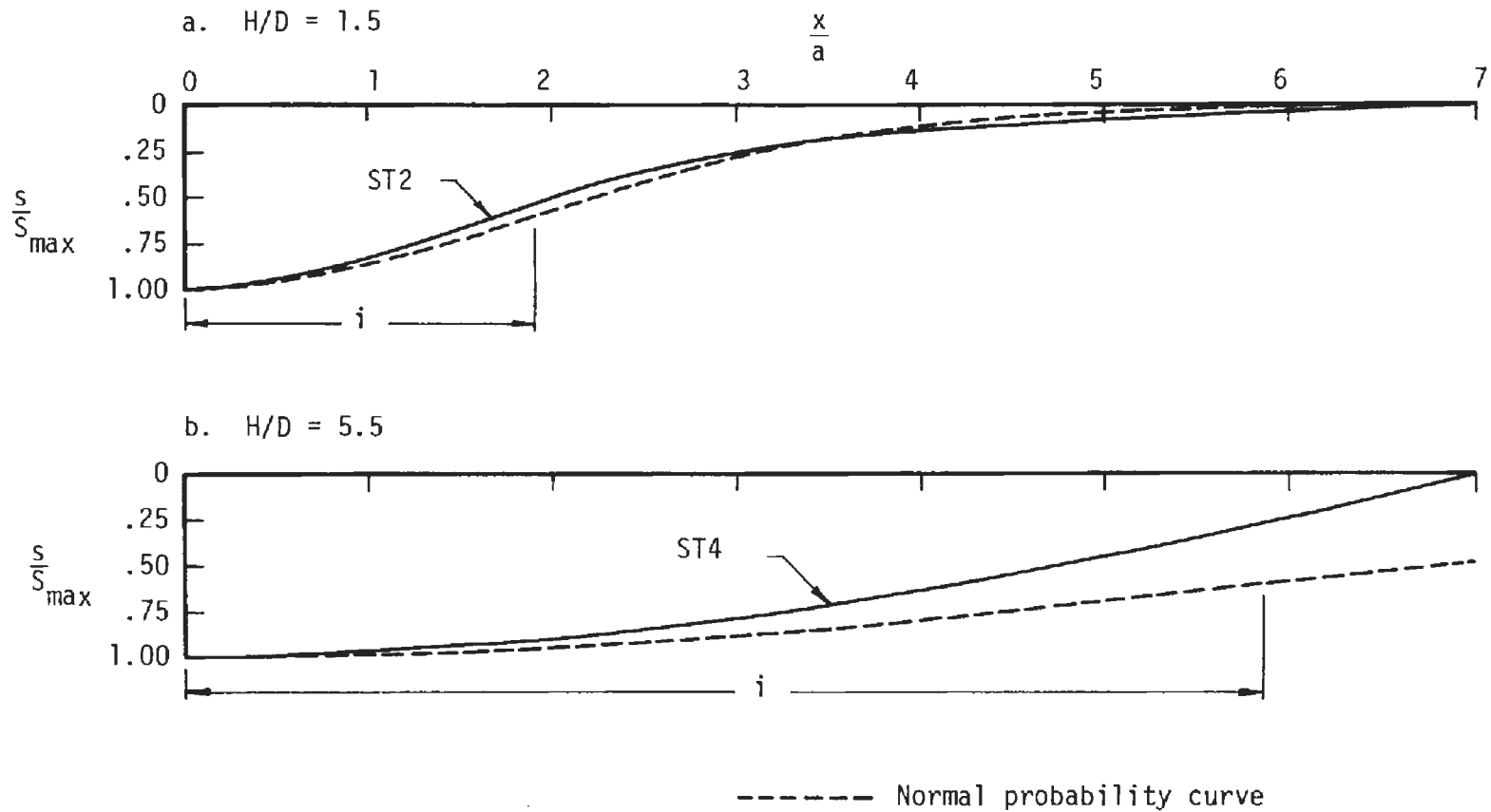


FIGURE 4.3 COMPARISON OF SURFACE SETTLEMENTS FROM SINGLE TUNNEL FINITE ELEMENT ANALYSES AND NORMAL PROBABILITY CURVE

for $i = 1.9a$. However, it cannot be concluded that the elastic finite element analysis accurately predicts surface settlements without first comparing finite element results with actual field data. Cairncross [12] has reported that finite element analyses of tunnels in elastic media tend to give wider settlement troughs (larger β values) than those commonly observed in the field.

For two adjacent and parallel tunnels it seems reasonable to expect that the settlements at the ground surface would consist of two components. The first component would be equal to the settlements resulting from the superposition of the two single tunnel troughs, assuming that the two tunnels are so spaced that their individual troughs overlap. The second component would consist of additional displacements resulting from interaction of the two tunnels (pillar shortening, increased crown displacements), assuming the two tunnels are close enough together so that interaction will occur. These two components are illustrated in Fig. 4.4.

The additional settlement due to two tunnel interaction is illustrated in Figs. 4.5 through 4.8 wherein the surface displacement profiles obtained from the finite element analyses are compared to profiles obtained by superimposing two single tunnel curves. Settlements were normalized with respect to S_{\max} which is the maximum settlement from the single tunnel analyses.

Figure 4.5 gives the comparison for the symmetrical case analyses of shallow, unlined tunnels at three different pillar widths. This figure indicates that the additional surface settlement due to interaction between the two tunnels increases as the pillar width is decreased. The pattern of increasing additional settlements over the tunnel crown ($x/a = 0$) corresponds to the pattern of increasing crown displacement shown in Fig. 3.6.

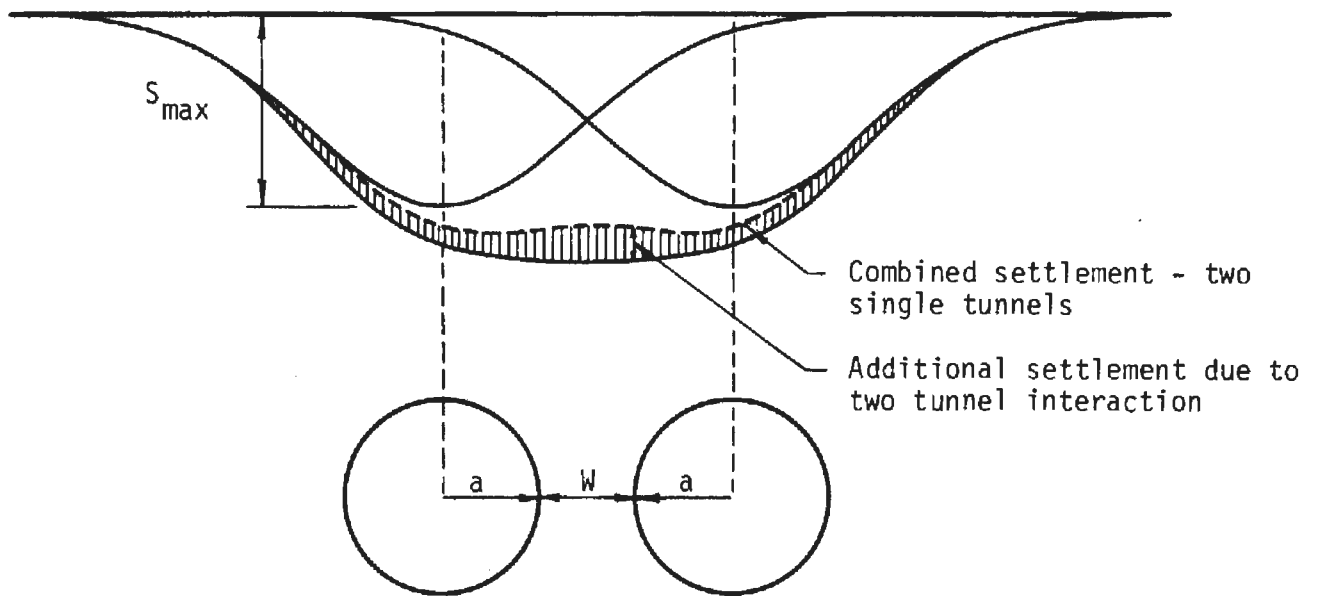


FIGURE 4.4 SCHEMATIC REPRESENTATION OF ADDITIONAL SURFACE SETTLEMENT ARISING FROM TWO-TUNNEL INTERACTION (SYMMETRICAL CASE)

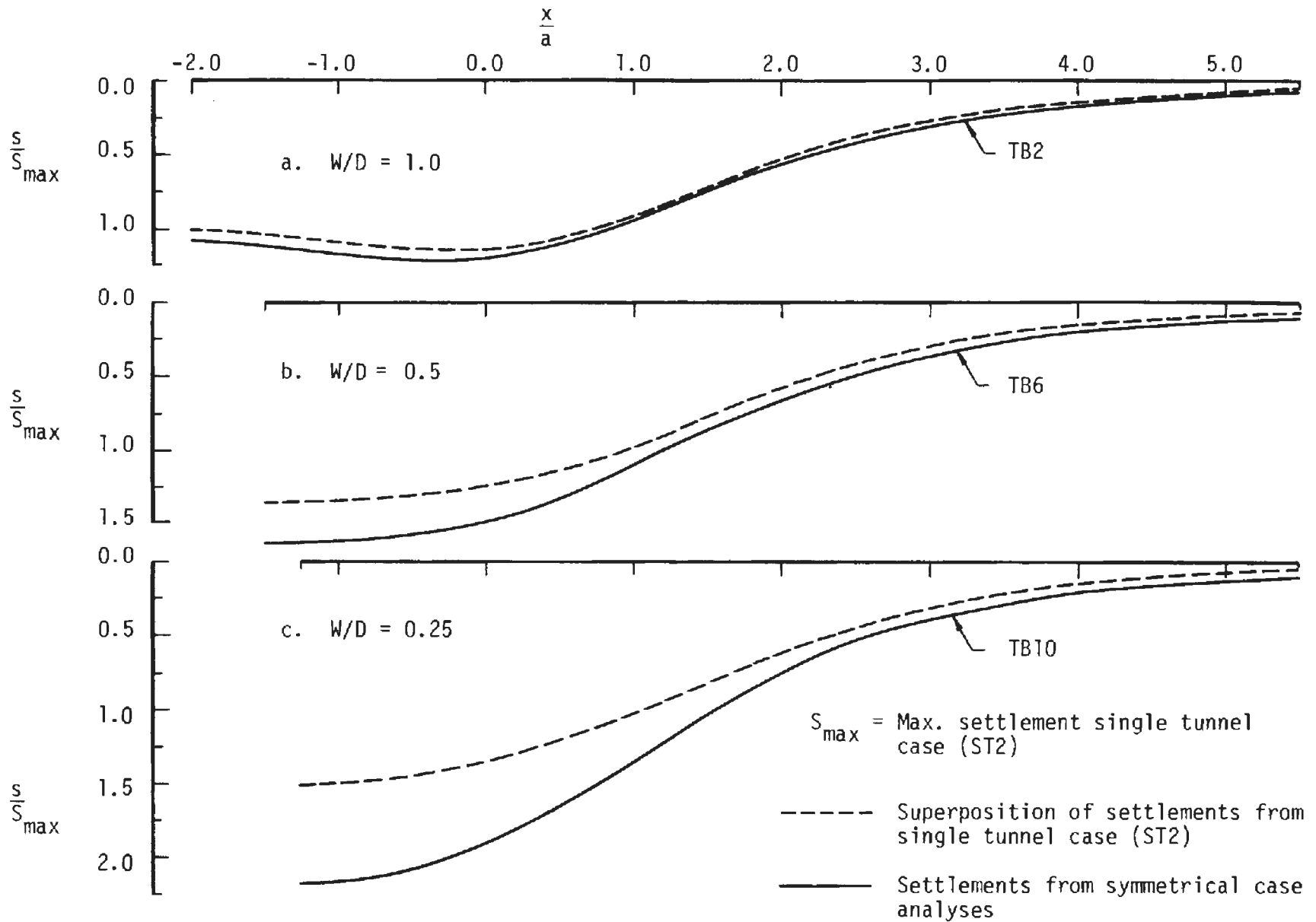


FIGURE 4.5 SETTLEMENT TROUGHS FROM SYMMETRICAL TWO TUNNEL ANALYSES AND FROM SUPERIMPOSING TWO SINGLE TUNNEL TROUGHS - $H/D = 1.5$

The comparison for the symmetrical case analyses of deep, unlined tunnels is shown in Fig. 4.6. Here the additional surface settlement due to two tunnel interaction also increases as the pillar width decreases, but at a less rapid rate than for the shallow tunnels. This pattern can be related to the relationship between displacements of the tunnel opening and pillar width (Fig. 3.7). Because of the depth of these tunnels the width of the individual settlement troughs is large and for two parallel tunnels the amount of overlap is extensive.

Figure 4.7 shows the differences between settlement troughs given by the superimposed single tunnel curves and the settlements obtained from four of the unsymmetrical finite element analyses. The solid circles represent settlements obtained from the analyses in which both tunnels were unlined. The broken lines represent settlements that resulted when the first tunnel was lined just prior to excavation of the second tunnel. It can be seen that the presence of the liner resulted in less settlement than when both tunnels were unlined.

Additional settlements due to interaction between the two shallow tunnels were not especially great (Fig. 4.7a). For both analyses TB13 and TB17 the settlement of Tunnel II was greater than that over tunnel I. The presence of the liner in tunnel I (TB17) restricted surface settlements above that tunnel to a magnitude less than that predicted by the superposition of two single tunnel settlements. A substantial amount of interaction settlement was indicated by both deep tunnel analyses (Fig. 4.7b). Despite the presence of the liner in tunnel I the settlement trough from analysis TB34 is essentially symmetrical about a vertical plane through the pillar centerline. The ground displacements from the two deep tunnels have overlapped to such an extent by

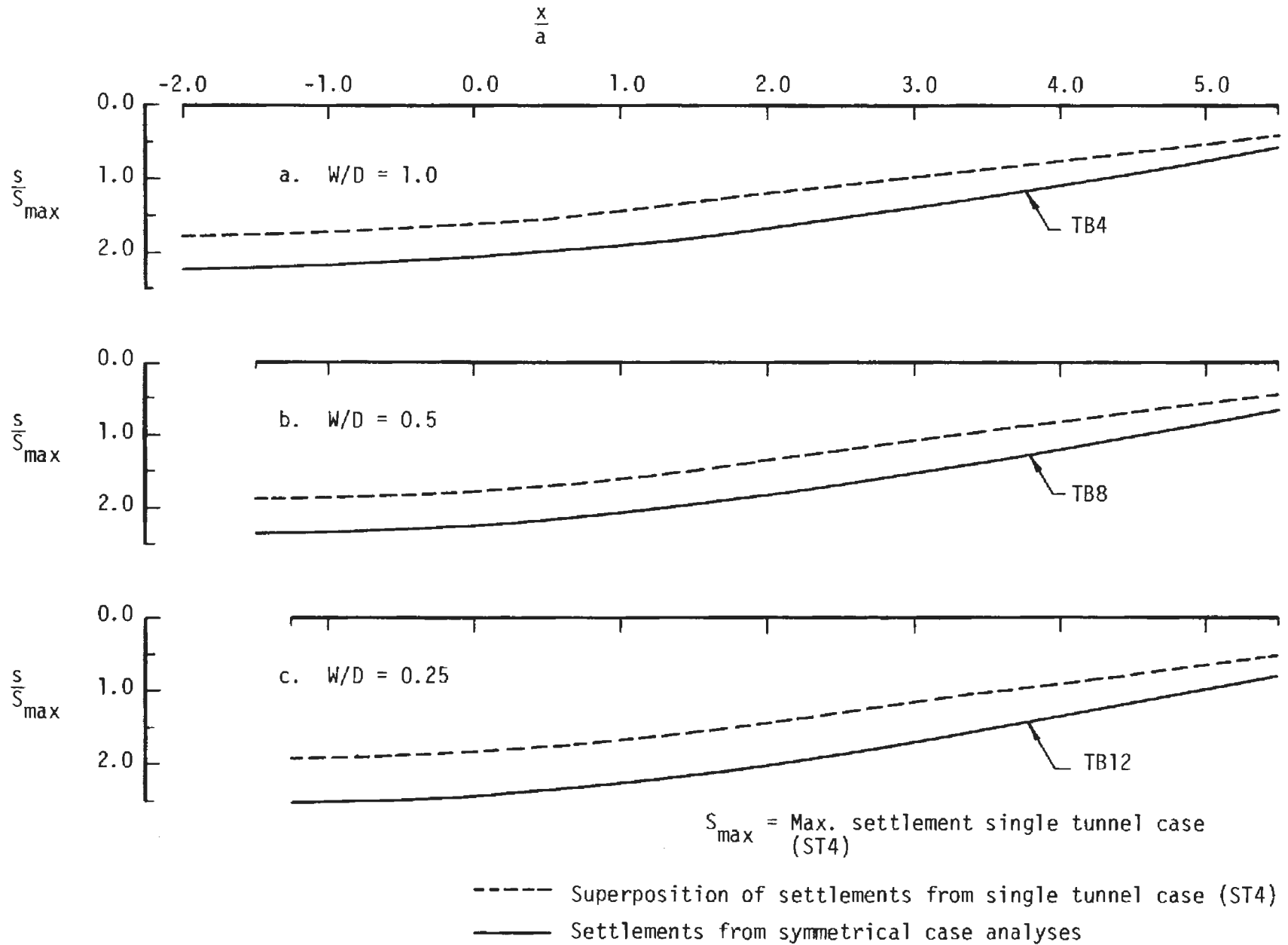


FIGURE 4.6 SETTLEMENT TROUGHS FROM SYMMETRICAL TWO TUNNEL ANALYSES AND FROM SUPERIMPOSING TWO SINGLE TUNNEL TROUGHS - $H/D = 5.5$

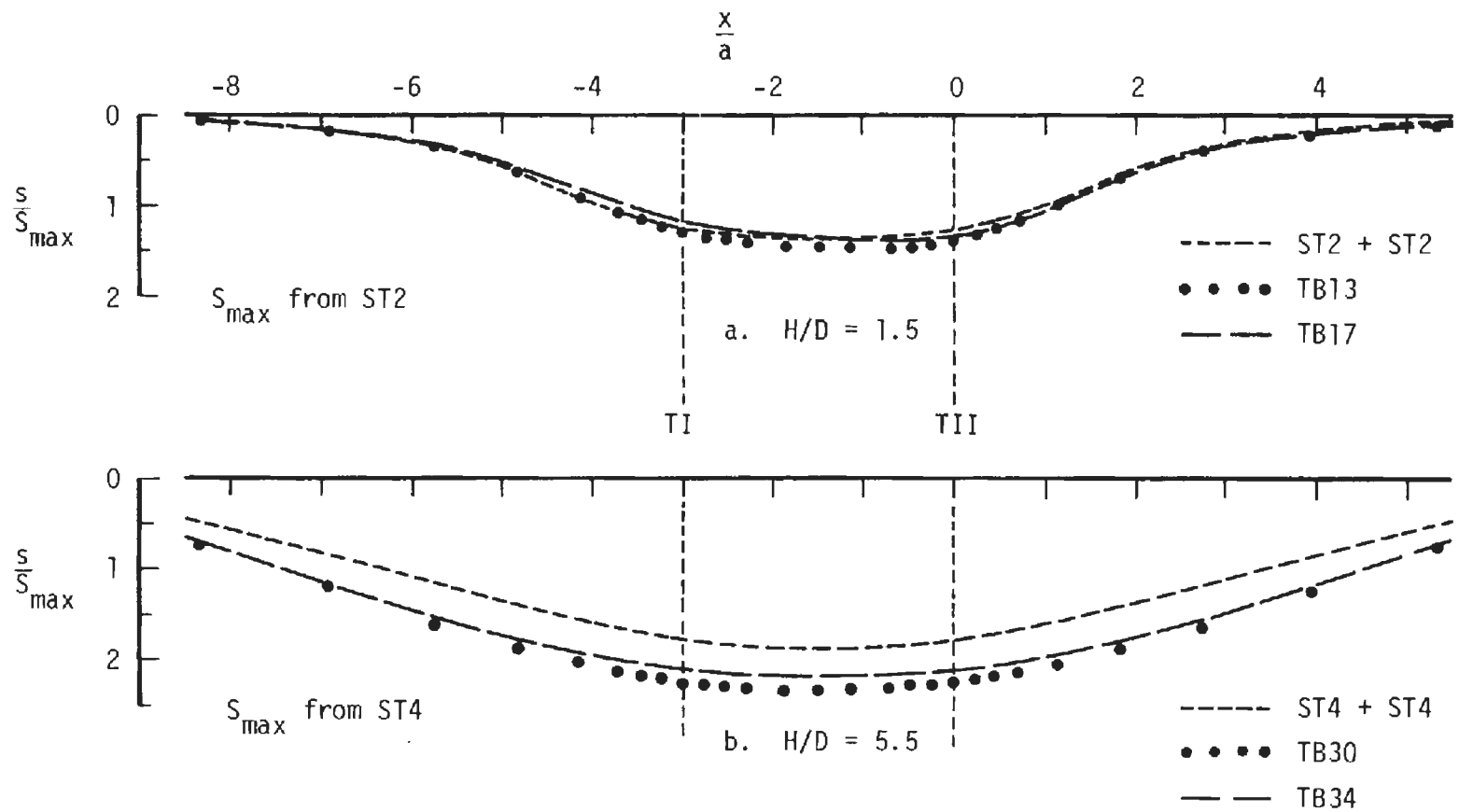


FIGURE 4.7 SETTLEMENT TROUGHS FROM UNSYMMETRICAL TWO TUNNEL ANALYSES AND FROM SUPERIMPOSING TWO SINGLE TUNNEL TROUGHS

the time they reach the ground surface that the shape of the settlement trough gives no indication that support conditions are not the same in both tunnels. That the presence of the liner in tunnel I has restricted the interaction settlements arising from the passage of tunnel II is indicated by the difference in settlements for analysis TB34 and analysis TB30 in which tunnel I was left unlined until after passage of tunnel II.

Another way of illustrating the additional settlement due to two tunnel interaction is to compare the settlement occurring upon excavation of the second tunnel to the settlement that would have resulted had that tunnel been the only one present. Such a comparison is shown in Fig. 4.8 for unsymmetrical analyses TB13 and TB30 in which both the first and second tunnels were unlined. In this figure the curves labeled A represent the settlements of the ground surface occurring upon excavation of tunnel II. These settlements were obtained by subtracting the settlements due to tunnel I from the final total settlements due to both tunnels. The curves labeled B represent the surface settlements that would have resulted had tunnel II been the only tunnel present. The volume of this settlement trough is designated V_S . The difference between curves A and B is the additional settlement that occurred as a result of interaction between the two tunnels. The volume of the interaction settlements is designated ΔV .

For the shallow tunnels it is clearly evident that most of the additional settlement occurs over the crown of tunnel II and over the pillar. As the vertical displacements migrate from the deep tunnels to the ground surface they spread out laterally. As a result, the displacements from each of two parallel tunnels overlap to a considerable extent at the ground surface

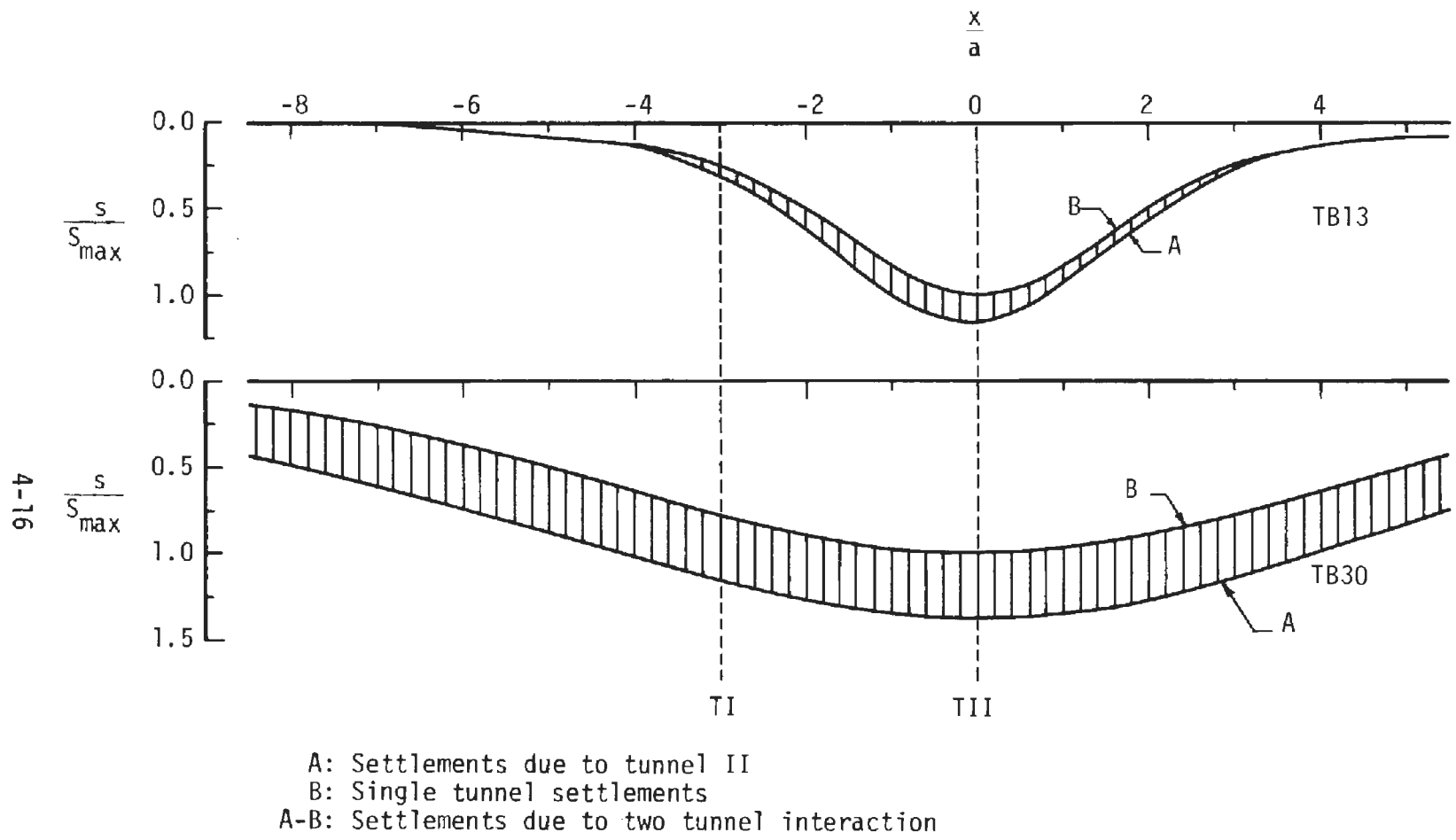


FIGURE 4.8 DISTRIBUTION OF INTERACTION SETTLEMENTS OBTAINED FROM FINITE ELEMENT ANALYSES OF TWO UNLINED TUNNELS (UNSYMMETRICAL CASE)

yielding what might be termed a homogenized settlement pattern. The interaction settlements are spread out over a wide distance rather than being concentrated over the tunnels.

The ratio obtained by dividing the interaction settlement volume by the settlement volume for a single tunnel, $\Delta V/V_s$, (Hansmire [1]) was calculated for the finite element analyses in which both tunnels were assumed to be unlined. These ratios are plotted versus pillar width in Fig. 4.9. The results from the symmetrical analyses show that the additional settlements due to two tunnel interaction increase as the pillar width decreases. The data also indicate that the volume ratio is greater for deep tunnels than shallow tunnels. If this relationship is valid it means that the deeper two tunnels are located the wider must be the pillar between them before no interaction would occur. However, while this may be true to a certain extent, it is difficult to believe that the upper dashed curve, for the deep tunnels, would continue on to the right (increasing pillar width) at the low rate of descent indicated.

All of the unsymmetrical analyses considered the same tunnel spacing ($W/D = 0.5$). Thus, curves similar to those for the symmetrical analyses are not available. However, the volume ratios obtained for the two unsymmetrical analyses in which both tunnels were left unlined are indicated in Fig. 4.9 by the solid square ($H/D = 5.5$) and solid circle ($H/D = 1.5$) points.

The symmetrical and unsymmetrical analyses of the deep tunnels yielded essentially identical distributions of surface settlements. This is reflected in the identical settlement volume ratios shown in Fig. 4.9. For elastic behavior it seems reasonable to expect the same final result regardless of whether the two unlined tunnels are excavated at the same time or at different

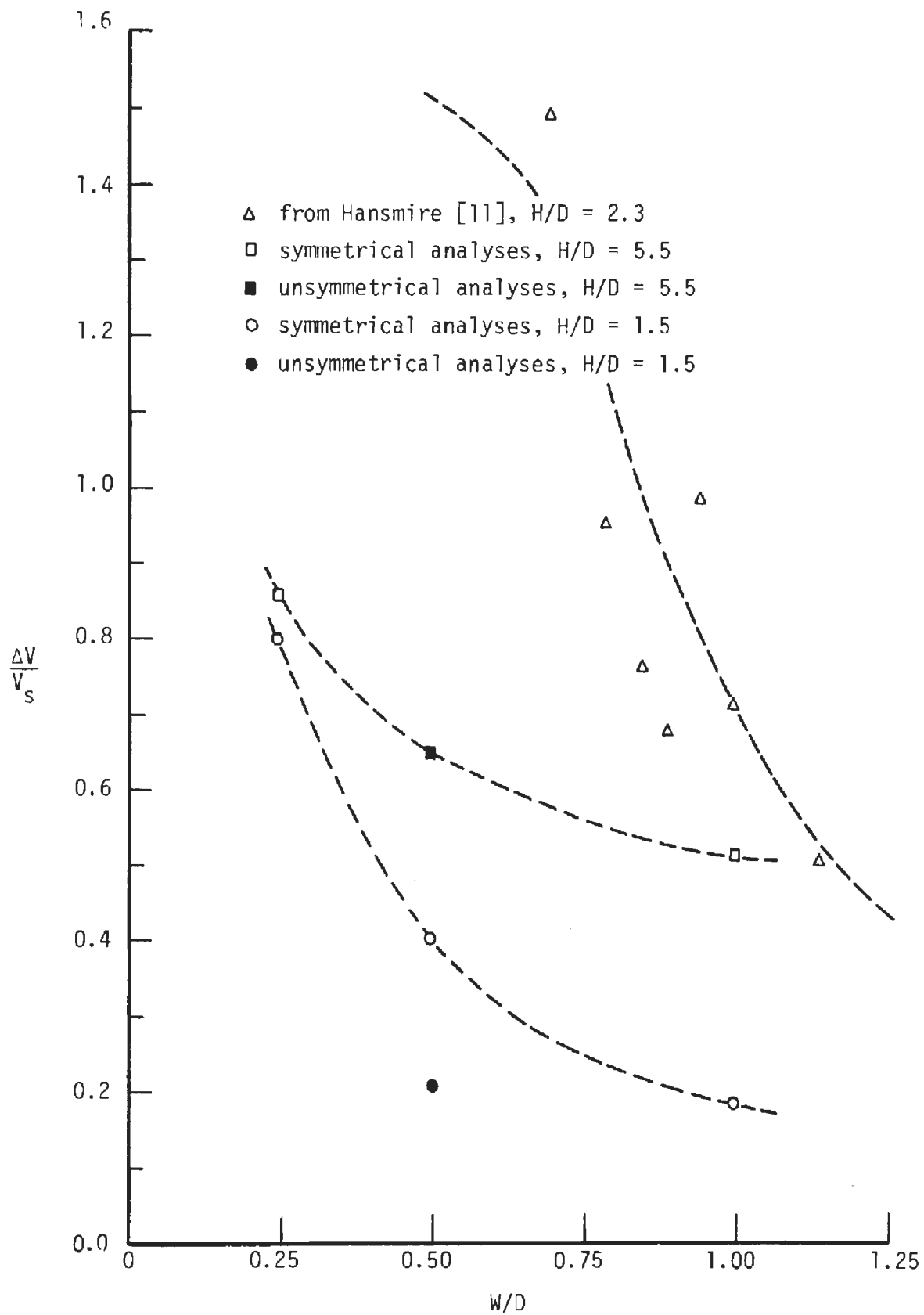


FIGURE 4.9 INTERACTION SETTLEMENT VOLUME AT GROUND SURFACE VERSUS PILLAR WIDTH

times. However, the results from the shallow tunnel analyses indicate that this may not be universally true. Figure 4.9 shows that the interaction settlement volume obtained from the unsymmetrical analysis of the two shallow tunnels was almost 50 percent less than that found for the symmetrical case. Final surface settlements from the unsymmetrical analyses were everywhere less than those from the symmetrical analysis. As shown in Fig. 3.33 the surface settlements obtained in the unsymmetrical analysis were not the same over both tunnels. The greatest settlements occurred over tunnel II.

The reason for a discrepancy between the results from the two types of analysis when shallow, but not deep, tunnels are considered is not entirely clear from the available data. Indications are that the cause is related to the influence of the ground surface.

When both tunnels are excavated at the same time the response of the system is necessarily symmetrical about a vertical plane through the pillar centerline. Additional settlements due to interaction between the two tunnels are forced to be the same over both tunnels regardless of depth. When the two tunnels are excavated separately it may be that the boundary constituted by the ground surface interferes with the interaction (as expressed by displacements) between the two tunnels resulting in less interaction settlement volume and restricting most of that which does occur to the region around the tunnel that was excavated last. The interference caused by the ground surface would vary with the depth of the tunnels, being greatest for shallow tunnels and minimal or nonexistent for deep tunnels.

Also shown in Fig. 4.9 are the volume ratios calculated by Hansmire [11] from field measurements of surface settlement over two parallel tunnels

constructed in Washington, D. C. The data from the Washington Metro indicates that the interaction volume ratio, $\Delta V/V_s$, for dense sands is two to three times larger than predicted from elastic theory. The difference is primarily due to soil volume decreases and disturbance that occurred in the sands and gravels but which were not modeled by the elastic analyses.

4.3 LINER FORCES, MOMENTS AND STRESSES

The tunnel liner modeled in the various analyses of this study was assigned properties and dimensions that most closely simulate a liner of unreinforced concrete, or shotcrete, of uniform thickness. To determine whether or not this liner would be adequate as a tunnel support system in the various situations considered, the liner forces and moments must be examined with respect to their contributions to the distribution of stresses in the liner.

There are three types of liner failure that must be investigated. The first of these is the simple compression failure resulting from liner compressive stresses that exceed the compressive strength of the concrete. Second, tensile stresses in a liner can induce tensile cracking, which, if it became too severe, would be unacceptable. Finally, the liner shear forces should also be examined to check the possibility of a diagonal tension failure.

At various locations around the liner perimeter the maximum and minimum circumferential stresses induced by the combined thrust and moment can adequately be determined using the familiar equation:

$$\sigma = \frac{T}{A} \pm \frac{Mc}{I} \quad (4.4)$$

Examination of the distributions of liner stresses for the single tunnel analyses performed indicates that, for both the shallow and deep tunnels,

at no point around these liners does the maximum compressive stress approach the compressive strength of the concrete. However, for both shallow and deep tunnels the bending moments near the crown and invert are sufficiently large, with respect to the thrust magnitude, that small tensile stresses are mobilized on the inner fiber of the liners at these locations.

The symmetrical analyses of the two tunnel problem, which simulated the special case of advancing both lined tunnels, side by side, at the same pace, indicated an even more favorable stress distribution than the single tunnel analyses. For analysis TB11 ($H/D = 5.5$, $W/D = 0.25$) liner thrusts either increased or remained unchanged, while the moments decreased in the critical areas around the crown, invert and springlines. Maximum compressive stresses were still well below the allowable value while the tensile stresses were either eliminated or reduced to negligible values. The results from the symmetrical analyses indicate that, in terms of liner stresses, if two parallel tunnels could be constructed in the manner simulated the liners could conservatively be designed on the assumption that each was a single tunnel.

It is seldom that two parallel tunnels are constructed in the manner assumed for the symmetrical analyses. Thus, the unsymmetrical analyses represents a step toward a more realistic approach to the two tunnel problem. For analyses TB14, TB15, TB31, TB32 and TB32EP the first tunnel was excavated and lined simultaneously, as was the procedure for the single tunnel analyses. Thus, before the passage of the second tunnel liner forces and stresses were the same as those obtained in the single tunnel analyses. However, as the second tunnel passed, the forces in the first tunnel's liner were altered.

When the second tunnel was also lined the change in liner forces was, in general, toward a more favorable distribution of thrusts and moments. The stress distributions in both liners approached those found in the symmetrical analyses and were less severe than those found in the single tunnel analyses.

When the second tunnel was left unlined (TB15, TB32 and TB32EP) the changes in liner forces and moments for tunnel I were, in general, toward a less favorable distribution of thrusts and moments. As indicated by Figs. 3.39 and 3.40 the trend was toward increased thrusts in that portion of the liner adjacent to the pillar and substantial increases in bending moments at most locations around the liner. In the vicinity of the right springline the increases in bending moments were significantly greater than the thrust increases. This led to very high compressive stresses on the inside of the right springline in addition to tensile stresses on the outside of the liner at that location. Compressive stresses actually exceeded the allowable value. Similar results were found for both the linear-elastic and elasto-plastic analyses, but the adverse stress concentrations were more severe in the elasto-plastic case, as illustrated in Table 4.1.

In analyses TB16, TB17, TB33 and TB34 the tunnel I liner was not installed until after all excavation displacement had occurred. This approximated the condition of installing the liner far behind the face. Forces and moments in this liner were due entirely to the disturbance created by the passage of tunnel II. Liner thrusts were very small relative to those for the single tunnel case. Moments in this liner were also generally small, except near the right springline where they exceeded 50 percent of the single tunnel values at that location when the second tunnel was unlined. In all of these

TABLE 4.1
 MAXIMUM AND MINIMUM STRESSES AT SELECTED LOCATIONS
 AROUND LINER FOR ANALYSES TB32 AND TB32EP

	TB32		TB32EP	
	σ_{\max}	σ_{\min}	σ_{\max}	σ_{\min}
	$.85f'_c$	$.85f'_c$	$.85f'_c$	$.85f'_c$
Crown	0.691	-0.214	0.660	-0.116
Left springline	0.855	0.018	0.871	0.045
Invert	0.738	-0.220	0.780	-0.218
Right springline	1.078	-0.103	1.455	-0.422

Negative sign indicates tensile stress.
 At crown and invert: σ_{\max} occurs at extrados, σ_{\min} at intrados.
 At springlines: σ_{\max} occurs at intrados, σ_{\min} at extrados.

analyses the distributions of liner thrusts and moments were such that they combined to cause tensile stresses in regions around the crown, invert and both springlines of the tunnel I liner. This was a result primarily of the very small thrust values that were mobilized. The compressive stresses contributed by these small thrusts were not sufficient to cancel out the tensile stresses contributed by the bending moments.

When the second tunnel was lined the thrusts and moments mobilized in its liner were generally greater in magnitude than those for a single tunnel. However, the increase in thrusts generally kept pace with the increase in moments and the resulting stress distributions were only slightly less favorable than those for a single tunnel.



CHAPTER 5

SUMMARY AND CONCLUSIONS

An investigation has been conducted of the interaction that occurs between two parallel circular tunnels. The finite element method of analysis was employed. The two tunnel system variables considered in greatest detail were the depth of burial, tunnel spacing and construction sequence. The ground mass was assumed to be a continuous, isotropic and homogeneous medium subjected to a free-field stress system with $K_0 = 0.5$. The vertical stress at any point in the medium was taken as the weight of the overburden at that point. Thus, the increase of stress with depth was considered. The majority of analyses assumed linear-elastic stress-strain behavior for the medium, although three elasto-plastic analyses were performed. The tunnels were assumed to be lined right at the face or far behind the face.

The various analyses were divided into three main categories. A set of four single tunnel analyses, considering unlined and lined tunnels at two different depths (shallow, $H/D = 1.5$ and deep, $H/D = 5.5$) comprised category one. These analyses provided the control data with which to compare the two tunnel results. Category two consisted of a series of two-tunnel analyses in which it was assumed that both tunnels advanced together at the same rate. Excavation and, when lined tunnels were considered, liner placement were considered to occur for both tunnels simultaneously. Both shallow and deep tunnels were analyzed and three different pillar widths were considered ($W/D = 1.0, 0.5, 0.25$). Construction sequence was the variable on which the category three analyses concentrated. Although both shallow and deep depths of burial

were considered, only one pillar width ($W/D = 0.5$) was examined. These analyses assumed that one of the tunnels was already in place before the second tunnel was excavated (tunnel I face far ahead of tunnel II face). Tunnel I was simulated as having been lined right at the face, lined behind the face but ahead of tunnel II, or not lined until after passage of tunnel II. Tunnel II was assumed to have been either lined right at the face or lined far behind the face.

Category two analyses, the symmetrical cases, indicated that the amount of two tunnel interaction that occurs increases as the pillar width decreases. With respect to the behavior of the tunnel openings it was found that the interaction was reflected most strongly in the displacements and liner forces on the pillar side of the tunnels. At the outer springlines little difference was found from the single tunnel results. Liner moments in the vicinity of the pillar springlines were significantly reduced from their single tunnel magnitudes as the pillar width was reduced. Average liner thrust increased only slightly from the single tunnel average as the pillar width decreased. In general, it appears that for this special sequence of parallel tunnel construction the liners need not be designed for conditions more severe than those for a single tunnel. Interaction between the two tunnels was also reflected by settlements of the ground surface that were in excess of what would be expected from simple superposition of the settlement troughs for two single tunnels. The additional interaction settlements increased as the pillar width was reduced and were larger for the deep tunnels than for the shallow tunnels.

Field data from tunnels in sands and gravels show larger interaction settlements than those obtained here due to the volume changes occurring in the sands and gravels that were not modeled by the finite element analyses.

Analyses of the unsymmetrical case gave results similar to those of the symmetrical case when both tunnels were either unlined or lined right at the face. The major exception to this statement was the difference between the surface settlements over shallow unlined tunnels given by the two types of analysis. Settlements obtained when the two tunnels were excavated separately were less than those obtained when both tunnels were excavated at the same time. The two types of analysis gave essentially identical surface settlements for the deep tunnels. This suggests that the additional medium displacements due to interaction between the two tunnels are influenced by the ground surface boundary and that this influence varies with the proximity of the source of displacement to the ground surface.

The unsymmetrical analyses indicated that when tunnel I is lined the passage of an unlined second tunnel (at a pillar width of $W = 0.5D$) causes significant changes in the initial distribution of liner displacements, forces and moments. Large bending moments are mobilized in the vicinity of the liner's pillar springline leading to the development of tensile stresses in that part of the liner. Bending moments become especially large if plastic yielding of the pillar occurs. When the second tunnel is assumed to be kept lined right up to the face the interaction between the two tunnels is reduced, because displacements of the ground mass are decreased.

Tensile stresses occurred in the region of the pillar springline of the tunnel I liner for three out of the four construction sequences considered in the unsymmetrical analyses. The one sequence in which these tensile stresses did not appear was that in which both tunnels were kept lined right up to the face. All of these construction sequences can be interpreted as simulating

the practice of installing the tunnel I liner prior to passage of tunnel II. The adverse stress distributions obtained from these analyses suggest that a permanent liner should not be placed in one tunnel before passage of the second tunnel unless successful efforts can be made to prevent ground displacements prior to liner installation in both tunnels.

The following are the conclusions that have been drawn from the results of this investigation. These conclusions are necessarily limited to tunneling conditions as simulated herein.

1. Interaction between two parallel tunnels increases with decreasing pillar width.
2. Interaction between two parallel tunnels results in settlement of the ground surface in excess of what would be predicted by superposition of the surface settlements from two single tunnels.
3. Excess surface settlement volume (expressed as a percentage of settlement volume for a single tunnel at the same depth) due to interaction between two tunnels located in a continuous medium is greater for deep tunnels than for shallow tunnels.
4. The additional, interaction settlements can be reduced by keeping tunnel separation as great as possible and/or by taking steps to minimize the displacement of the surrounding ground mass into the tunnels.
5. Interaction between two parallel tunnels results in distribution of liner forces and moments that are different from those of a single tunnel. The greatest differences occur on

that side of the liner adjacent to the pillar. Liner bending moments are influenced more than liner thrusts by interaction.

6. If ground displacements can be prevented, or at least held to a minimum,, prior to liner installation in both tunnels the distributions of liner forces and moments, while different from what would exist in a single tunnel, are not necessarily more adverse to liner performance than those for a single tunnel.



REFERENCES

1. Ranken, R. E. and Ghaboussi, J., Tunnel Design Considerations: Analysis of Stresses and Deformations Around Advancing Tunnels, Report No. FRA-ORD&D 75-84, Federal Railroad Administration, Department of Transportation, August 1975.
2. Fotieva, N. N. and Sheinin, V. I., "Distribution of Stresses in the Lining of a Circular Tunnel when Driving a Parallel Tunnel," Soil Mechanics and Foundation Engineering, No. 6, Nov.-Dec. 1966.
3. Barla, G. and Ottoviani, M., "Stresses and Displacements Around Two Adjacent Circular Openings Near to the Ground Surface," Proceedings, Third International Congress on Rock Mechanics, Vol. II, Denver, 1974.
4. Peck, R. B., Deere, D. U., Monsees, J. E., Parker, H. W. and Schmidt, B., Some Design Considerations in the Selection of Underground Support Systems, Report for U.S. Department of Transportation, Office of High Speed Ground Transportation, Contract 3-0152, November 1969, (Order No. 190 443 from NTIS, Springfield, VA 22151).
5. Deere, D. U., Peck, R. B., Monsees, J. E. and Schmidt, B., Design of Tunnel Liners and Support Systems, Report for U.S. Department of Transportation, Office of High Speed Ground Transportation, Contract No. 3-0152, February 1969, (Order No. PB 183799 from NTIS, Springfield, VA 22151).
6. Ward, W. H. and Thomas, H.S.H., "The Development of Earth Loading and Deformation in Tunnel Linings in London Clay," Proceedings, 6th International Conference on Soil Mechanics and Foundation Engineering, Vol. 2, pp. 432-436.
7. Terzaghi, K., "Liner-Plate Tunnels on the Chicago Subway," Proceedings, ASCE, Vol. 68, No. 6, pp. 862-899, 1942.
8. Peck, R.B., "Deep Excavations and Tunneling in Soft Ground," Proceedings, 7th International Conference on Soil Mechanics and Foundation Engineering, State of the Art Volume, 1969, pp. 225-90.
9. Schmidt, B., Settlements and Ground Movements Associated with Tunneling in Soil, Ph.D. Thesis, University of Illinois, Urbana, IL, 1969.
10. Cording, E. J. and Hansmire, W. H., "Displacements Around Soft Ground Tunnels," General Report: Session IV, Tunnels in Soil, 5th Pan American Congress on Soil Mechanics and Foundation Engineering, Buenos Aires, November 1975.

11. Hansmire, W. H., Field Measurements of Ground Displacements About a Tunnel in Soil, Ph.D. Thesis, University of Illinois, Urbana, IL., 1975.
12. Cairncross, A. M., Deformations Around Model Tunnels in Stiff Clay, Ph.D. Thesis, Corpus Christi College, Cambridge University, 1973.